



Optimization of Riboflavin Production by Fungi on Edible Oil Effluent

This work is submitted in fulfilment for the requirements for the degree of Doctor of Technology: Biotechnology in the Faculty of Applied Sciences at the Durban University of Technology.

Feroz Mahomed Swalaha
M.Sc. (cum laude): Microbiology

MAY 2010

PROMOTER: Professor Bharti Ohav

DECLARATION BY STUDENT

Optimization of Riboflavin Production by Fungi on Edible Oil Effluent

F.M. Swalaha

2010

I declare that the thesis herewith submitted for the D Tech: Biotechnology at the Durban University of Technology, has not been previously submitted for a degree at any other University.

Feroz Mahomed Swalaha

I hereby approve the final submission of the following thesis.

Prof. B. Odhav
Ph.D. (UKZN)

This _____ day of _____ 2010, at Durban University of Technology.

ABSTRACT

South African edible oil processing plants produce approximately 3×10^5 tonnes of oil annually with up to 3 tonnes of water for every tonne of oil produced. Wastewater that contains oil extracts varies in organic loading from 30,000 to 60,000 mg.l⁻¹ COD. This wastewater can be used to grow oleophilic fungi to produce valuable industrial products. The global vitamin B market is approximately R25.5 billion with 4500 metric tonnes being produced. A large proportion of this is produced using the fungus *Eremothecium gossypii* using oil substrates. The aim of this study was to develop a novel method to produce riboflavin with the aid of fungi, using edible oil effluent (EOE) as substrate, and to optimize the production thereof by statistical experimental design. Four fungi were surveyed for their growth potential on EOE and two, *E. gossypii* (CBS109.51) and *C. famata* (ATCC 208.50) were found to produce sufficient riboflavin for further study. Mutation of these organisms using ethylmethane sulphonate (EMS) increased riboflavin production from 3.52 mg.l⁻¹ to 38.98 mg.l⁻¹, an 11-fold increase. An enzyme pathway responsible for this was found to involve isocitrate lyase and comparison of this enzyme's activity in the mutant against the wild-type using Michaelis-Menten kinetics showed a higher reaction velocity (V_{\max}) with a reduced substrate affinity (K_m) indicating that the mutation was associated with this enzyme. Biomass comparisons were fitted to the sigmoid Gompertz model which was used to compare the wild-type to the mutant and increased specific growth rates and doubling times were observed in mutated cultures of *E. gossypii*. A strategy of statistical experimental design was pursued to optimize media components and iterative fractional factorial experiments culminating in a central composite optimization experiment were conducted. Statistically verified mathematical models were developed at each stage to identify important media components, predict media interactions, show directions for improvement and finally, predict maximum riboflavin production. An eight-factor resolution IV fractional factorial increased riboflavin production to 112 mg.l⁻¹ followed by a four-factor resolution V experimental design which increased riboflavin production to 123 mg.l⁻¹. A two-factor (yeast extract and NaCl) central composite experimental design predicted a maximum riboflavin production of 136 mg.l⁻¹ which was a 3.5-fold increase from the mutant, and 38.6-fold higher than the *E. gossypii* wild-type. The optimized value was achieved within predicted confidence intervals in confirmatory experiments. Cost implications for production of riboflavin on EOE were calculated and a 10% technology uptake by the edible oil industry could yield a riboflavin industry with a 63.65 million rand turnover and a potential 24.96 million rand gross profit margin.

DEDICATION

To my daughters, Nafeesa and Naseeha, who taught me the true lesson of unconditional love.

To my mother who persevered through untold trials to raise me - I can never repay the debt.

ACKNOWLEDGEMENTS

Thank you to my wife Anisa, for keeping everything at home going and taking over when I needed her.

Thank you Professor Bharti Odhav for being a friend, supervisor, inspiration and role model. I am deeply grateful and you will always find me beside you when you need me.

Thank you to Doctor George Nikolaev Tivchev for supervising me during the early part of this project.

Thank you to the NRF for funding parts of this project.

Thank you to PGDS of Durban University of Technology for funding for a laptop and associated peripherals.

Thank you to the various students who assisted me when I needed it, especially Nazihah Khan.

TABLE OF CONTENTS

TITLE	i
DECLARATION BY STUDENT	ii
ABSTRACT	iii
DEDICATION	iv
ACKNOWLEDGEMENTS	v
TABLE OF CONTENTS	vi
LIST OF FIGURES	xii
LIST OF TABLES	xvi
LIST OF ABBREVIATIONS	xix
CHAPTER 1 : INTRODUCTION	1
CHAPTER 2 : LITERATURE REVIEW	4
2.1 EDIBLE OIL EFFLUENT	4
2.2 RIBOFLAVIN (VITAMIN B ₂)	5
2.2.1 Structure	6
2.2.2 Stability and solubility	7
2.2.3 Uses of riboflavin	7
2.2.3.1 Clinical uses	8

2.2.4	Riboflavin Detection Methods	9
2.3	RIBOFLAVIN PRODUCTION METHODS	9
2.3.1	Chemical Production	9
2.3.2	Biosynthesis of Riboflavin	9
2.3.2.1	Bacterial producers	12
2.3.2.1.1	<i>Bacillus subtilis</i>	13
2.3.2.1.2	<i>Other bacterial producers</i>	15
2.3.2.2	Fungal producers	16
2.3.2.2.1	<i>Candida famata</i>	16
2.3.2.2.2	<i>Eremothecium gossypii</i>	17
2.3.2.2.3	<i>Eremothecium ashbyi</i>	21
2.3.3	Other Microorganisms	22
2.4	INDUSTRIAL RIBOFLAVIN PRODUCTION METHODS	22
2.4.1	Patents for Riboflavin Production Processes	22
2.4.2	Riboflavin Purification after Fermentation	24
2.5	RIBOFLAVIN OVERPRODUCTION MECHANISMS	24
2.5.1	Genetic Pathway	24

2.5.2	Regulatory Mutants	25
2.5.3	Nutrient Supplements	25
2.6	EXPERIMENTAL DESIGN FOR PROCESS OPTIMIZATION	27
2.6.1	Strategies for Problem Solving	27
2.6.2	Clear Signal Designs	28
2.6.3	Design Types	28
2.6.4	Optimizing Designs	29
2.6.5	Estimating Effect Magnitude and Data Transformation	30
2.6.6	Statistical Designs for Media Optimization	34
	CHAPTER 3: MATERIALS AND METHODS	38
3.1	STRAIN SELECTION, MEDIA AND CULTIVATION	38
3.1.1	Strain Selection	38
3.1.1.1	<i>Eremothecium (Ashbya) gossypii</i> wild type WT (ATCC 10895)	39
3.1.1.2	<i>Eremothecium gossypii</i> (CBS 109.51)	39
3.1.1.3	<i>Eremothecium ashbyi</i> (CBS 206.58)	39
3.1.1.4	<i>Candida famata</i> (ATCC 20850)	39
3.1.2	Media and Cultivation	40

3.2	COMPOSITION OF EDIBLE OIL EFFLUENT	41
3.2.1	Determination of Fatty Acid Composition of Edible Oil Effluent by Gas Chromatography	41
3.2.2	Instrumentation	42
3.3	FUNGAL GROWTH MEASUREMENT	43
3.3.1	Growth Curve Determination	43
3.4	OPTIMIZATION OF RIBOFLAVIN DETECTION ASSAY	44
3.5	FUNGAL GROWTH ON EDIBLE OIL EFFLUENT	47
3.6	MUTATIONAL STUDIES	48
3.6.1	Ultraviolet Light Mutation	48
3.6.2	N-Methyl-N-Nitrosoguanidine (MNNG)	49
3.6.3	Ethylmethane Sulphonate (EMS)	49
3.6.4	Sodium Azide (NaN_3)	49
3.6.5	Screening for Riboflavin-overproducing Mutants	49
3.6.6	Isocitrate Lyase Assay to Compare Mutant Enzyme Activity to Wild-Type	50
3.6.6.1	Enzyme extraction procedure	50
3.6.6.2	Enzyme assay procedure	51

3.7	SUPPLEMENTATION TO EDIBLE OIL EFFLUENT	51
3.7.1	Experimental Design for Media Optimization	52
3.7.1.1	Primary screening experiment to determine factor effects ..	52
3.7.1.1.1	<i>Inoculum Preparation</i>	52
3.7.1.2	Secondary screening experiment to identify important factors	55
3.7.1.3	Response surface experiment to optimize important factors	56
3.7.1.4	Confirmatory experiment to determine validity of prediction	59
	CHAPTER 4 : RESULTS	61
4.1	RIBOFLAVIN PRODUCTION UNDER DEFINED CONDITIONS	61
4.1.1	Wild type and Mutant Fungal Growth	61
4.1.2	Localisation of Riboflavin Production	64
4.2	EVALUATION OF FUNGAL GROWTH ON CONVENTIONAL MEDIA	65
4.2.1	Growth Curve	65
4.2.2	Specific Growth Rates and Doubling Times	66
4.3	COMPOSITION OF EDIBLE OIL EFFLUENT	67
4.4	RIBOFLAVIN DETECTION METHOD	69

4.5	FUNGAL GROWTH ON EDIBLE OIL EFFLUENT	71
4.6	RIBOFLAVIN PRODUCTION ON EDIBLE OIL EFFLUENT	73
4.7	MUTATIONAL STUDIES TO ADAPT MICROORGANISMS FOR GROWTH ON EDIBLE OIL EFFLUENT	75
4.8	ENZYME ACTIVITY OF SELECTED MUTANT	79
4.9	NUTRIENT SUPPLEMENT SCREENING	81
4.9.1	Primary Screen	81
4.9.2	Secondary Screen	89
4.9.3	Optimization Experiment	95
4.9.4	Confirmatory Experiment	98
CHAPTER 5 : DISCUSSION		101
CONCLUSIONS		117
REFERENCES		118
APPENDICES		132

LIST OF FIGURES

Figure 2.1	Structure of Riboflavin (Choe <i>et al.</i> , 2005)	7
Figure 2.2	Biosynthesis of riboflavin by bacteria and fungi (Bacher <i>et al.</i> , 2000)	11
Figure 2.3	Riboflavin production in <i>E. gossypii</i> showing relationship between growth (dashed line) and riboflavin production (solid line). mRNA samples were for study of transcriptional regulation (Karos <i>et al.</i> , 2004).	19
Figure 2.4	Strategy for selection, optimization and confirmation of experimental factors.	33
Figure 3.1	Representation of a central composite design for two factors showing six face-centered points around a replicated center point. The four corners of the square represent the factorial (+/- 1) design points and the four star points represent the axial (+/- α) design points (Statease, 2007).	57
Figure 4.1.1	Seven-day growth of four fungi on Ozbas and Kutsal agar plates (a) <i>E. gossypii</i> wild type (ATCC 10895), (b) <i>E. gossypii</i> (CBS 109.51), (c) <i>E. ashbyi</i> (CBS 206.58), (d) <i>C. famata</i> (ATCC 20850).	61
Figure 4.1.2	Sparingly septate mycelia showing dichotomous branching for (a) <i>E. gossypii</i> and (b) <i>E. ashbyi</i> . Darkfield images at 400 x (bar =25 μ m).	63
Figure 4.1.3	Spore formation showing (a) needle-like clavate spores in <i>E. gossypii</i> Phase contrast image at 400 x (bar=25 μ m) and (b) budding and short chain formation in <i>C. famata</i> Phase contrast image at 1000 x (bar=10 μ m).	63
Figure 4.2	Light and UV micrographs at 1000x of two fungi showing intracellular localisation of riboflavin. (a) and (b) <i>E. gossypii</i> (CBS 109.51) and (c) and (d) <i>C. famata</i> (ATCC 20850) light and UV illuminated micrographs respectively. Bar = 25 μ m.. . . .	65

Figure 4.3	Growth curves of four fungi grown on Ozbas and Kutsal liquid medium and fitted to the Gompertz growth model to determine growth parameters . Grey droplines indicate mid-log phases and times of inoculation for each fungus. <i>E. gossypii</i> wild type (ATCC 10895) (yellow triangle), <i>E. gossypii</i> (CBS 109.51) (red circle), <i>E. ashbyii</i> (CBS 206.58), (black circle) and <i>C. famata</i> (ATCC 20850) (green inverted triangle)	66
Figure 4.4	Total ion chromatogram of edible oil effluent.	67
Figure 4.5	Base Peak Chromatogram of edible oil effluent sample showing two peaks that were later identified using mass spectrometry.	68
Figure 4.6	Scan of 26 riboflavin concentrations from 200 to 820 nm showing three linear areas (indicated by white arrows) that were further investigated for standard curve preparation.	69
Figure 4.7	Standard curves for three wavelengths, 265 nm (black circle), 347 nm (red circle) and 444 nm (green inverted triangle) investigated for riboflavin measurement.	70
Figure 4.8	Growth curves of four fungi on EOE, fitted to the Gompertz model. <i>E. gossypii</i> wild-type (ATCC10895) (red circle) <i>E. gossypii</i> (CBS109.51) (green inverted triangle) <i>E. ashbyii</i> (CBS206.58) (yellow triangle), and <i>C. famata</i> (ATCC 20850) (blue square) and negative control (black circle). Error bars are standard deviations of triplicates.	72
Figure 4.9	Riboflavin production by four fungi grown on EOE after 168 hours. <i>E. gossypii</i> wild-type (ATCC 10895) (inverted red triangle), <i>E. gossypii</i> CBS 109.51 (green square), <i>E. ashbyii</i> (CBS 206.58) (yellow diamond), <i>C. famata</i> (ATCC 20850) (blue triangle) and control (black circle). Error bars are standard deviations of triplicates.	74
Figure 4.10	Riboflavin production by mutants of <i>E. gossypii</i> subjected to mutagens a) EMS, b) U.V. irradiation, c) MNNG and d) sodium azide. Black circle is 10 mins of exposure, red circle is 20 mins of exposure and green inverted triangles are 30 mins of exposure. Control lines are indicated by blue squares. A summary of the mutant riboflavin production levels is given in Table 4.7.	76

Figure 4.11	Riboflavin production by mutants of <i>C. famata</i> subjected to mutagens a) EMS, b) U.V. irradiation, c) MNNG and d) sodium azide. Black circle is 10 mins of exposure, red circle is 20 mins of exposure and green inverted triangles are 30 mins of exposure. Control lines are indicated by blue squares. A summary of the mutant riboflavin production levels is given in Table 4.7.	77
Figure 4.12	Michaelis-Menten plots of enzyme activity of a wild-type <i>E. gossypii</i> (black circle) and an EMS 30/1 <i>E. gossypii</i> mutant (red square).	79
Figure 4.13	Half-normal probability plot to indicate which of the factors were selected to be included in the model. Shapiro-Wilk p -value=0.121.	83
Figure 4.14	Pareto chart to indicate the magnitudes of positive (orange) and negative (blue) effects on riboflavin production in the eight-factor design. Bars above the Bonferroni limit are certainly significant while those above the t -value limit are possibly significant and are included in the model.	83
Figure 4.15	Box-Cox plot to determine if a mathematical transformation is required for data to fit a higher-than linear model.	84
Figure 4.16	Interactions among three factors, yeast-extract, NaCl and minerals to show increased riboflavin production.	86
Figure 4.17	Three-dimensional plot to show effect of low NaCl concentration on riboflavin production and the interaction of yeast-extract and minerals.	88
Figure 4.18	Three-dimensional plot to show effect of high NaCl concentration on riboflavin production and the interaction of yeast-extract and minerals.	88
Figure 4.19	Half-normal probability plot to indicate which of the factors were selected to be included in the model.	91
Figure 4.20	Pareto chart to indicate the magnitudes of positive (orange) and negative (blue) effects on riboflavin production in the eight-factor design. Bars above the Bonferroni limit are certainly significant while those above the t -value limit are possibly significant.	91

Figure 4.21	Interactions among yeast-extract, NaCl and minerals to show increased production of riboflavin.	93
Figure 4.22	Three-dimensional plot to show the effect of low minerals concentration on riboflavin production.	94
Figure 4.23	Three-dimensional plot to show the effect of high minerals concentration on riboflavin production.	94
Figure 4.24	Interaction between yeast extract and NaCl to show a peak riboflavin production.	97
Figure 4.25	Contour plot to show location of peak riboflavin production with varying yeast extract and NaCl concentrations.	97
Figure 4.26	A comparison of biomass production by <i>E. gossypii</i> prior to mutation (black circle), after mutation (green inverted triangle) and after statistical media optimization (red circle).	99
Figure 4.27	A comparison of riboflavin production by <i>E. gossypii</i> prior to mutation (black circle), after mutation (green inverted triangle) and after statistical media optimization (red circle).	99
Figure 4.28	Riboflavin production in a 2-litre fermenter confirmatory test using a mutated strain of <i>E. gossypii</i> and optimized growth conditions. Show are riboflavin production (yellow), biomass (blue), residual oil in medium (blue) and pH (green).	100

LIST OF TABLES

Table 2.1	Effluent discharge standards from the vegetable oils processing industry (World Bank Group, 2007) compared to a Pakistani environmental draft report on process water from the vegetable oil producing industry (Anon, 2002)	5
Table 2.2	Highest yields of riboflavin production by various microorganisms.	18
Table 2.3	Microbial products optimized by DOE and/or RSM methodologies	35
Table 3.1	Gas chromatograph and oven and injector conditions	42
Table 3.2.	Concentrations of riboflavin used to prepare standard curve to use for spectrophotometric riboflavin measurement	46
Table 3.3	Media components for determination of fungal growth on EOE	47
Table 3.4	Concentrations of variables added per litre of EOE in the first 2 ⁸ - ⁴ screening fractional factorial experiment indicating low, high and center points	52
Table 3.5	Experimental design of an eight-factor 1/16th fractional factorial, FF0816, with five center points, showing coded factor levels and randomized run order to determine effect on riboflavin production of eight medium additives to EOE	54
Table 3.6	Concentrations of variables in the second full factorial experiment indicating low, high and center points	55
Table 3.7	Experimental design of a four-factor full-fractional factorial experiment, FF0416 with five center points, showing coded factor levels and randomized run order to determine effect on riboflavin production of four medium additives to EOE	56
Table 3.8	Concentrations of variables in the central composite experiment indicating low, high and center points along with alpha values ($\alpha = \pm 1.41421$)	57
Table 3.9	Experimental design of a two-factor central-composite experiment showing coded factor levels with randomized run order to determine effect on riboflavin production of two medium additives to EOE	58
Table 3.10	Media components optimized using DOE and RSM and used to confirm predicted results.	59

Table 4.1	Colony and cellular morphologies of four fungi grown on standard Ozbas and Kutsal agar plates after seven days of incubation at 30°C.	62
Table 4.2	Gompertz parameters and resultant calculations of specific growth rates, doubling times and times of inoculation as well as fit to the curve (R^2).	66
Table 4.3	Compounds found in edible oil effluent sample	68
Table 4.4	Range and sensitivity of riboflavin detection and linear curve fitting values (R^2) calculated by Corel Quattro Pro version 13 spreadsheet for each of the standard curves.	71
Table 4.5	Gompertz parameters and resultant calculations of specific growth rates, doubling times and times of inoculation as well as fit to the model (R^2)	73
Table 4.6	Maximum rate of riboflavin production and the time interval at which they are produced in four fungi grown on EOE.	74
Table 4.7	Composite table showing best mutants of <i>E. gossypii</i> and <i>C. famata</i> after exposure to each of four mutagenic agents for three time intervals each. Characteristics are ranked within each organism grouping to find the best mutant producer	78
Table 4.8	Determination of maximum enzyme velocity (V_{max}) and Michaelis-Menten constant (K_m) of a wild-type <i>E. gossypii</i> and mutant EMS30/1 strain after non-linear curve-fitting. Also included is the goodness-of-fit (R^2)	80
Table 4.9	Eight-factor, two-level, half-fraction, resolution IV, fractional factorial design for screening of nutrients to support riboflavin production using EOE as a carbon substrate showing actual/predicted riboflavin production and residuals.	81
Table 4.10	Analysis of variance of the linear model applied to the eight-factor screening experiment, indicating also, significance of one- and two-factor interactions applied to the model. Also shown, are curvature and lack-of-fit results for the applied model	85
Table 4.11	Four-factor, two-level, full factorial design for screening of nutrients to support riboflavin production using EOE as a carbon substrate	89

Table 4.12	Analysis of variance of the linear model applied to the four-factor screening experiment, indicating also, significance of one- and two-factor interactions applied to the model. Also shown, are curvature and lack-of-fit results for the applied model	92
Table 4.13	Two-factor, face-centered, central composite design for optimization of nutrients to support riboflavin production using EOE as a carbon substrate showing actual/predicted riboflavin values as well as residuals. Alpha is set at 1.414	95
Table 4.14	Analysis of variance of the quadratic model applied to the two-factor optimizing experiment, indicating also, significance of one- two- and squared-factor interactions applied to the model. Also shown, are curvature and lack-of-fit results for the applied model	96
Table 4.15	Optimized solutions from the model generated for the two remaining factors, yeast extract and NaCl to maximize riboflavin production	98
Table 5.1	Progressive increase in riboflavin production over the various steps including mutation, screening, optimization, batch and fermenter production.	115
Table 5.2	Cost of medium and purification for riboflavin production on edible oil effluent in South African cents	116

LIST OF ABBREVIATIONS

ABE	- activated bleaching earth
ARS	- Agricultural Research Service
ATCC	- American Type Culture Collection
BOD	- biochemical oxygen demand
cAMP	- cyclic adenosine-3',5'-monophosphate
CBS	- Centraalbureau voor Schimmelcultures
CCD	- Central Composite Designs
COD	- chemical oxygen demand
CSL	- cornsteep liquor
df	- degrees of freedom
DOE	- Design of Experiments
EMS	- ethylmethane sulphonate
F-value	- Fisher's value
GRAS	- generally regarded as safe
ICL	- isocitrate lyase
MNNG	- N-methyl-N'-nitro-N-nitrosoguanidine
NaN ₃	- sodium azide
NRRL	- National Center for Agricultural Utilization Research
OFAT	- one factor at a time
RSM	- Response Surface Methodology
T _d	- doubling time
UV	- ultraviolet
μ	- specific growth rate
μ _{max}	- maximum specific growth rate
WT	- wild type

CHAPTER 1 : INTRODUCTION

South African edible oil processing plants produce approximately 3×10^5 tonnes of oil annually, with the concomitant consumption of nearly two billion litres of water. Potentially potable water entering these processing plants is either discharged to sewers as effluent or vapourised in cooling circuits (Steffen *et al.*, 1989). The effluents in the vegetable oil processing industry are produced when oils are extracted from various sources. The washing, boiling and extraction process is primarily aqueous, followed by a hexane extraction of the liquid oil. Any remaining oil is obtained by evaporation and approximately two to three tonnes of wastewater are generated per tonne of oil produced (Anon, 2002). Previous reports indicate liquid waste volumes as high as 295 tonnes of wastewater per tonne of product (Khan and Akhthar, 1998). Although the quantity and physico-chemical characteristics of the effluents produced vary considerably for different refineries, these characteristically have a high quantity of fats, oils and grease (FOG), sulphates and phosphates which causes a high inorganic and organic loading of wastewater treatment works. The wastewater usually has a biochemical oxygen demand (BOD) range of 20,000 to 30,000 mg.l⁻¹, a chemical oxygen demand (COD) range of 30,000 to 60,000 mg.l⁻¹, a high dissolved solids content of 10,000 mg.l⁻¹, oil and fats residues of between 5000 - 10000 mg.l⁻¹, organic nitrogen (500-800 mg.l⁻¹) and ash residues (Anon, 2002). These effluents with high CODs result in huge expenses as the industries pay severe fines for discharging these high COD effluents into the sewage system, resulting in a loss of profit. Thus, processes that can utilize these chemicals from the effluent can lower CODs thus decreasing disposal costs whilst increasing profits and are also environmentally beneficial. Thus it is only prudent to use this effluent for industrially viable processes.

Riboflavin (vitamin B₂) is an essential vitamin that needs to be supplemented in the diets of humans at a concentration of 1.1 – 1.3 mg per day (Food and Nutritional Board, 1998). It is a vital precursor to the coenzymes flavin mononucleotide (FMN) and flavin adenine dinucleotide (FAD). Both these compounds are co-factors of a variety of enzymes in energy metabolism, particularly the dehydrogenases and oxidases (Choe *et al.*, 2005). This vitamin is also used extensively in the animal feed industry for supplementing the diets of poultry and cattle. Although many vitamins are produced microbially, riboflavin production by microorganisms has been a particular success.

The huge market value for this vitamin, coupled to its successful microbial production, makes it an important biotechnological fermentation product (Burgess *et al.*, 2009).

Riboflavin is an excellent example of the successful application of biotechnology to produce a vitamin on an industrial scale. Approximately 4000 tonnes of this vitamin are consumed annually, and chemical and biological synthesis are both employed for its production (Adrio and Demain, 2003). Biological synthesis is preferred because it can utilize renewable resources, utilizes less energy and produces less waste but most importantly, costs approximately half that of chemical synthesis (van Loon *et al.*, 1996). Fungi are utilized primarily for production on complex carbon sources especially plant oils and secondarily because they secrete this vitamin copiously into the culture medium. Of the various fungal producers, *Eremothecium ashbyi*, *Candida famata* and *Ashbya gossypii* (*Eremothecium gossypii*) have been the most studied. Patents have been filed on production processes from simple and refined carbon sources, but there remains a large variety of cheaply available materials such as fish meal, molasses, and hog casings that have been investigated as media for riboflavin production. The possibility exists to use *E. gossypii*, *E. ashbyi* and *C. famata* on edible oil effluent (EOE) as a no-cost substrate to produce riboflavin. If the COD levels in the effluent are reduced by the fungi, which is a distinct likelihood, an effluent bioremediating technology with a valuable product will have been developed as well.

The aim of this study was therefore, to develop a novel method to produce riboflavin with the aid of fungi, using edible oil effluent as substrate, and to optimize the production thereof by statistical experimental design.

To achieve this aim our objectives were to:

- i) Establish suitable nutrient requirements of *E. gossypii*, *E. ashbyi* and *C. famata* in batch cultures using edible oil effluent as a substrate and to determine:
 - The optimum growth and maximum riboflavin production.
 - The additional supplements required in the edible oil effluent.
 - The periods during which growth and riboflavin production occur.

- ii) Having established the optimum growth parameters of the fungi, our second objective was to evaluate *E. gossypii*, *E. ashbyi* and *C. famata* for their riboflavin-producing capacity on edible oil effluent in order to select fungi for mutational improvement.
- iii) Having selected fungi producing riboflavin, our third objective was to increase riboflavin production by mutation with physical and chemical mutagens in order to select mutants that have adapted both to growth and riboflavin production on edible oil effluent.
- iv) Our fourth objective was to establish a laboratory-scale riboflavin production process using edible oil effluent, growth supplements and the selected fungus in batch culture using statistical design of experiments and response surface optimization procedures.
- v) Lastly, we endeavoured to determine the feasibility of riboflavin production from edible oil effluent.

CHAPTER 2 : LITERATURE REVIEW

Edible oil has a variety of uses in food preparation and there are 16 South African industries, run by 10 separate company groups, that produce approximately 250,000 tonnes of edible oils annually. The most commonly refined oils are sunflower, groundnut and maize but other seeds, such as cotton and soya, are also processed including fish oil and animal fat. Water usage is estimated to be between 1.75 to 2 billion litres per annum, 35% of which is discharged as effluent. This effluent has a high organic loading of fats, oils and greases and is normally treated by the various wastewater treatment plants (Steffen *et al.*, 1989).

2.1 EDIBLE OIL EFFLUENT

Effluents in the vegetable oil processing industry are produced when oils are extracted from various sources. The washing, boiling and extraction process is primarily aqueous, followed by a hexane extraction of the liquid oil. Any remaining oil is obtained by evaporation and approximately two to three tonnes of wastewater is generated per tonne of oil produced. (Anon, 2002). Previous reports have indicated liquid waste volumes of 295 tonnes of wastewater per tonne of product which is far in excess of the ratios reported in the previous study (Khan and Akhthar, 1998).

The wastewater has a high organic content and usually has a BOD range of 20,000 to 30,000 mg.l⁻¹ and a COD range of 30,000 to 60,000 mg.l⁻¹. The wastewater also has a high dissolved solids content of 10000 mg.l⁻¹, oil and fats residues of between 5,000 - 10,000 mg.l⁻¹, organic nitrogen (500-800 mg.l⁻¹) and ash residues (Anon, 2002). This effluent clearly has the ability to support microbial and, more specifically, fungal growth. Emissions levels when applying for funding to the World Bank Group for financing of an oil from vegetable sources industrial development are listed in Table 2.1.

Table 2.1 Effluent discharge standards from the vegetable oils processing industry (World Bank Group, 2007) compared to a Pakistani environmental draft report on process water from the vegetable oil producing industry (Anon, 2002)

Parameter	World Bank Group recommendations	Pakistani Environmental Report
BOD	50	450-700
COD	250	1300-2100
TSS	50	2000-16500
Oil and grease	10	100-180
Total nitrogen	10	nd
pH	6-9	11-12
Temperature increase	$\leq 3^{\circ}\text{C}$	40-50 $^{\circ}\text{C}$

Note: All values in mg.l^{-1} except for pH and temperature. nd = not determined.

In practical applications these limits are normally set by the country's local legislation and may exceed the specified limits by several fold as seen in the comparative table above (Table 2.1). Khan and Akhtar (1998) found that fats and oils, BOD, COD and suspended solids were much higher than the Pakistani National Environmental Quality Standards. They also found a discharge rate of 9.14 kg of solid waste generated per tonne of ghee and cooking oil produced. The impacts of these high oil and grease emissions to water courses is a reduction in the oxygen absorptive ability of the receiving water body and a subsequent depletion in dissolved oxygen. Photosynthesis is also affected by oil films on the surfaces of water courses that reduce light transmission. In addition, suspended and emulsified oil may be harmful to aquatic animals (Anon, 2002). Therefore, there is a requirement for treatment of the wastewater from the vegetable oil processing industry, and for a reduction in the COD and BOD of the waste oil effluent (Roux-Van der Merwe *et al.*, 2005).

2.2 RIBOFLAVIN (VITAMIN B₂)

Riboflavin is commonly known as vitamin B₂ and is a yellow-coloured, partially water soluble vitamin that is a natural component of foods containing other members of the B-vitamin complex family. It was discovered in 1920 and first isolated in egg albumin (Hoffman, 2000). It was isolated, characterised, synthesised and the structure was

determined in 1935 to be composed of a ribose sugar unit and a three-ring flavin structure known as lumichrome (Dunne, 1990). It has an empirical formula $C_{17}H_{20}N_4O_6$ and is also known as 7,8-dimethyl-10-(D-ribo-2,3,4,5-tetrahydroxypentyl)-isoalloxazine as well as 7,8-dimethyl-10-ribitylisoalloxazine. Riboflavin has a molar mass of 376.37.

In its free form it is only present in whey, urine and in the retina. In all other living cells it is found as a co-enzyme. It is necessary for metabolism in all living organisms in trace quantities, however, it is synthesised by microorganisms and not vertebrates. The inability of the human body to produce this vitamin coupled with its water soluble property, causes a loss of excess vitamin, emphasising the need for replenishment (Survase *et al.*, 2006).

Riboflavin has conjugated double-bonds and nitrogens in its ring structure (Figure 2.1) and the lumichrome portion of the riboflavin molecule emits a characteristic yellow-green fluorescence (Hoffman, 2000) which has shown absorption maxima at approximately 225, 275, 370 and 450 nm at pH 7. Cationic riboflavin (pH<4) is strongly fluorescent while neutral riboflavin is fluorescent and anionic riboflavin (pH>9.7) is weakly fluorescent. (Drossler *et al.*, 2002). Absorption in the visible spectrum either by absorbed or fluorescent light is used for detection of this vitamin (Vandamme, 1989).

Riboflavin is produced by both by chemical and fermentation processes [major producers, Hoffmann- La Roche (Switzerland), BASF (Germany), ADM (USA), Takeda (Japan)]. The current world production of riboflavin is about 2,400 tonnes per annum, of which 75% is used as feed additive and the remaining is used for food and pharmaceutical purposes. This vitamin is industrially produced mainly by two closely related ascomycete fungi, *E. ashbyi* and *E. gossypii*, (Ozbas and Kutsal, 1986; Stahmann *et al.*, 2000).

2.2.1 Structure

Riboflavin's chemical structure was determined in 1935 and it has two distinct parts: a ribose sugar unit and a three-ring flavin structure, known as the lumichrome (Dunne, 1990). This portion emits a characteristic yellow-green fluorescence and can be used for quantitative determination of riboflavin in feeds or tissues (Hoffmann, 2000). The term riboflavin was derived from the sugar alcohol moiety, ribitol, and its yellow colour (the

Latin word for yellow is flavus). Riboflavin has many conjugated double bonds and nitrogens in its ring structure, as shown in Figure 2.1.

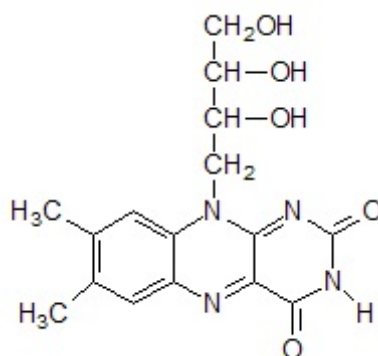


Figure 2.1 Structure of Riboflavin (Choe *et al.*, 2005)

2.2.2 Stability and solubility

Riboflavin, in its crystalline form is resistant to oxidation, even when heated in air for long periods of time. It melts and decomposes at 280°C which makes it resistant to destruction during cooking of foods. It darkens in colour at 240°C. Its decomposition is fairly rapid in alkaline solutions although it is resistant to acids of low pH. It readily decomposes when it is exposed to light and should be kept in the dark. The heat-stable, yellow-orange crystals of riboflavin are only sparingly soluble in water (10 mg per 100 ml water at 20°C) (Hoffman, 2000). This vitamin has a slight odour and a bitter taste. It is soluble in water to the extent of 10 - 13 mg in 100 ml water at 25 - 27.5°C, 19 mg in 100 ml water at 40°C and 230 mg in 100 ml water at 100°C. This vitamin is easily degradable in the presence of light and is also hygroscopic, forming lumps when moisture is absorbed (Vandamme, 1989, Takeda Vitamin and Food USA Inc., 2002).

2.2.3 Uses of riboflavin

Riboflavin acts as structural component of the coenzymes flavin mononucleotide (FMN) and flavin adenine dinucleotide (FAD). Both coenzymes catalyse non-enzymatic oxidation-reduction reactions by functioning as dehydrogenating hydrogen carriers in the transport system involved in ATP production (Dunne, 1990). Hence riboflavin is essential in cellular metabolism and respiration and particularly with regard to

carbohydrates, fats and proteins. It is also an antioxidant in that it works with glutathione reductase to produce glutathione which is a cellular protector against free radicals (Garrison and Somers, 1990). The vitamin is essential for healthy growth of skin, hair and nails and the production and regulation of hormones responsible for erythropoiesis. It cannot be stored in the body and is excreted primarily via the urine. It has to be replenished daily as a food additive in both humans and animals through the diet or supplementation. It is also necessary as a feed supplement in poultry, pigs, ruminants, horse, rabbit and fish feeds (Anon., 2002).

2.2.3.1 Clinical uses

Neonatal hyperbilirubinaemia or jaundice is commonly treated with phototherapy where infants are irradiated with light to degrade bilirubin in surface blood vessels. A side effect of phototherapy is a decrease in serum concentrations of riboflavin and tocopherol. Both these are supplied intravenously when a neonate undergoes phototherapy (Maisels and Watchko, 2000).

Migraine headache patients have been found to show mitochondrial dysfunction. A co-treatment with β blockers and riboflavin was shown to improve symptoms of migraine headaches and the authors found that β blockers and riboflavin act on separate and distinct pathophysiological mechanisms. They recommended co-treatment with these two chemical compounds because the treatment showed no additional central nervous system side-effects (Sandor *et al.*, 2000). Another study proposed prophylactic treatment of migraine with high doses of riboflavin (400 mg). They found that there was a decrease in attack frequency, headache days and migraine severity compared to the placebo group (Breen *et al.*, 2003).

Bacterial infection of blood products can be treated with a combination of riboflavin and photoinactivation using either ultraviolet or visible light. Riboflavin has been found to associate closely with bacterial nucleic acids and photoinactivation of the riboflavin has been shown to affect bacterial replication. This allows for blood and blood products to have their bacterial loadings reduced (Fung and Triulzi, 2003).

2.2.4 Riboflavin Detection Methods

Riboflavin can be measured by the following methods :

- UV Spectrophotometrically at 445 nm (Ozbas and Kutsal 1986),
- Fluorescence Spectrophotometrically at an excitation wavelength of 440 nm and an emission wavelength of 565 nm (Long, 2000) and
- Using an HPLC equipped with a Supercosil™ LC8DB column and a diode-array detector at 240 nm (Bretzel *et al.*, 1999).
- Using an HPLC equipped with fused silica microcapillaries and laser-induced fluorescence detection (Hustad *et al.*, 1999)

The variety of wavelengths used especially with regards to UV/visible spectrophotometry indicate an uncertainty with regards to the method required. Riboflavin also is poorly soluble in water although it is listed as a water-soluble vitamin and acidification was advocated for both solubilisation and stabilisation of this chemical (Long, 2000).

2.3 RIBOFLAVIN PRODUCTION METHODS

2.3.1 Chemical Production

Chemical production of riboflavin still accounts for a large proportion of industrial riboflavin. D- ribose is reacted with 3,4-xylydine in methanol with the subsequent riboside being hydrogenated to give N-(3,4-dimethylphenyl)-D-1'-ribamine. This is coupled with a phenyl diazonium halogenide, and the azo compound is cyclocondensed with barbituric acid to give riboflavin (Howe, 1957; Wolf *et al.*, 1982). The comparative disadvantages of chemical processes are :

- Aniline is found as a trace element in chemically synthesised riboflavin.
- The maximum yield is 60% generating large quantities of chemical waste.
- The process is $\pm 25\%$ more energy intensive than bacterial production.

2.3.2 Biosynthesis of Riboflavin

Riboflavin is produced in varying amounts by bacteria, yeasts and molds. Commercial production was first attempted as early as 1937 with the submerged anaerobic bacterium *Clostridium acetobutylicum* being employed in the USA and Japan. In 1940, *E. gossypii* was discovered to produce riboflavin from industrial waste products at concentrations ranging between 200 and 400 mg.l⁻¹ in a submerged aerobic fermentation with no iron

sensitivity. Steel containers could thus be used as fermenters producing beers with sufficiently concentrated riboflavin to crystallize it. The yields of *E. gossypii* were rapidly improved to between 1 and 2 g.l⁻¹ and in 1946, the filamentous ascomycete *E. gossypii* was reported to produce 1 to 1.5 g.l⁻¹. Both these molds accumulated lipid droplets within cells which were later metabolised to riboflavin and this advanced the idea of using lipids as carbon substrates for riboflavin production (Hickey, 1954).

In 1965, riboflavin was produced on a commercial scale by Commercial Solvents, Grain Processing Corporation, and Premier Malt Products. Unfortunately, they were not successful at competing with the prevalent chemical processes at the time and were shut down (Lago and Kaplan, 1981). In 1974, BASF began producing riboflavin with *E. gossypii*. BASF has run simultaneous chemical and biological riboflavin production from 1990 to 1996, after which they shut down the chemical process and are currently producing riboflavin using *E. gossypii* using a glucose supplemented substrate (Stahmann *et al.*, 2000).

The biotechnical production of riboflavin is a good example of a successful story of replacing an established chemical process with a biological one (De Baets *et al.*, 2000). When biologically-produced riboflavin entered the market in 1990, it contributed to about 5% of the global vitamin B₂ market. Today about 75% of the 4000 tonnes vitamin B₂ market is produced via the cultivation of microorganisms. A further shift towards biotechnical production of this vitamin can be envisaged (Karos *et al.*, 2004). The ascomycete *E. gossypii* is known to be a natural riboflavin over-producer. It was the first organism used in industrial large-scale riboflavin production, followed by *C. famata* and finally by *Bacillus subtilis*. A common characteristic of all three organisms is that riboflavin production is recognised by the yellow colour of the colonies (Stahmann *et al.*, 2000).

The biosynthetic pathway is summarized in Figure 2.2. The starting point is when the imidazole ring of GTP (structure 1 of Figure 2.2) is opened by hydrolysis and releases formate and pyrophosphate, which is catalyzed by GTP cyclohydrolase II. The product 2,5-diamino-6-ribosylamino-4(3H)-pyrimidinone 5'-phosphate (2 in Figure 2.2) is converted to 5-amino-6-ribitylamino-2,4(IH,3H)-pyrimidinedione 5'-phosphate (5 in Figure 2.2) by two reaction steps, involving the hydrolytic cleavage of the position 2

amino group of the heterocyclic ring and the reduction of the ribosyl side chain affording the ribityl side chain of the vitamin. The sequence of these reaction steps varies in different organisms. In eubacteria, the deamination precedes the side chain reduction. In yeasts and fungi, the reduction precedes the deamination. The 5'-Phosphate of structure 5 cannot serve as substrate for 6,7-dimethyl-8-ribityllumazine synthase. Hence, the compound must be dephosphorylated prior to further conversion. Nothing is known about that reaction step (Bacher *et al.*, 2000).

The dephosphorylated 5-amino-6-ribitylamino-2,4(1H,3H)-pyrimidinedione (6 in Figure 2.2) is condensed with 3,4-dihydroxybutanone 4-phosphate (7 in Figure 2.2) by 6,7-dimethyl-8-ribityllumazine synthase. The carbohydrate-type substrate (7 in Figure 2.2) of that enzyme has been discovered only relatively recently. It is formed from ribulose 5-phosphate (10 in Figure 2.2) by an unusual reaction involving the loss of carbon atom 4 via an intramolecular rearrangement (Bacher *et al.*, 2000).

The final step of the biosynthetic pathway is the dismutation of 6,7-dimethyl-8-ribityllumazine (8 in Figure 2.2) catalyzed by riboflavin synthase. The second product of the dismutation is 5-amino-6-ribitylamino-2,4(1H,3H)-pyrimidinedione (6 in Figure 2.2). This compound is a substrate of lumazine synthase and is recycled in the biosynthetic pathway. Stoichiometrically, the formation of riboflavin requires one equivalent of GTP and two equivalents of ribulose 5-phosphate. Of the 17 carbon atoms of the riboflavin molecule, all but four are thus derived from the pentose phosphate pool (Bacher *et al.*, 2000).

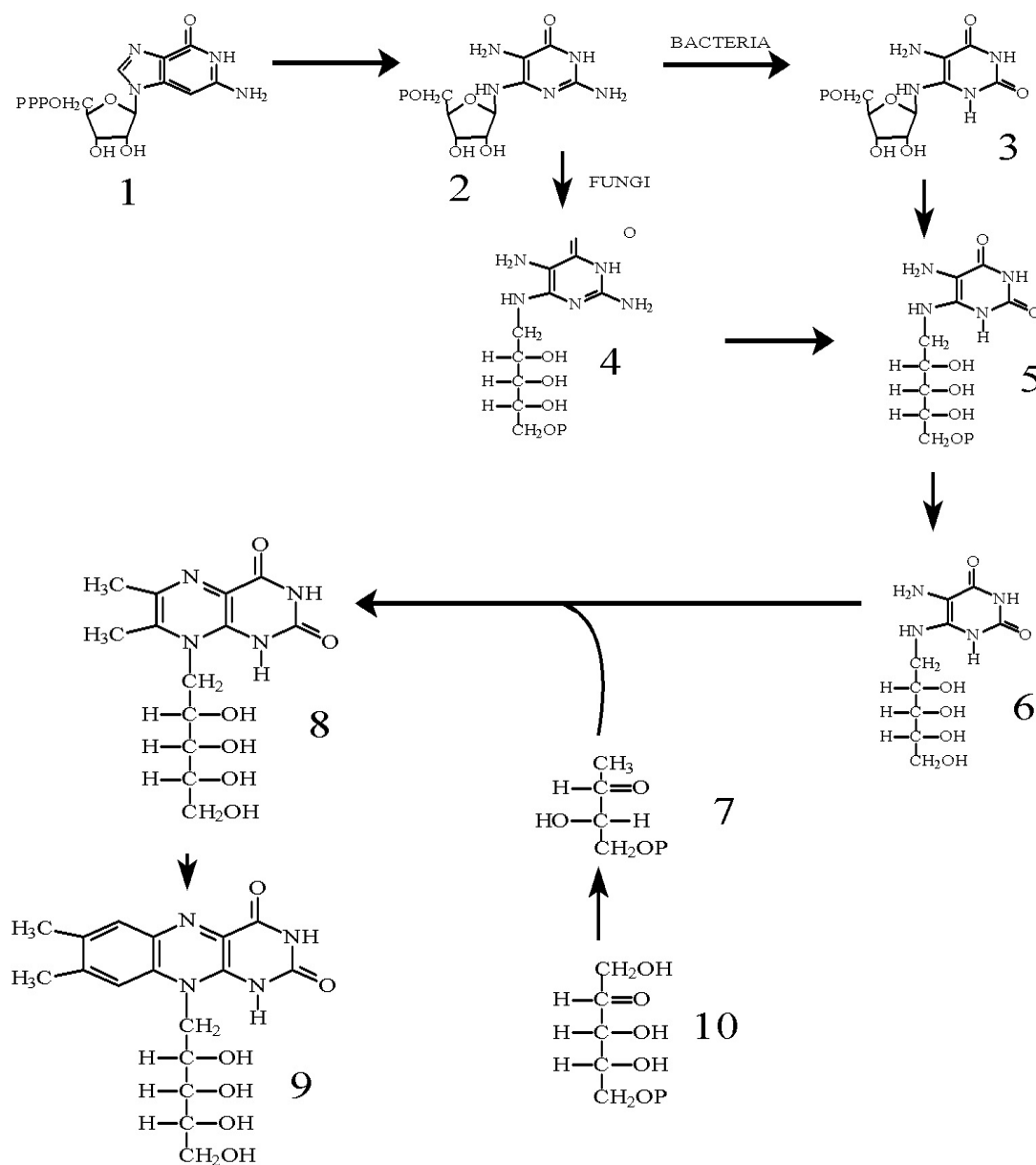


Figure 2.2 Biosynthesis of riboflavin by bacteria and fungi (Bacher *et al.*, 2000)

2.3.2.1 Bacterial producers

Like the other B-vitamins, the synthesis of riboflavin by microorganisms occurs in the rumen. Pigs, poultry and horses also have microorganisms that synthesise riboflavin, but microbial activity occurs in the caecum and the large intestine instead (Hoffman, 2000). Many laboratory strains have been investigated and these are summarized in Table 2.2.

2.3.2.1.1 *Bacillus subtilis*

Riboflavin producing bacteria are faster growing organisms when compared to the fungi. With the high growth rate particularly of *B. subtilis* and its growth-linked riboflavin production, it is susceptible to non-producing mutants (Stahmann *et al.*, 2000). Species of the genus *Bacillus* are generally regarded as safe (GRAS) and because they grow faster, they have shorter production cycles and are therefore important in industrial processes (Schallmeyer *et al.*, 2004). To obtain riboflavin production using *B. subtilis*, purine synthesis is deregulated and a mutation in a flavokinase/FAD synthetase is required. A structural analogue of riboflavin - roseoflavin, is then used for selecting riboflavin overproducing mutants of *B. subtilis* (Stahmann *et al.*, 2000).

The riboflavin synthase gene in *B. subtilis* has been found to contain an α and a β subunit, making it a bifunctional enzyme (Bacher and Milander, 1973). The authors of this paper obtained strains that were deficient in the β subunit and showed that riboflavin synthase activity is mediated by the alpha subunits whereas the beta subunits are necessary for an earlier biosynthetic step.

Sauer *et al.*, (1996) examined the metabolic fluxes in the production of riboflavin by *B. subtilis* and concluded that the oxidative branch of the pentose phosphate pathway was enhanced in the mutants overproducing riboflavin. In 1998, Sauer *et al.*, again examined metabolic pathways in *B. subtilis* overproducing riboflavin and used stoichiometric models in order to relate the various metabolic compounds in the process. They showed that purine nucleosides including riboflavin were metabolically limited in the respective pathways and that *B. subtilis* was able to reoxidise NADPH. The significance of this was that *B. subtilis* could continue the purine-pathway synthesis, and this increased the ability of *Bacillus* species to produce increased amounts of purine products including riboflavin as compared to *E. coli*.

Sauer and Bailey (1999) examined P-to-O ratio and its effect on riboflavin production. Their rationale was that increasing glucose concentration correlated to increased cell growth of mutants so energy pathways in the form of ATP had to be examined in order to increase riboflavin production in *B. subtilis*. They found that a wild-type *B. subtilis* had a P-to-O ratio of $1\frac{1}{3}$ mmol.g⁻¹.h⁻¹ ATP per unit oxygen under glucose-limited

conditions and that increasing the ratio to $1\frac{1}{2}$ mmol.g⁻¹.h⁻¹ could increase riboflavin yield by 20%.

Perkins *et al.*, (1999) engineered a *B. subtilis* strain with multiple copies of the *rib* operon at two sites in the chromosome. They also included a strong phage promoter and found that the operon was expressed constitutively. They also introduced two mutation sets into the operon, a purine analog resistant mutation and a *ribC* mutation that allowed the mutant to be analog-resistant. Their engineered organisms yielded between 6.3 and 14 g.l⁻¹ of riboflavin on various laboratory media in 14 l batch fermentations.

Bretzel *et al.*, (1999) developed a down-stream processing method for purifying riboflavin from a *B. subtilis* producer. Their process involved centrifugation, acid-washing and crystallization using concentrated HCl to produce two grades of riboflavin, a 96% feed grade and a 98% food/pharma grade of riboflavin. The purification was from two 35 m³ pilot scale batch fermenters. Their product had small amounts of riboflavin and a riboflavin precursor dimethyl-ribityl-lumazine. Importantly, their end product did not contain any DNA.

Dauner *et al.*, (2002) employed a co-feeding strategy in glucose-limited chemostat cultures in order to circumvent some of the metabolic bottlenecks in the two pathways related to riboflavin viz., the pentose-phosphate pathway and the citric acid cycle. They supplemented with gluconate, acetate, citrate and acetoin. From an energy-yield perspective, they found that none of the supplements were more energy-efficient than glucose alone in producing riboflavin but acetoin co-supplementation was able to increase yields, although not in an energy-efficient manner. Energy efficiency was calculated by a mol carbon substrate to mmol riboflavin conversion.

Wu, *et al.*, (2007) used a statistical experimental design strategy to produce riboflavin from *B. subtilis* RH44. They employed the Plackett-Burman design to screen media components and a central composite design to show relationships and optimize yield. They identified glucose, NaNO₃, K₂HPO₄ and, ZnSO₄ and MnCl₂ as important media components by their significance after the screening experiments. Optimal values of the five variables were calculated after running a central composite experiment and they obtained a riboflavin maximum of 6.65 g.l⁻¹ which was 76.4% higher than the basal

medium. They further scaled up this experiment to a 5-l fed-batch fermenter under glucose-limited conditions and produced a maximum riboflavin concentration of 16.36 g.l⁻¹ in 48 h.

2.3.2.1.2 *Other bacterial producers*

A mutant strain of *Aerobacter aerogenes* 62-1 AB was found to produce riboflavin and xanthosine from adenine, hypoxanthine, xanthine, guanine. The authors found that guanine was the primary compound incorporated into riboflavin after ¹⁴C labelling the four precursors (Bacher and Mailander, 1973).

Fuller and Mulks, (1995) isolated four riboflavin producing genes from *Actinobacillus pleuropneumoniae* and cloned them into *E. coli*. These genes were coded *RibA*, *RibB*, *RibG* and *RibH*. Their rationale for studying the pathway was not for industrial purposes but for attenuating the pathogenic *Actinobacillus pleuropneumoniae*. This avenue of research is rather dubious since metabolic inhibition can easily be reversed by environmental back mutation and a fully functional pathogen would then be the result. They did, however, manage to compare the four genes isolated to various strains of industrial riboflavin producers and pathogens and found homologies of between 58 and 73% among them.

Corynebacterium spp. have also been investigated for their riboflavin producing capabilities and Coccagn *et al.*, (1993) investigated various carbon substrates for riboflavin production by *C. glutamicum*. They grew the organism under glucose/lactate and lactate/acetate conditions and found that pyruvate accumulated in the former but not the latter case. This pyruvate overflow was assumed to be caused by the rate-limiting pyruvate dehydrogenase enzyme. This was confirmed by the lactate/acetate supplementation not showing pyruvate overflow. *Corynebacterium ammoniagenes* was investigated by Koizumi and Teshiba (1998) and they mutated strains of this organism to find that strain RK122 was able to accumulate a riboflavin precursor 6,7-dimethyl-8-ribityllumazine. They further cloned and sequenced the biosynthetic genes of *C. ammoniagenes* and found them to be significantly similar to genes in *B. subtilis*. A further study on this organism involved metabolically engineering it using a transformed strain. The strain was transformed with a plasmid containing riboflavin biosynthetic genes and the resulting mutant produced 17 times more than the wild-type. A further

investigation of the promoters on the plasmid showed a DNA fragment (P54-6) to enhance two enzyme activities viz., GTP cyclohydrolase II and riboflavin synthase. They found a 2.4 fold and 44.1 fold increase in both enzyme activities respectively. Their final strain was able to produce 15.3 g.l⁻¹ of riboflavin in a 5-l jar fermenter after 72 hours.

Enzymes from a member of the Archaea were even investigated for riboflavin synthesis. The riboflavin synthase gene from the archaebacterium *Methanococcus jannaschii* was cloned into *E. coli*, but was poorly expressed (Fischer *et al.*, 2004). These authors did, however, find a similar mechanism of action for the enzyme, that of binding two substrate molecules in an antiparallel manner. The structure of the archaebacterial enzyme was very different to eubacteria and eukaryotes. They did apparently find some eubacterial-type riboflavin synthase genes in other Archea and postulated that these may be acquired by lateral gene transfer rather than via a conserved evolutionary pathway.

2.3.2.2 Fungal producers

Primarily, riboflavin is produced by the filamentous ascomycetes *E. gossypii* and *E. ashbyi* which secrete riboflavin to the medium and are overproducers (Bigelis, 1989). Although bacteria are faster growing organisms than fungi their riboflavin production is linked with their growth rates. With the high growth rate particularly of *B. subtilis* and its growth-linked riboflavin production, it is susceptible to non-producing mutants (Stahmann *et al.*, 2000). In *E. gossypii* the risk is absent, compared to *B. subtilis*, since growth and riboflavin production are not linked. Another advantage of *E. gossypii*, *E. ashbyi* and *C. famata* is their ability to grow on plant oil as substrate. They can grow on both the liquid and solid varieties which would allow higher charging of fermenters. An advantage of *E. gossypii* over *E. ashbyi* is that it is genetically more stable than the latter, which was a major factor in its choice as BASF's producing organism. *Candida famata* has already been genetically modified to overproduce riboflavin but the product has yet to find acceptance due to its GM links.

2.3.2.2.1 *Candida famata*

Candida famata is also known as *Debaryomyces hansenii* and is synonymous with *C. flareri* (Stahmann *et al.*, 2000). Colonies of this culture are white to cream coloured with a glabrous yeast-like appearance. The yeast has ovoid cells with budding but no pseudohyphae and does not possess a capsule. It is a common environmental isolate and

is rarely pathogenic making it a good candidate for industrial development. Heefner *et al.*, (1992) have lodged a patent on behalf of Zeagen Inc., identifying *C. famata* as a riboflavin overproducer and claiming to have produced 20 g.l⁻¹ in 200 hours. They developed the overproducing strain by mutation and selection using a purine riboflavin analogue, tubercidin. Their strain was also reported to have come from a combination of two ATCC strains, viz., ATCC 20849 and 20850. Although they make mention of iron inhibiting flavogenesis in their strain, they go on further to say that their patented strains can produce high concentrations of riboflavin with elevated iron concentrations.

Yatsyshyn, *et al.*, (2009) attempted to metabolically engineer *C. famata* to produce FMN. They used a gene cassette including the *FMN1* from the yeast *Debromyces hansenii* and a promotor *TEF1* from *C. famata*. The resulting plasmid was transformed into and expressed in a strain of *C. famata*. They reported that their transformed strain produced a 30-fold increase in riboflavin kinase activity and 400-fold increase in FMN production. However, the quantities they reported produced were very small, in the region of 200-250 mg.l⁻¹. They did show that it was possible to transform the cell and overcome metabolic bottlenecks for the production of riboflavin.

2.3.2.2.2 *Eremothecium gossypii*

Eremothecium gossypii, a filamentous ascomycete, was first isolated as *Nematospora gossypii* by Ashby and Nowell in 1926 as a plant pathogen causing stigmatomycosis on cotton plants and other citrus fruits (Wendland and Walther 2005). It was renamed *Ashbya gossypii* by Guilliermond in 1928 and was also called *Ashbia gossypii* by Ciferri and Frago in 1928 (Kurtzman and Fell, 1998), before being renamed *Eremothecium gossypii* by Kurtzman in 1995 based on rDNA sequence analysis (Kurtzman, 1995). It is able to overproduce riboflavin (Maeting *et al.*, 1999) and it was the first microorganism to be used in the industrial production of riboflavin (Kato and Park, 2006). On Yeast-malt extract agar, it produces tan colonies with yellow pigmentation. Colonies are smooth or finely floccose, moist, wrinkled at the center and have a sharp lobed margin. Hyphae are branched and some cells may contain needle-shaped riboflavin crystals. Asci containing between 12 and 32 ascospores in parallel packets, are clavate to fusiform and disarticulate at maturity to produce individual ascospores. Ascospores are needle- or spindle-shaped and measure 2-3.5 μ m. They may produce terminal filiform appendages that are slimy and thus bind ascospores into small groups. *Eremothecium*

gossypii appears to be homothallic (Kurtzman and Fell, 1998). The highest production of riboflavin by various bacteria and fungi is summarised in Table 2.2.

Table 2.2 Highest yields of riboflavin production by various microorganisms.

Bacteria	Titre (g/L)	Authors
<i>Bacillus subtilis</i>	15	(Sauer <i>et al.</i> , 1998)
<i>Rhizobium</i> sp (GRH28)	14×10^{-6}	(Sierra <i>et al.</i> , 1999)
<i>Corynebacterium ammoniagenes</i> pFM76	15.3	(Koizumi <i>et al.</i> , 2000)
<i>Lactococcus lactis</i> (pNZGBAH)	24×10^{-3}	(Burgess <i>et al.</i> , 2004)
<i>Leuconostoc mesenteroides</i>	5×10^{-4}	(Burgess <i>et al.</i> , 2006)
Fungi		
<i>Eremothecium gossypii</i>	15	(Bigelis, 1989)
<i>Eremothecium ashbyi</i>	15	(Bigelis, 1989)
<i>Candida famata</i>	20	(Heefner <i>et al.</i> , 1992; Stahmann <i>et al.</i> , 2000)
<i>Candida boidinii</i>	0.09	(Suryadi <i>et al.</i> , 2000)
<i>Pichia guilliermodii</i>	14.4	(Leathers and Gupta, 1997)

Riboflavin yield improvements in *E. gossypii* were initially achieved by random mutagenesis and colony colour screening which was followed by antimetabolite screening after multiple rounds of mutagenesis. Genetic manipulation by introducing genes and triggering gene activity has further enhanced riboflavin production although genetically manipulated strains are not used in industrial production. A split between growth and riboflavin production can be recognised by the profiles in Figure 2.3 and this allows for separate manipulation of genes associated with growth and riboflavin production. The mRNA samples were analysed by Karos *et al.*, to study transcriptional regulation during biomass and riboflavin production phases (Karos *et al.*, 2004).

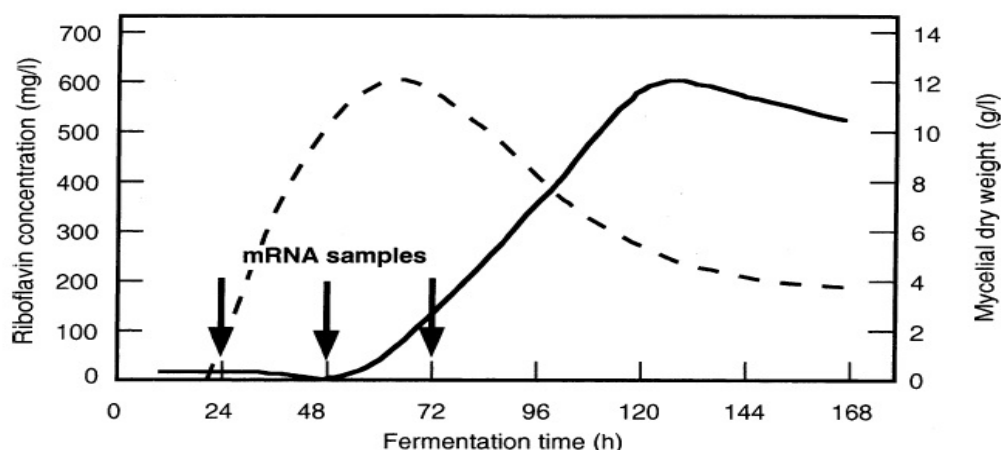


Figure 2.3 Riboflavin production in *E. gossypii* showing relationship between growth (dashed line) and riboflavin production (solid line). mRNA samples were for study of transcriptional regulation (Karos *et al.*, 2004).

Tanner *et al.*, (1949) investigated low-cost media and culture conditions for riboflavin production using *E. gossypii*. They found a narrow temperature range of 26 to 28°C to be optimum for riboflavin yields with maximum production in the 6.0 to 7.0 pH range. Above 28°C, yield was sharply decreased and starting pHs of between 4.5 and 5.5, although providing good cellular multiplication, did not give maximal riboflavin yields. Starting pH is thus an important factor in the production process. Since *E. gossypii* possesses little saccharifying power they found that starches and pentoses were not suitable for this organism's growth. Rather, they found glucose as the most adequate carbohydrate for growth. They also proposed corn-steep liquor as a substitute for yeast extract which was used as a nitrogen source. They also investigated times of sterilization to release riboflavin from the mycelia after growth and found a time of 30 minutes to be the most appropriate autoclave time to release bound riboflavin. They produced riboflavin at 1050 mg.l⁻¹ in shake-flasks and 1060 mg.l⁻¹ and 1420 mg.l⁻¹ in parallel 30 l batch fermentations. These were obtained using a 4% glucose and 0.25% peptone medium.

Ozbas and Kutsal, (1986) compared production of riboflavin between *E. gossypii* and *E. ashbyi* using combinations of simple and complex carbohydrates. They found that *E. ashbyi* gave highest yields of riboflavin with a combination of glucose (5 g.l⁻¹) and sunflower oil (15 g.l⁻¹). The maximum titre obtained when using *E. ashbyi* was 1.84 g.l⁻¹. They also tested whey as a substrate and found that *E. ashbyi* was able to produce more

riboflavin (1.36 g.l^{-1}) on it than *E. gossypii* (0 g.l^{-1}) and the reason they advanced was that *E. gossypii* lacks the necessary enzymes to break lactose down into its monomer components to utilise it as carbon source.

Ertrk *et al.*, (1998) used whey as a substrate for riboflavin production with *E. gossypii* and added various supplements. Of the six supplement combinations that they used, they found that whey supplemented with bran was able to produce the highest amount of riboflavin after an incubation period of eight days. This was four times higher than their whey-only medium. Also, when scaling up from flasks to a fermenter, they were able to increase riboflavin production four-fold to a maximum of 1227 mg.l^{-1} after an eight-day incubation period.

Stahmann, *et al.*, (2001) examined the protective ability of riboflavin on spores of *E. gossypii*. They postulated that it is a spore protective response to ultraviolet light. They found that spores of both *E. gossypii* and *Aspergillus nidulans* were more resistant to UV light in the presence of riboflavin. They further examined sporulation and riboflavin production in *E. gossypii* using cyclic adenosine-3', 5'-monophosphate (cAMP) to inhibit spore production and found that both sporulation and riboflavin overproduction stopped in the presence of cAMP. Further, they examined the growth phase in which riboflavin was produced and found that it was a secondary metabolite. Contrary to other findings, they determined that glucose limitation did not trigger riboflavin production but exhaustion of amino acids and other unquantified compounds in the yeast extract led to a decrease and cessation in growth with a subsequent overproduction of riboflavin. Riboflavin was thus overproduced as a secondary metabolite and they concluded that riboflavin was a mechanism for protecting spores against UV light.

Park *et al.*, (2007) used vegetable oil as a carbon source to produce riboflavin by *E. gossypii*. They examined isocitrate lyase activity and identified it as a key enzyme in riboflavin production. They then mutated *E. gossypii* and produced a strain ZP4, that produced riboflavin at a concentration of 8.7 g.l^{-1} after five days with rapeseed oil as a carbohydrate source and activated bleaching earth (ABE) as a support medium. They batch-fed their culture with 50 g.l^{-1} of rapeseed oil at the start of incubation and 25 g.l^{-1} after 36 hours. The production rate from the oil consumed was 0.13 g.g^{-1} . They postulated that the ABE provided a larger surface area for the mycelia to grow upon and

degrade oil. They also advanced the theory that the charged ABE particles play a role in increasing riboflavin production.

2.3.2.2.3 *Eremothecium ashbyi*

Eremothecium ashbyi is also a filamentous ascomycete, isolated by Guilliermond, that has been used in the production of riboflavin. It was previously known as *Spermophthora gossypii* and *Crebothecium ashbyi* before being named *Eremothecium ashbyi* by Guilliermond in 1935 (Kurtzman and Fell, 1998). They form tan colonies on Yeast-malt extract agar but later as they excrete riboflavin into the medium the colonies turn yellow. Colony surfaces are initially smooth and develop deep radial furrows as the organism grows with a sharply lobed margin. Hyphae are dichotomously branched, sparingly septate and asci are ellipsoidal to fusiform containing 8-16 ascospores. Ascospores are evenly distributed in the ascus and appear hyaline, narrow and sickle-shaped with a rounded tip at one end and a basal spine at the other (Kurtzman and Fell, 1998).

Osman and Chenouda, (1965), grew *E. ashbyi* on a glucose medium and found that riboflavin was produced when the carbon source was depleted. They also found that total nitrogen and lipid content of the mycelium decreases when riboflavin is being produced. This led them to postulate that cell reserves are redirected to riboflavin production.

Kolonne *et al.*, (1994) showed the effect of pH on riboflavin production by this organism in an airlift and a stirred-tank bioreactor. Their findings indicated that this organism preferred a constant pH of between 4.5 and 5.5 in the airlift reactor and a pH of 4.5 in the stirred tank in order to maximally produce riboflavin. Kalingan and Krishnan, (1997) supplemented growth of *E. ashbyi* with various plant seed extracts with a molasses, peanut-seed oil medium base. They found that seeds of *Eriodendron anfractosum* (cotton plant) increased riboflavin by 10% compared to their controls. They were unable to advance concrete reasons for this increase and assumed that the seeds were providing amino acids or vitamins to stimulate riboflavin production in this organism. Kalingan and Liao (2002) determined the suitability of various low-cost organic wastes as substrate using *E. ashbyi* to produce riboflavin. They found hog casings and fish meal substrates combined and used as flavinogenic stimulants provided a maximum yield of riboflavin in a medium containing molasses and peanut seed cake as carbon and nitrogen sources respectively.

2.3.3 Other Microorganisms

Apart from *Bacillus subtilis*, *Escherichia coli* is the second most chemically characterised microorganism for riboflavin production (Fuller and Mulks, 1995). *Corynebacterium ammoniagenes* has also been investigated for riboflavin production and a recombinant strain has been found to accumulate 17-fold as much riboflavin as the host strain (Koizumi *et al.*, 2000)

2.4 INDUSTRIAL RIBOFLAVIN PRODUCTION METHODS

Little is known about proprietary methods and most reviews on aspects of riboflavin production do not include any specific information on the scale, productivity and downstream processing for recovery of riboflavin. The following is information obtained from various patents by the companies producing riboflavin industrially.

2.4.1 Patents for Riboflavin Production Processes

Coors Biotechnology of the U.S.A. used a strain of *C. famata*, most likely ATCC 20849 or a mutant thereof to produce riboflavin from a fed-batch process feeding both glucose (up to 5 g.l⁻¹) and glycine at various intervals. They mutated the strain previously with NTG and were able to isolate one with increased copper resistance. They were also able to grow this culture in a diphasic continuous process, with a feeding scheme for biomass production where glucose feed was limited and the dilution rate of the process was controlled to give a specific growth rate of 5% (0.09 to 0.11 h⁻¹) of the U_{max} . This, they claimed, encouraged the microorganism to produce more riboflavin when fed with glucose and glycine during secondary production. With this process, they were able to produce riboflavin at a rate of 0.17 g.l⁻¹.h⁻¹ to a final maximum concentration of 19.5 g.l⁻¹. They also maintained pH between 5.0 and 7.5 and used ammonium sulphate as their nitrogen source. No indication of the scale of production was given and no indication of extraction or purification methods were given in this patent (Bailey, *et al.*, 1992).

Ajinmoto Corporation of Japan described a process of producing riboflavin using an NTG induced mutant of *B. subtilis* AJ12644. They used a batch fermentation process with a starting glucose concentration of 80 g.l⁻¹ and additional 10 g.l⁻¹ glutamate. They reported production of 1.05 g.l⁻¹ of riboflavin with pH controlled at 6.5 using ammonia and an incubation temperature of 34°C after 16 hours. They further reported a purification

process using heating and hydrosulphite which precipitated the riboflavin. This was then recovered by centrifugation and further purified by solubilising in 1N acetic acid and oxidation using potassium permanganate to produce a precipitate of 560 mg of pure crystals. This was done with a 5 l starter volume in a fermenter. No indication of a scaled-up process was given (Usui *et al.*, 1994)

Archer Daniels Midlands Company of the USA filed a patent for a *C. famata* strain that produced 10 g.l⁻¹ riboflavin from a starting glucose concentration of 60 g.l⁻¹ and additional glycine once the glucose was depleted. The unique method of isolation of a mutant was described in this patent and this was the use of a pre-depleted medium at 50% concentration to isolate NTG-induced mutants that produced riboflavin. The selective agent in the medium was tubercidin. No indication of any form of process scale-up was given (Heefner *et al.*, 1994)

CJ Corporation filed a patent using a mutated strain of *B. subtilis* (KCCM 10446) that was able to tolerate a high concentration of threonine analogue DL-beta-hydroxynorvaline. This organism was also reported to produce up to 26.5 g.l⁻¹ riboflavin which was 18.4% higher than the parent strain. The organism was grown on a complex medium comprising among other components 30 g.l⁻¹ molasses and 15 g.l⁻¹ CSL. The production medium comprised among others, an absence of molasses with glucose at 26.7 g.l⁻¹ as carbon replacement and an equivalent amount of CSL. No further scale-up was described (Lee *et al.*, 2006).

2.4.2 Riboflavin Purification after Fermentation

The first riboflavin purification process from organic sources such as beef liver, egg yolk and milk is described by Pasternak and Ellis in 1943. A second industrial recovery process, this time from fermentation broths utilizing *E. gossypii* to produce riboflavin was patented by Morehouse in 1958, from a fermenter with a volume of 45,5 kl producing approximately 50,000 g of riboflavin of which 91.4% was recovered by adjusting the pH to 4.5, boiling at 100°C for 30 minutes before filtering through a leaf-type filter. The crystallized riboflavin was blown off the mycelium with hot air and was 79% pure. The remaining beer was treated with sodium hydrosulphite and adjusted to pH 11, after which the solubilised riboflavin was oxidised by bubbling oxygen through the solution for 30 minutes. The solution was adjusted to pH 6.5 with sulphuric acid and the riboflavin

crystallized from solution which was then recovered by filtration and drying at 93°C. This riboflavin was 87% pure. The overall recovery rate was 95% from the fermentation broth.

The Morehouse method was said to have shortcoming in that it cannot recover the majority of riboflavin since it solubilises riboflavin by heating and this method is not suitable for concentrations greater than 1 g.l⁻¹. Coors Biotechnology Incorporated developed a purification process that involved an alkaline solubilisation at a pH of between 12.4 and 12.8 in the presence of at least 50% oxygen as a riboflavin oxidant bubbled into the solution. The solution was also heated to 25 to 30 °C. This solubilised riboflavin was separated from cells and debris using ultrafiltration to ensure purity of the final product. The solubilised riboflavin was then precipitated by bubbling oxygen to oxidise it at a pH of 5.8 to 6.2. The resultant riboflavin crystal slurry was recovered by rotary vacuum filtration to a 96% purity (Gyure and Lauderdale, 1992).

2.5 RIBOFLAVIN OVERPRODUCTION MECHANISMS

2.5.1 Genetic Pathway

Random mutagenesis and genetic engineering improves the productivity of the organism and allows for industrial application (Stahmann *et al.*, 2000). The key factor to a successful biotechnical process is strain development. *Eremothecium gossypii* has been used for over a decade in the biotechnological production of vitamin B₂ and strain improvement is ongoing. Along with the improvement of *E. gossypii* strains, many different approaches have been used to enhance productivity. Random mutagenesis followed by screening by colony colour were the main strategies, followed by the use of many different antimetabolites in combination with several rounds of mutagenesis. The introduction of gene technology in the strain development process made the changing of methods possible for further improvement. Today it is still possible to further enhance productivity by introducing genes or triggering gene activity. For a better understanding of gene activity during riboflavin biosynthesis, Karos *et al.* (2004) took advantage of the characteristic behavior of *E. gossypii* fermentation, and showed that a split between the growth phase and the production phase in a typical *E. gossypii* fermentation can be recognised and therefore a differentiation between the genes responsible for growth and riboflavin production can be made.

2.5.2 Regulatory Mutants

The role of the glyoxylate pathway has been elucidated in the production of riboflavin by *E. gossypii* and it is thought that this pathway is essential for the metabolism of complex substrates such as plant oils and lipids (Stahmann *et al.*, 1997). These are degraded to fatty acids and glycerol and are considered precursors for the production of riboflavin in *E. gossypii* (Maeting *et al.*, 1999). The subsequent conversion of these two precursors via gluconeogenesis to riboflavin via the glyoxylate pathway provides an indication that the enzyme isocitrate lyase (ICL), also known as isocitratase, plays an important role in riboflavin metabolism. This enzyme catalyzes the cleavage of isocitrate to glyoxylate and succinate.

Mutational studies to deregulate ICL in order to improve riboflavin production have involved the suppression of its activity by mutagens such as ethylmethane sulphonate and a correlation has been found between the activity of this enzyme and riboflavin production in *E. gossypii* (Schmidt *et al.*, 1996). The authors found that this enzyme is repressed by glucose, derepressed by glycerol and induced by soybean oil. Deregulation and monitoring of this enzyme's activity is thus an important consideration in metabolism of complex carbon sources.

2.5.3 Nutrient Supplements

Since complex carbon sources may be lacking in some supplementary nutrient requirements, several supplements have been used in the production of riboflavin, the earliest attempt of which was by Tanner *et al.*, (1949), who investigated the production of riboflavin by *E. gossypii* with glucose at a starting concentration of 2-3% and they found riboflavin production to be between 340 and 365 mg.l⁻¹. They also found that corn-steep liquor was an adequate replacement for yeast extract but they were unable to find a lower-cost replacement to peptone having tried various beef, and fish waste liquors. They also tested inoculum growth times and showed that a 24-hour inoculum far exceeded riboflavin production than older inocula. Lastly, they found that an autoclave time of 30 minutes after incubation produced the highest amount of riboflavin in the medium and they suggested acidifying with 1N HCl or a pH 4.7 acetate buffer before autoclave extraction.

Ozbas and Kutsal, (1986) compared the varying factors on the growth of *E. gossypii* and *E. ashbyi* and their subsequent production of riboflavin. Their assessment of pH found that both fungi produced u_{\max} and highest rates of riboflavin production at pH 6.5. A temperature of 30°C was found to produce u_{\max} in both fungi as well and they further went on to determine carbohydrate combinations that produced the highest amount of riboflavin. From glucose, sunflower oil, glycerol and whey, and various combinations of these carbon sources, they found the most efficient combination to be glucose : sunflower oil in the ratios 10 g.l⁻¹ : 10 g.l⁻¹ for *E. gossypii* and 5 g.l⁻¹ :15 g.l⁻¹ for *E. ashbyi*. Quantities produced were in the region of 1.76 g.l⁻¹ for *E. gossypii* and 1.84 g.l⁻¹ for *E. ashbyi* from an initial total of 20 g.l⁻¹ carbon source which gives a carbon to riboflavin conversion percentage of 8.8% and 9.2% respectively.

In subsequent experiments Ozbas and Kutsal, (1991) investigated the effects of inositol, D(+)-biotin and thiamine on riboflavin production by *E. gossypii*. They found that when doing a one factor at a time experiments, that the optimum meso-inositol, biotin and thiamine concentrations were 0.5 g.l⁻¹, 0.4 ug.l⁻¹ and 0.04 g.l⁻¹ respectively. However, when tested with a glucose, sunflower oil medium, the additives decreased the riboflavin yield from 1.496 g.l⁻¹ to 1.131 g.l⁻¹. No further experiments were conducted to determine the factors contributing to the negative effect on yield of riboflavin.

Ertrk *et al.*, (1998) used a whey carbon source and supplemented it with bran, soybean flour, glycine+peptone and sucrose. They grew *E. gossypii* and measured riboflavin production over eight days in shake-flasks and a fermenter. Their best combination of carbon/supplement was whey/bran in a fermenter to give a yield of 1.23 g.l⁻¹ after eight days which was four times greater than in flask experiments. The addition of glycine+peptone produced 0.4 g.l⁻¹ of riboflavin, which was unexpected as glycine is a riboflavin precursor. They postulated that better oxygen transfer was the reason for better performance in the fermenters when comparing fermenters to flask cultures.

Elucidation of the riboflavin pathway has pointed to key components in the metabolic chain that can be used as supplements (Jiminez *et al.*, 2005). Overproduction of riboflavin by *E. gossypii* and *C. famata* can be achieved by supplementing the medium with precursors of GTP, the first metabolite of the riboflavin production pathway (Stahmann *et al.*, 2000).

2.6 EXPERIMENTAL DESIGN FOR PROCESS OPTIMIZATION

The two primary bottlenecks in empirical problem-solving are time and resources (Haaland, 1989). The one factor at a time (OFAT) strategy is both time-consuming due to its iterative nature and resource-intensive due to the duplication involved in repeating experiments with step-wise factor variation. Also, one-factor experiments do not elucidate interactions among the various other factors that affect the complex biological processes and their fermentation surroundings. Due to these drawbacks, a more holistic approach to bioprocess problem solving was needed that provided faster optimization and clearer understanding of synergistic effects of factors. The other two strategies, matrix design and factorial design are largely ignored, the former, because of the high experimental numbers leading to high cost and time implications and the latter, because of traditional resistance and poor understanding (Anderson and Whitcomb, 2000).

2.6.1 Strategies for Problem Solving

A strategy for problem-solving used in the science and engineering industry is statistical experimental design. Its advantage over both matrix and OFAT design strategies is cost and time. Its primary disadvantage is a loss of some resolution within the design space. The statistical experimental design strategy has not been employed widely in biotechnology partly due to few biological examples being available. However, a few researchers have attempted to adapt this strategy for problem solving using biological systems and this section will discuss them.

2.6.2 Clear Signal Designs

In order to employ this strategy, the practice of clear-signal designs needs to be applied to biological systems. These are designs developed by statisticians to incorporate more than two factors into an experiment and differentiate whether the factors have a clear effect or are part of the background noise. The additional benefit is that they can also measure the effects and rank them in order. This is helpful in selecting a direction for further designs in that, effects due to noise can be dropped or set at low values if necessary, and highly significant effects can be further optimized using further experiments. Thus, signals are separated from the background noise and signals can be clearly distinguished from each other (Haaland, 1989).

The most commonly used tool in differentiating effects is the pareto chart. It lists, as a histogram, effects and their magnitudes and may include statistical reference lines to indicate factor significance. Included in the pareto chart are significance lines (in the Design Expert 7.1.6 software package); the t-value of effects and the Bonferroni limit. Effects lying above the t-value of effects line are significant and those above the Bonferroni limit, a more stringent test for significance of effects, are definitely significant (Statease, 2007).

2.6.3 Design Types

Typically, when considering several factors, the most common experimental choice is one called a factorial experiment. This allows for factors to be set at two levels (low/high) and for their individual effects and possible interactions to be elucidated. A general equation for determining the number of experiments needed for a full factorial experiment would be $n=2^k$ where k = number of factors. From this, it can be seen that increasing the number of factors will exponentially increase the number of experiments. In order to bring the number of experiments to a manageable level, and investigate several factors as well, fractions or fractional factorial experiments are utilized. These have the general equation $n=2^{k-p}$ where p = natural number that determines the $k-p/k$ fraction of the experiment. This would allow an experiment to be run in half the number of runs or a lesser fraction (Anderson and Whitcomb, 2000).

A fractional factorial experiment loses fidelity in that some interactions may be aliased with others, losing the ability to differentiate amongst them. This is termed a loss of resolution, and fractional factorial experiments are graded according to their resolutions. A resolution IV experiment is generally accepted as the lowest level at which biological experiments may be conducted for screening of effects although lower resolutions may be used. This implies that one and three-factor interactions would be aliased. However, when screening for individual effects this resolution of experiment is sufficient to differentiate single factors from one another and even two-factor interactions. Resolution IV experiments usually decrease experimental runs by up to a quarter of their full-factorial counterparts, i.e., a 12-factor screening experiment requiring 128 runs may be done in as little as 32 runs (Haaland, 1989). Resolution V experiments are almost as good as full-factorial experiments with all main effects and two-factor interactions being resolved. The benefit is that a resolution V experiment can be achieved using a smaller

number of runs than a full-factorial experiment. In addition, two-factor interactions can be resolved from other two-factor interactions which is not possible in resolution IV experiments (Statease, 2007).

A further consideration in factorial experiments is center points. These set the factor usually at the center of the minimum and maximum values. These are replicated three (Haaland, 1989) or five times (Anderson and Whitcomb, 2000) and sometimes more. The reasons for this replication is to estimate the standard errors of the design points and to determine the inherent standard error of the experiment. Failure to include center points in the design would not allow estimation of standard error as mentioned previously.

Other design types include the Plackett-Burman and Taguchi design sets. Plackett-Burman designs were set up in the second world war, by Robin Plackett and Peter Burman to develop proximity fuses for anti-aircraft shells. They were set up to fill gaps in fractional factorial experimental designs whose number of runs n are usually in powers of 2, that is, 4, 8, 16, 32. . . . and as the number of runs increase, so to do the gaps between the numbers. Plackett-Burman designs were available as multiples of 4, that is n is 12, 20, 24, 28, 36 . . . runs (Box *et al.*, 2005). These are low-resolution designs and assume no interaction between factors or the pairwise factors will be aliased to the single factors. Taguchi designs explore main effects and no interactions. They should be used with care in biological systems where interactions often exist and experimenters are advised to explore factorial designs as alternatives to Taguchi arrays (Statease, 2007).

2.6.4 Optimizing Designs

Fractional factorial experiments only elucidate the magnitudes of effects and possible interactions. The optimization of those interactions can be done using space filling designs, one of which is the central composite model. This design type allows five instead of three levels to be investigated around a focused point where an optimum is expected. The ideal is to narrow down factors in fractional-factorial experiments to two or three factors before attempting this type of optimization. Since these experiments involve five levels and center points, more than three factors make the number of runs very large. A two-level central composite would give a face-centered design and a three level central composite would give a rotatable sphere design. Both these designs encompass the design space sufficiently to allow prediction of optima. The mathematical

models developed here, can be used to minimise or maximise the required result whilst predicting the levels of each of the factors (Anderson and Whitcomb, 2005).

Once a design is set up and data is inserted into the relevant tables, checks can be made on the data to determine its validity. Firstly, the maximum quantity produced, in this case riboflavin, can be determined and it should be greater than previous experiments. Secondly, center points, which are three to five or more replications of an experiment at a central point, should yield similar results. Thirdly, the ratio of maximum to minimum response would give an indication of whether data responses can be described using a linear model or if data transformation is required. Usually, a maximum to minimum ratio of less than 10 indicates a linear relationship between response and parameters. Greater than 10 would then require an interactive transformation to determine the best fit of the response data to descriptive models. A square-root or natural log transformation of data is often sufficient to fit descriptive models. Higher transformation formats very often would indicate that response data are suspect, and that an experiment or parts of the experiment need to be repeated (Box *et al.*, 2005).

On the issue of center points; orthogonal designs require this to estimate the error at each node of the design. Since each node is not replicated, the center point serves as the estimation of error at the center of the design. The rationale for this is that variability is inherent in the experimental setup and this variability will be replicated at any node of the design. Also, center points, because they are replicated, serve to indicate whether the experimental method applied is sound or not. Hence, center points essentially serve two purposes; a means to estimate error and a quality check for the experimenter's accuracy (Box *et al.*, 2005).

2.6.5 Estimating Effect Magnitude and Data Transformation

The effects of each variable are then estimated and this entails subtracting the effect of the sum of values of each variable set on high from the sum of values of each value set on low. In this manner, a variable can have either a positive or negative effect on the outcome. In media optimization, effects of media components can be determined on fermentation products such as riboflavin and extraneous factors such as temperature and agitation rates can also be estimated. Normal plots, which are plots of residuals, can be used to determine the magnitudes, directions and deviations from the normal, of effects.

Half-normal plots usually show negatively directed effects as positive, allowing the experimenter to view the magnitudes of both positive and negative effects on one axis. Effects can be conveniently plotted onto a pareto chart which gives the magnitude and direction of effects on outcomes in a convenient bar chart. Variables with highest effects can then be selected to be included in a mathematical model to describe data. The model could then be used to illustrate the interaction among effects and to explore the design spaces between experimentally set data points (Montgomery, 2005).

Once choices are made for transformation or not, data is fitted to the selected model and its fit to the best mathematical description of the model is statistically estimated. An ANOVA between the model and its predicted value is conducted to determine whether each factor fits the model and the overall fit of the model to all selected data points. Probability of fit is set at $p=0.05$. Effects that are significant are included in the model to generate the resultant mathematical equation to describe a dataset.

Data sometimes do not fit a linear model and need to be transformed. A logarithmic or power transformation is usually applied. If transformation of a dataset to fit the model is required, a Box-Cox plot is used to assess the validity of the currently applied transformation and to indicate both the need for a transformation and the possible transformation required. (Montgomery, 2005). Design Expert 7.15 offers the option to assess several model types on a dataset and suggest the most likely one to fit data.

The suggestion is based on the correlation of data to the models applied via a correlation coefficient. The correlation coefficient used is Pearson's' least-squared correlation coefficient r^2 and the associated adjusted- r^2 which is the correlation coefficient adjusted for the number of observations in the data compared to the number of observations in the selected design (Anderson and Whitcomb, 2000).

For fermentation supplements, individual factor interactions are often not investigated in one-at-a-time experiments. In Design of Experiments (DOE), interactions and their magnitudes are identified on the normal plots or pareto chart and their directions and significance can be visualised using interaction plots. Two interactions can be investigated in this way. Three interactions can be investigated with box plots. Three-dimensional plots and contour plots can be used to visualise the direction of the

interactions and, subsequently point to the direction following experiments should take (Anderson and Whitcomb, 2000).

After screening experiments when important components are identified and unimportant ones are either set at a concentration or omitted, response surface methodology (RSM) can be applied to optimize important factors. Central composite designs (CCD) are a subset of DOE that allow investigation of the few important factors and optimization of the effect they have. If two chemical compounds have an effect on a fermentation product, their interaction can be mapped with contour plots and “sweet-spot” can be found in the experiment to optimize the product. A face-centered central-composite design is the most often used type of CCD. This design type can handle two or three factors and extends the design parameters over five points to map a surface interaction (Anderson and Whitcomb, 2005).

Again, data is analysed with both R^2 and ANOVA to determine its fit to a selected model. The quadratic transformation of data is usually selected but other transforms are possible to fit data to mathematical equations (Anderson and Whitcomb, 2005). A quadratic equation would normally yield curved data surfaces and these can be of the classical peak, saddle or often the rising ridge forms seen in biological optimizations. These indicate the peaks and directions required by factors to obtain them. An example of the general form of the quadratic model construct is given in equation 1.1.

$$Y = b_0 + b_1X_1 + b_2X_2 + b_{11}X_1^2 + b_{22}X_2^2 + b_{12}X_1X_2 \quad (1.1)$$

Where Y is the response, b_0 the regression coefficient and X_{ij} the factors and (b_{ij}) their coefficients.

Coefficients are calculated as half of the effect and the independent regression coefficient is calculated as half of the sum of effects (Montgomery, 2005).

Simple mathematical reductions of the quadratic model would yield solutions to the peak points that are give as point predictions in Design Expert 7.1.6. Point predictions in this programme are given along with a confidence interval of 95% to indicate the expected range of optimization. These can be examined to see which factor conditions would best fit the experimental conditions and the best yielding point prediction can be confirmed in a series of confirmatory tests.

The overall strategy of experimentation is summarised in Figure 2.4.

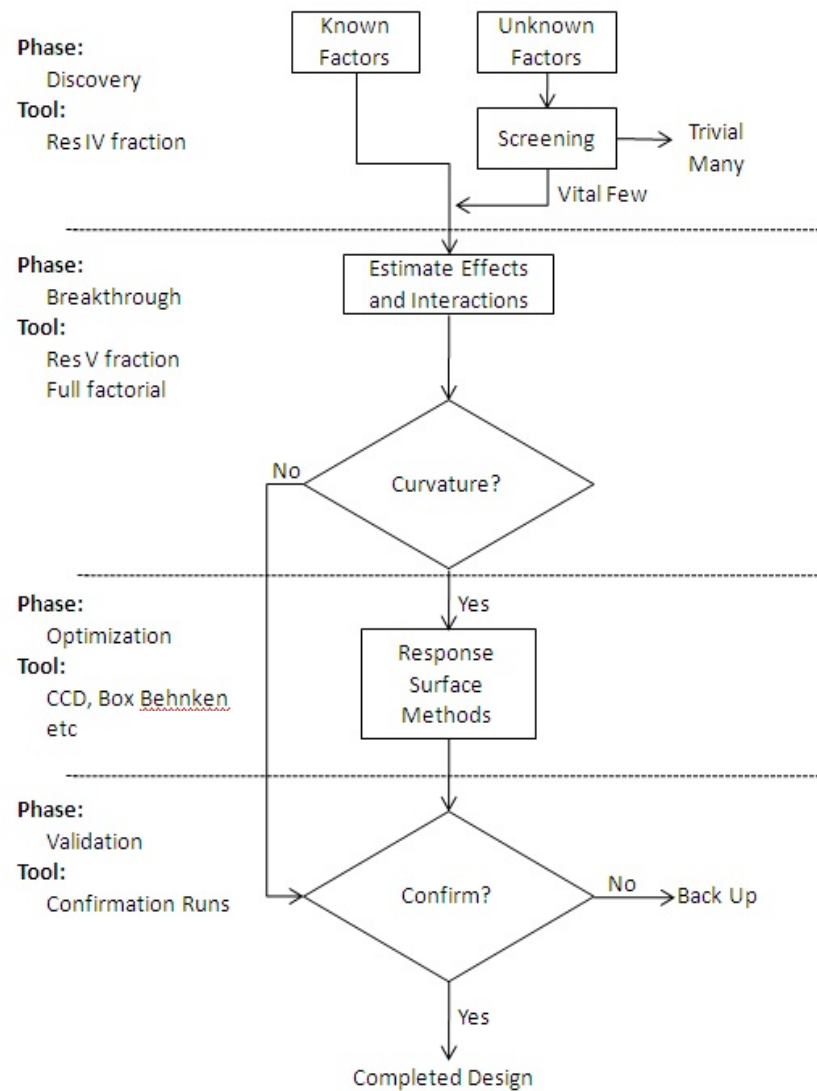


Figure 2.4 Strategy for selection, optimization and confirmation of experimental factors. (Anderson and Whitcomb, 2005)

2.6.6 Statistical Designs for Media Optimization

Several researchers have, to-date, published optimizations using RSM on various biological systems. Very little information is available on fungi in particular and riboflavin production specifically. Below is a summary of some attempts at applying RSM to optimize biological systems.

Liu and Tzeng, (1998) attempted to optimize production of spores from *Bacillus thuringiensis* using RSM. They investigated four factors, tapioca, fishmeal, ammonium sulphate and calcium carbonate in a half-fraction fractional factorial design to identify which of the four had the largest effect on spore-production. Their fractional factorial design was of sufficiently high resolution to resolve both one and two-factor interactions. Their fractional factorial was run, surprisingly, with no center-points which then would not allow estimation of variability within their design model. This was probably why they did not include a statistical table of data for their fractional factorial experiment. Additionally, they did not indicate which of the four factors significantly affected spore-formation, so their choices for the following experiment were not statistically sound. They did choose three of the four factors that had positive effects on spore-formation to investigate in a central-composite design. Their choice was not obvious and had to be inferred from the provided mathematical equation. The CCD gave three interaction graphs, all three of which were published, only one of which, was a significant interaction, which was the fishmeal/ammonium sulphate combination. Their point-prediction indicated 8.56×10^8 spores could be obtained but their actual experiment obtained 8.35×10^8 . No confidence interval or probability of obtaining the predicted variable was given so the experimental result could not be estimated to lie within a confidence interval. Their conclusions indicated that there may be more factors causing variability in the experiment, hence the shortcomings in their data. In reality, the experimenters were unable to correctly design and analyse the experiments, and this was the shortcoming.

Costa *et al.*, (2002) attempted to optimize *Spirulina platensis* production in fresh water using a central composite design. They designed an experiment to optimize media components, urea and sodium bicarbonate. Their CCD showed variability among center points which is essentially a replicated experiment and they attempted to explain that this variability is due to the experiments being carried out at different times. They do not

make the distinction between replicates or repeated experiments. The completed RSM experiment was found to produce an interaction that was not significant, but the authors do show the three-dimensional graph and make inferences from it in their conclusions. They even go as far as predicting the optimum urea and sodium bicarbonate for *Spirulina platensis* production from the insignificant interaction.

The following table summarises some of the other studies that have used either DOE and/or RSM to optimize microbial products:

Table 2.3 Microbial products optimized by DOE and/or RSM methodologies

Compound	Organism	Methods	Comments	Authors
Phycocyanin	<i>Spirulina platensis</i>	2-factor CCD for RSM	3D diagrams show linear or steeply increasing trends. Optima not reached.	Silviera <i>et al.</i> , 2007
Acetonin	<i>Bacillus subtilis</i> CICC 10025	Plackett-Burman for DOE 2-factor CCD for RSM	Plackett-Burman does not determine interaction factors but interactions investigated in CCD.	Xiao <i>et al.</i> , 2007
Extracellular polysaccharide	<i>Agaricus blazei</i>	3-factor Box-Behnken RSM	Authors investigated insignificant 2-factor interaction ignoring significant ones	Liu and Wang, 2007
Growth for inhibition of cocoa pathogen, <i>Phytophthora megakarya</i>	<i>Trichoderma asperellum</i> (4 strains)	3-factor CCD reported	Design is a factorial and not RSM. No interactions are explored. Only positive and negative interactions are mentioned.	Begoude <i>et al.</i> , 2007
α -amylase	<i>Bacillus subtilis</i>	2-factor CCD with $\alpha=1.68$	Interactions are given but no significances are calculated for interactions.	Zhi <i>et al.</i> , 2005
Cellulose	<i>Gluconobacter hansenii</i>	5-factor, $\frac{1}{2}$ fraction FFD	Some interactions are discussed but none shown	Hutchens <i>et al.</i> , 2007

Table 2.3 contd... <i>α</i> -galactosidase	<i>Aspergillus foetidus</i>	5-factor FFD and 2-factor CCD	Good progression of linear design logic to finally explain significant interaction	Liu <i>et al.</i> , 2007
Xylanase	<i>Alternaria mali</i> ND-16	10-factor Plackett-Burman FFD and 3-factor Docheleert RSM	Plackett-Burman does not elucidate interactions but authors chose 3 interactive factors for RSM	Li <i>et al.</i> , 2007
Lovastatin	<i>Monascus purpureuse</i> MTCC 369	5-factor Box-Behnken RSM	Very large design due to many factors. Authors explore 2-factor interactions without giving significance.	Sayyad <i>et al.</i> , 2007

A few studies have been done to attempt to optimize riboflavin production using both DOE and RSM. Pujari and Chandra (2000) attempted to optimize riboflavin production in a UV mutant of *Eremothecium gossypii*. Their yield was an extremely small 800-900 pg/ml to start with. They then attempted a Plackett-Burman DOE design with six factors. Plackett-Burman designs are generally used for screening large numbers of factors and when factors do not interact with each other and if factors do interact, the assumption is that there are no two-factor interactions (Haaland, 1989). The design flaw of using a Plackett-Burman design becomes apparent in the authors' next step where they use a full-factorial central composite to examine four factors, molasses, sesame seed cake, KH_2PO_4 and $\text{MgSO}_4 \cdot 7\text{H}_2\text{O}$. This experiment shows interaction among all four factors! If the interactions were present initially as was demonstrated subsequently, use of the Plackett-Burman design is wholly inappropriate for screening. Also, to choose four factors for a CCD is extremely confusing in terms of results generation which the authors subsequently show, being unable to focus on which interaction is most important. The authors should have chosen a fractional factorial screening experiment with the equivalent number of runs to isolate fewer important factors before running a CCD. This way, they would have avoided using a dummy variable to fill the design space for the seventh variable. Although the model generated in the CCD was shown to be significant, the interactions shown in contour plots have no indication of being significant and are questionable.

Wu *et al.*, 2007, attempted to optimize riboflavin production in *Bacillus subtilis* RH44 using both a 15-factor screening Plackett-Burman screening design DOE and a 4-factor CCD for their RSM component. They had a large number of factors to screen and some logic was applied to using the Plackett-Burman design as it allows a small $k+1$ design meaning one run more than the factors involved. One limitation of Plackett-Burman designs is that the numbers of factors used are fixed by the design e.g. a 7-run 6-factor design, a 12-run 11-factor design, and the one used here, a 20-run 19-factor design. The authors had 15 factors and had to insert a further four dummy factors. The risk in inserting dummy factors is that they may be significant and create confusion in the experimental analysis - significant factors cannot be ignored. The question then arises as to how these would be further incorporated into an RSM design? They did, however, manage to reduce the 15 to five factors in the initial screening using a pareto chart. They should have screened the five again using a further factorial experiment to reduce the number of factors to run a CCD on. However, they designed and ran a five-factor CCD and produced just one significant interaction. Glucose, the component with the highest effect on riboflavin production, in the DOE component was part of this interaction but manganese chloride, the lowest of the five effects in DOE was the other factor in the CCD. They do go on to explore the effect and optimize it, finally obtaining a high of 6.65 mg.l⁻¹ riboflavin in shake-flask and 110.8 g.l⁻¹ glucose. They also explored the interaction of a non-significant manganese chloride interaction with dipotassium hydrogen phosphate, ignoring the other eight non-significant reactions. No reason was given for choosing this interaction over others. Their fermentation culture seems to have performed far better than this optimization, with a final yield of 16.36 g.l⁻¹ from *Bacillus subtilis* with a fed-batch culture of glucose being kept at between 5-10 g.l⁻¹.

In general and considering the above sample of researchers using DOE and RSM to optimize media supplements for microbial systems, most have applied designs without much justification and some seem to have used designs that are inappropriate to the task at hand. Analysis and interpretation are often superficial without checking if the model is statistically significant, or if the data requires transformation. Some of the examples above show a shallow naivete in both the experimental approach and interpretation of subsequent data. A deeper understanding is thus required of the statistical basis of DOE and RSM before application to these systems or results, as seen in the discussions above, are questionable.

CHAPTER 3 : MATERIALS AND METHODS

This chapter details methods used to accomplish each objective in this study. Three fungal and one yeast strain were initially investigated for riboflavin production on a standard medium with glucose as carbon source, yeast extract, peptone, malt extract, magnesium sulphate-heptahydrate and di-potassium hydrogen phosphate. This medium was reported to be successfully used to grow the selected ascomycetes (Ozbas and Kutsal, 1986). This medium was used to determine the growth phases of each fungus and growth curves were fitted to a mathematical model which was used to calculate the mid-log phase, doubling time and maximum growth. Edible oil effluent was then investigated as a carbon source for riboflavin production by incorporating the effluent as a carbon source. Riboflavin yields were then compared in order to establish which fungus was producing the most riboflavin. A series of fractional factorial experiments that involved the five nutrient supplements of the standard medium, yeast extract, peptone, malt extract, magnesium sulphate-heptahydrate and, di-potassium hydrogen phosphate, were designed using the statistical software, Design Expert 7.1.6 (Statease, 2007). This program statistically analysed the experimental data, generating a mathematical model for each experiment. The models, described with mathematical equations, were used to guide the direction in which steps should be taken for subsequent experiments. These experiments allowed for screening of significant factors affecting riboflavin production in each round of screening (fractional factorial experimental designs). Once factors were reduced to the two most significant ones, response surface methodology, based on central composite experimental designs, was applied to optimize riboflavin production using point prediction solutions generated from quadratic equations generated to describe the production of riboflavin in the central composite design. The optimized medium was verified in confirmatory experiments and compared to predicted values. Since riboflavin is light-sensitive, in order to prevent its degradation, all experiments were conducted in foil-covered flasks and, where possible, all analyses were conducted under low light conditions.

3.1 STRAIN SELECTION, MEDIA AND CULTIVATION

3.1.1 Strain Selection

Four riboflavin overproducing fungal strains were used in this study, three of which are known to accumulate lipids in vacuoles and subsequently, to use it for riboflavin

production. The substrate on which these were to be eventually grown contained oils and fats and the choice of fungi was made based on their saprophytic nutrition, as well as their previous abilities to grow on complex oil substrates. Therefore, the four fungi chosen were the molds *Eremothecium (Ashbya) gossypii* wild type WT (ATCC 10895), *Eremothecium gossypii* (CBS 109.51), *Eremothecium ashbyi* (CBS 206.58) and the yeast *Candida famata* (ATCC 20850).

3.1.1.1 *Eremothecium (Ashbya) gossypii* wild type WT (ATCC 10895)

This strain was noted to overproduce riboflavin long before it was utilised as an industrial producer. It was deposited in the National Center for Agricultural Utilization Research (NRRL) by W.J. Robbins and later deposited at the ATCC. The culture is more popularly known as *Ashbya gossypii* and several research articles are published under this organism name. It has been shown to produce 2.5 g.l⁻¹ of riboflavin on soybean oil (Lim *et al.*, 2003) and 1.1 g.l⁻¹ on rapeseed oil (Park and Ming, 2004). It was selected to compare against other mutated strains in this study and was kindly provided by Dr K.-P. Stahmann of the Institut für Biotechnologie, Jülich, Germany.

3.1.1.2 *Eremothecium gossypii* (CBS 109.51)

This strain was a high riboflavin producing mutant deposited at the Centraalbureau voor Schimmelcultures (CBS) from which it was purchased. It has been implicated in oil-droplet accumulation (Stahmann *et al.*, 1997) and was thus considered a candidate for growth on EOE. It has been reported to produce riboflavin at concentrations of 15 g.l⁻¹ (Bigelis, 1989).

3.1.1.3 *Eremothecium ashbyi* (CBS 206.58)

This strain has also been reported to overproduce riboflavin at 15 g.l⁻¹ (Bigelis, 1989) and was able to grow on solid oil waste in the form of sesame seed cake and produce 1 g.l⁻¹ (Pujari and Chandra, 2000). It was thus considered suitable to attempt to grow on EOE and was purchased from CBS.

3.1.1.4 *Candida famata* (ATCC 20850)

This is a high riboflavin producing yeast strain, able to produce up to 20 g.l⁻¹ on simple carbon substrates (Heefner *et al.*, 1994). It has also been shown to grow on various oils

including flaxseed oil and produce riboflavin albeit at lower concentrations (Suzuki *et al.*, 2009) than reported above. It was included in this study to test whether it could grow and produce riboflavin on EOE as carbon source. This strain was purchased from the ATCC.

3.1.2 Media and Microorganism Storage

The four organisms mentioned above were grown at a pH of 6.5 at 30°C on three types of solid media, Malt Extract agar, Potato Dextrose agar (both Sigma) and a medium formulated by Ozbas and Kutsal, (1986) (O&K agar) (Appendix 1). The latter supported growth best and was subsequently used for growth and subculturing of all four fungal strains.

Colony morphologies of the four isolates were observed after a seven-day incubation on O&K agar plates in order to show qualitative differences in riboflavin production as well as describe the physical features of colonies. Microscopic evaluations were conducted using both light and fluorescence microscopy. The cultures were stained with lactophenol blue before viewing and comparative views were observed using both light and UV microscopy to determine the location of riboflavin within the physical structure of cells.

Medium-term stocks were prepared by growing fungal strains on O&K agar. One cm² blocks were cut using a sterile scalpel from the inoculation point in order to increase the number of spores collected. These blocks were stored under 20 ml of sterile distilled water in universal bottles at 4°C for six months as described by Diogo *et al.*, (2005). Cultures were resuscitated when needed by aseptically removing one square from below the water level, resuspending it in five ml of O&K liquid medium (agar was omitted) and incubating at 30°C for five days with agitation at 150 rpm. Cultures were checked microscopically for bacterial and other yeast contamination before one loopful each was centrally inoculated onto three O&K agar plates and incubated for five days at 30°C. Plates were monitored for contamination before continuing with the culture.

Long-term stocks were stored in Microbank™ vials (Prolab Diagnostics) which contained porous beads that serve as support for microorganisms. Twenty five beads were packed into Nunc cryovials. The bacterial cryopreservative was removed by aspiration and one ml aliquots of five-day old fungal cultures grown on O&K liquid

medium were dispensed into cryovials. Vials were inverted four to five times to mix the culture with the beads, allow absorption of the microorganisms onto them and vials were then frozen to -70°C . These vials were kept at -70°C for a year. Cultures were resuscitated when needed by removing one bead from cryovials and resuspending in five ml of O&K medium and incubating at 30°C for five days with agitation at 150 rpm. Cultures were checked microscopically for bacterial and other yeast contamination before one loopful each was centrally inoculated onto three O&K agar plates and incubated for five days at 30°C . Plates were monitored for contamination before continuing with the culture by checking for yeast or bacterial colonies and gram staining and examining under a light microscope if contamination was suspected.

Working stocks were prepared by subculturing the four strains on a weekly basis using a 3-point inoculation for molds and streak-planting for yeasts, in 90 mm petri dishes on O&K agar and incubated at 30°C until used.

3.2 COMPOSITION OF EDIBLE OIL EFFLUENT

Edible oil effluent (EOE) was obtained from an edible oil producing industry in Pietermaritzburg. Samples were collected in 20 litre plastic jerry cans and immediately stored at 4°C until used. The Chemical Oxygen Demand of EOE was measured whenever aliquots were withdrawn using a CSB COD Cell Test kit (500-10,000 mg.l^{-1} range) (Merck). The method of COD measurement is analogous to EPA 410.4, US Standard Methods 5220 D and ISO 15705. The method, briefly, oxidizes organic material in the presence of a hot sulphuric acid solution of potassium dichromate with silver sulphate as a catalyst. Chloride is masked with mercury sulphate. The evolution of the reduced green Cr^{3+} ions was determined photometrically using a Spectroquant Pharo 300 Spectrophotometer (Merck) and converted COD value was read from the pre-programmed method. The conversion factor is: 1 mol $\text{K}_2\text{Cr}_2\text{O}_7$ is equivalent to 1.5 mol O_2 with $1\text{mg.l}^{-1} \text{O}_2$ equal to $1\text{mg.l}^{-1} \text{COD}$.

3.2.1 Determination of Fatty Acid Composition of Edible Oil Effluent by Gas Chromatography

Fatty acid composition of EOE was carried out by Gas Chromatography-Mass Spectrometry analysis which was carried out by Umgeni Water. The method is detailed below and is an adaptation of the US EPA method 625 (Umgeni Water Methods Manual, 2002).

Sample Preparation

A sample of the EOE (five drops) was dissolved in methylene chloride (one ml) before analysis.

3.2.2 Instrumentation

One microlitre of the above sample was injected into the HP 6890 series Gas Chromatograph interfaced to an HP 5973 Mass Selective Detector (MSD) and controlled by HP Chemstation software (version b.02.05, 1989-1997). The chromatographic separation was achieved using a DB-5 MS capillary column (30.0 m x 250 μ m x 0.25 μ m). The column stationary phase comprised of 5%-Diphenyl-95% Dimethylpolysiloxane. The GC conditions, oven and injector conditions are outlined in Table 3.1. The results were analysed and compounds were identified by comparing the resultant spectra with a Wiley 275 spectral library.

Table 3.1 Gas chromatograph and oven and injector conditions.

Oven Temperature Programme	
Initial Temp:	50°C
Initial Time:	2 minutes
Ramp Rate:	10°C/min
Final Temp:	300°C
Final time:	3 minutes
Injector Conditions	
Injection mode:	Splitless
Injector Temp:	250°C
Injector volume:	1 μ L

3.3 FUNGAL GROWTH MEASUREMENT

3.3.1 Growth Curve Determination

The objective of determining the growth curves of each fungus was to determine growth kinetics, maximum specific growth rates (μ_{\max}) and doubling times (T_d) in order to select the mid-log phase (x) of each fungus for transfer during inoculation. One cm² of the leading edge of a five-day old culture of the three filamentous fungi were inoculated into three 500 ml Erlenmeyer flasks containing 300 ml O & K liquid medium (Ozbas and Kutsal, 1986). Two colonies of the yeast were inoculated per 100 ml of medium for the yeast, *C. famata*. Flasks were incubated at 30°C for five days on an orbital shaker with a radial throw of 2.5 cm and a speed of 100 orbits per minute. Three five-millilitre samples were withdrawn daily at three-hourly intervals over five days from each flask. Growth of *C. famata* was measured at 600 nm on a spectrophotometer. Growth of *A. gossypii*, *E. gossypii* and *E. ashbyi* was determined gravimetrically, by filtering through a pre-dried preweighed Whatman no 1 filter paper and drying at 105°C overnight before being re-weighed. Results were presented as line graphs with means of three replicates as symbols and standard deviations indicated by T-bars. Supernatants were used for measurement of riboflavin at 445 nm using a spectrophotometer.

Growth curves were fitted from first principles of curve-fitting to the Gompertz model (Windsor, 1932). The general equation to describe a four-parameter Gompertz curve is given below:

$$y = ae^{-e^{-\left(\frac{x-x_0}{b}\right)}} \quad (\text{eq. 3.1})$$

From this equation, four parameters a , b , x_0 and y_0 were calculated using the program Sigmaplot 11 (Systat, Software Inc.). These parameters were further manipulated to give the maximum specific growth rate (μ_{\max}), doubling time (T_d) and mid-log time of inoculation (x) which was taken from the mid-log point. The equations used were derived from eq. 3.1 and are given below:

$$\mu_{\max} = \frac{a}{(b.e) \div 2} \quad (\text{eq 3.2})$$

$$x = \left\{ -\ln \left[-\ln \left(\frac{y - y_o}{a} \right) \right] b \right\} + x_o \quad (\text{eq 3.3})$$

$$T_d = \frac{\ln 2}{u_{\max}} \quad (\text{eq. 3.4})$$

The Gompertz curve was used in preference to the logistic curve on the basis of data presented by Satoh (2003) in which correlations between the two sigmoid-curve-fitting models above were measured against sample data. The results showed that when the number of data were low, the Gompertz model had a higher correlation than the logistic curve.

3.4 OPTIMIZATION OF RIBOFLAVIN DETECTION ASSAY

Due to the various methods advocated for riboflavin measurement mentioned earlier, this study attempted to validate the most appropriate method. Riboflavin was measured spectrophotometrically in this study because it is an uncomplicated method, requiring no sample pre-preparation, does not require sophisticated solvents, is a fast method for quantification and sample degradation for the period of measurement is negligible. A pH decrease with the addition of 0.02 M acetic acid is advocated by the AOAC Official Method 970.65 in order to solubilise and stabilise riboflavin (Long, 2000). Hence 0.02 M acetic acid was used as solvent and diluent for riboflavin to develop a method for UV/visible detection.

A riboflavin standard stock solution of 100 mg.l⁻¹ using USP riboflavin (Sigma-Aldrich) was prepared according to the above AOAC method in 0.02 M acetic acid (Sigma-Aldrich). The stock was diluted with 0.02 M acetic acid to concentrations ranging from 0.05 to 100 mg.l⁻¹ using calibrated pipetman autopipettes in A-grade 100 ml borosilicate volumetric flasks. Concentrations are listed in Table 3.2.

A WPA Lightwave Version 1.0 Model S2000 diode-array UV/Vis spectrophotometer was used to scan all concentrations of riboflavin solutions from 200 to 825 nm in steps of 1 nm using matched quartz cuvettes with a 1 cm light path. Riboflavin peaks were detected at 264 nm, 374 nm and 442 nm. It was decided to produce standard curves for each of these three wavelengths and to determine the straightness of the resulting

standard curve using first order regression and compare the calculated squared Pearson's least square correlation coefficient (R^2) for each line. A choice would then be made of wavelength to be used, based on the best R^2 value, sensitivity and range of detection of the wavelengths used. Sensitivity was determined by the slope of each regression line, the steeper the slope, the more sensitive the wavelength. Range of detection was determined by visually inspecting the highest and lowest values in the linear range of the prepared standard curve.

Table 3.2. Concentrations of riboflavin used to prepare standard curve to use for spectrophotometric riboflavin measurement

VOL STOCK ml	VOL DILUENT ml	FINAL VOL ml	CONCENTRATION mg.l ⁻¹
0.05	99.95	100	0.05
0.1	99.9	100	0.1
0.5	99.5	100	0.5
1	99	100	1
2.5	97.5	100	2.5
5	95	100	5
7.5	92.5	100	7.5
10	90	100	10
15	85	100	15
20	80	100	20
25	75	100	25
30	70	100	30
35	65	100	35
40	60	100	40
45	55	100	45
46	54	100	46
47	53	100	47
48	52	100	48
49	51	100	49
50	50	100	50
55	45	100	55
60	40	100	60
65	35	100	65
70	30	100	70
75	25	100	75
80	20	100	80
85	15	100	85
90	10	100	90
95	5	100	95
100	0	100	100

3.5 FUNGAL GROWTH ON EDIBLE OIL EFFLUENT

Utilization of edible oil as a carbon source was assessed by using the chemically defined medium described by Ozbas and Kutsal (1986), where they assessed the effects of carbohydrate sources on *A. gossypii*. Peptone, yeast extract, malt extract, MgSO_4 and K_2HPO_4 were added to EOE. For comparison purposes, glucose was substituted as carbon source in the O&K medium and a medium without any external carbon source was also used for comparison. These are detailed in Table 3.3. The pH of the media was adjusted to 6.5 before autoclaving at 121°C for 15 minutes in an autoclave.

Table 3.3 Media components for determination of fungal growth on EOE

Treatment	MEDIUM (g.l^{-1})	BASE DILUENT (ml)
Experiment (EOE as carbohydrate)	Peptone (5)	Edible Oil Effluent (1000) (COD = $\pm 5000 \text{ mg.l}^{-1}$)
	Yeast Extract (5)	
	Malt Extract (5)	
	$\text{MgSO}_4 \cdot 7\text{H}_2\text{O}$ (0.2)	
	K_2HPO_4 (0.2)	
Positive Control (glucose as carbohydrate)	Glucose (20)	Distilled water (1000)
	Peptone (5)	
	Yeast Extract (5)	
	Malt Extract (5)	
	$\text{MgSO}_4 \cdot 7\text{H}_2\text{O}$ (0.2)	
	K_2HPO_4 (0.2)	
Negative Control (no external carbohydrate)	Peptone (5)	Distilled water (1000)
	Yeast Extract (5)	
	Malt Extract (5)	
	$\text{MgSO}_4 \cdot 7\text{H}_2\text{O}$ (0.2)	
	K_2HPO_4 (0.2)	

-pH of the medium was adjusted to 6.5 with 0.1 N HCl before sterilising at 121°C for 15 minutes in an autoclave.

One cm^2 of the leading edge of a five-day old culture of the three filamentous fungi were inoculated into triplicate 500 ml Erlenmeyer flasks containing 300 ml liquid medium. Two colonies of the yeast were inoculated per 100 ml of medium for the *C. famata* isolate. These flasks were incubated at 30°C for five days on an orbital shaker with a radial throw of 2.5 cm and a speed of 100 orbits per minute. Three five-millilitre samples were withdrawn daily at three-hourly intervals over five days from each flask.

Gravimetric determination of biomass was conducted at 24-hour intervals using Whatman No 1 filter paper as described in section 3.3.1. Riboflavin levels were measured spectrophotometrically at 445 nm. The pH was also monitored in order to determine if the carbohydrate components in the respective samples were acidified during metabolism. Comparative line graphs were drawn for each organism on the above three parameters to determine the best riboflavin producer, highest biomass and least pH fluctuation on EOE. The best producer was then selected, based on comparison primarily of growth and riboflavin production on EOE and data was statistically analysed to ensure significant differences were identified. The statistical test used was ANOVA with Bonferroni's post-test to compare data columns and null-hypothesis probability was set at $p=0.05$.

3.6 MUTATIONAL STUDIES

Two of the four organisms showed the ability to tolerate and grow in EOE as well as produce some riboflavin. These two organisms were *E. ashbyi* (CBS 206.58) and *C. famata*. (ATCC 20850). The two fungi were subjected to a physical mutagen (UV light) and three chemical mutagens and grown on an O&K medium containing EOE as selective pressure to select for mutants that showed potential for adaptation to EOE. The medium was composed of components described in the "experiment" in Table 3.3 above.

3.6.1 Ultraviolet Light Mutation

Eremothecium ashbyi and *C. famata* were both grown in broth cultures of 200 ml in 500 ml Erlenmeyer flasks for five days. *E. ashbyi* mycelium was strained from the broth using eight layers of sterile cheese cloth, the filtrate being collected into sterile one-litre beakers. Spores were counted in a Nebauer counting chamber and adjusted to 1×10^8 spore. ml^{-1} . *Candida famata* cells were counted in a Nebauer counting chamber and adjusted to 1×10^8 cells/ml. Ten millilitre aliquots were dispensed into sterile polystyrene petri dish bases and exposed without lids to UV light at 280-320 nm for 10, 20 and 30 minutes at a distance of 20 cm from the light source (Barichevich and Calza, 1996). Each of the aliquots were then aseptically decanted into 100 ml of EOE base media. Biomass and riboflavin were measured at 24- hour intervals over five days as described above.

3.6.2 N-Methyl-N-Nitrosoguanidine (MNNG)

The two microorganisms were cultured in a 250 ml flask, with 100 ml O&K medium. This was then incubated at 30°C on a rotary shaker at 110 rpm for 24 h after which 5 ml of this was added to a stock of N-Methyl-N-Nitrosoguanidine (dissolved in 95% ethanol) at a concentration of 50 mg.ml⁻¹. Exposure times were 10, 20 and 30 minute intervals (Barichievich and Calza, 1996).

3.6.3 Ethylmethane Sulphonate (EMS)

The two microorganisms were cultured in a 250 ml flask, with 100 ml O&K medium. This was then incubated at 30°C on a rotary shaker at 110 rpm for 24 h, after which 5 ml of cultured organism was added to Ethylmethane sulphonate (EMS) diluted with 0.05 M potassium phosphate buffer, pH 7 (Moses, 2009), with exposure times of 10, 20 and 30 minutes.

3.6.4 Sodium Azide (NaN₃)

The two microorganisms were cultured in a 250 ml flask, with 100 ml O&K medium. This was then incubated at 30°C on a rotary shaker at 110 rpm for 24 h, after which 5 ml of this culture was added to the freshly prepared sodium azide at a concentration of 1, 1.5 and 2 g/l in 0.05 M phosphate buffer (pH 3) (Sapra *et al.* 2004). Exposure times were 10, 20 and 30 minutes.

3.6.5 Screening for Riboflavin-overproducing Mutants

After each exposure interval an aliquot of 0.1 ml was removed from exposed cultures. These were then inoculated onto a screening medium (Appendix 2) containing Itaconate (Stahmann, *et al.*, 2001). Itaconate is a riboflavin antimetabolite and represses the activity of the enzyme isocitrate lyase in wild-type riboflavin producers. Those mutants that continue producing riboflavin in the presence of the antimetabolite have a mutated variant of isocitrate lyase that is insensitive to the antimetabolite. Riboflavin overproducing mutants showed yellow growth, indicating strong riboflavin production even in the presence of the antimetabolite while the wild-type grew cream/white, or light yellow on the itaconate-containing plates. The colonies producing the most yellow pigment were isolated and these successful riboflavin-producing mutants were grown on the optimized growth medium and riboflavin analysis was carried out using

spectrophotometric methods described previously. Mutants were compared, ranked and selected for on the bases of the following parameters: maximum specific growth rates μ_{\max} , doubling times T_d , maximum riboflavin production and rates of riboflavin production.

3.6.6 Isocitrate Lyase Assay to Compare Mutant Enzyme Activity to Wild-Type

The itaconate antimetabolite screening method described by Stahmann, *et al.*, (2000) allowed for the isolation of an isocitrate lyase regulatory mutant from the wild type. In order to assess whether the activity was increased in the final selected mutant, an isocitrate lyase assay was conducted on the extracted enzyme from both the wild-type and mutant and the enzyme activities were statistically compared.

3.6.6.1 Enzyme extraction procedure

Both the wild-type and mutant were grown to mid-log phase growth and maximum riboflavin production phase. A 1 cm² area of agar from the leading edge of a culture of each organism was inoculated into each of six 50 ml broths containing O&K medium with EOE as diluent in 300 ml Erlenmeyer flasks. Cultures were incubated at 130 rpm at 30°C and the entire volume of three flasks was filtered through a Whatman No. 1 filter paper at the point of maximum riboflavin production to obtain the maximum amount of enzyme.

Biomass was adjusted to four grams wet weight and ground in a pestle and mortar after freezing with liquid nitrogen. Powdered mycelium was resuspended in a 40 ml volume of enzyme extraction buffer containing 10 mM 3-(N-morpholino)propanesulfonic acid (MOPS-NaOH), 1 mM ethylenediaminetetraacetic acid (EDTA) and 1 mM dithiothreitol (DTT). The mixture was vortexed to allow extraction of enzyme to the liquid fraction from biomass. Cellular contents were pelleted by centrifugation at 10,000 X g in an ALC PR110 centrifuge at 4°C for 10 minutes. The clear supernatant containing crude enzyme extract was stored on ice (De Lucas *et al.*, 1997).

3.6.6.2 Enzyme assay procedure

Isocitrate lyase activity was measured according to the E.C. 4.1.3.1 method (Chell *et al.*, 1978). The crude enzyme in the supernatant extract was exposed to an isocitrate substrate which cleaved isocitrate to succinate and glyoxylate at pH 6.8. Glyoxylate was then reacted with phenylhydrazine to produce a colour reaction with the evolution of the coupled glyoxylate-phenylhydrazine complex, which was spectrophotometrically measured using a Beckman DU 640 spectrophotometer. A continuous spectrophotometric method was used over a five-minute period with 15-second measurement intervals. The reaction cell was maintained at 30°C with a continuous water jacket. Measurements were made at 324 nm over a 1 cm light path. Matched quartz glass cuvettes were used to accommodate the measurement wavelength. An appropriate blank (Appendix 3) was used to correct for spontaneous product formation. The enzyme activity was measured over the five minutes as a linear slope and the gradient of the slope was used as the measurement of rate of activity using a standard spreadsheet linear regression analysis. The complete method is listed in Appendix 3.

One unit of isocitrate lyase was determined to be the amount that catalysed the formation of 1 μ mole of glyoxylate per minute at pH 6.8 at 30°C. The equation used to calculate this was:

$$\text{Units / ml enzyme} = \frac{(\Delta A_{324nm} / \text{min Test} - \Delta A_{324nm} / \text{min Blank})(l)(df)}{(16.8)(0.1)}$$

l = volume of assay (ml)

df = dilution factor

16.8 = millimolar extinction coefficient of phenylhydrazine glyoxylate at 324 nm

0.1 = volume of enzyme used (ml)

3.7 SUPPLEMENTATION TO EDIBLE OIL EFFLUENT

A large number of supplements have been screened previously for addition to various carbon-containing media as detailed previously in the literature review. Previous experiments described in this chapter showed that EOE has sufficient carbon to support microbial growth provided it has sufficient nitrogen, phosphorous and trace elements. The levels of supplementation of these latter three, as nutrient groups, were further investigated using Design of Experiments. In order to do so, experiments were designed and analysed with the aid of DOE software Design Expert version 7.1.6 (Statease 2007).

3.7.1 Experimental Design for Media Optimization

3.7.1.1 Primary screening experiment to determine factor effects

Eight nutrient factors were studied for riboflavin production in EOE, namely: yeast extract, malt extract, peptone, corn-steep liquor, dipotassium hydrogen orthophosphate, sodium chloride, a combined minerals solution (Appendix 4) and tween 80. These were selected on the basis of preliminary experiments previously conducted by various researchers in this laboratory. The concentrations used are listed in Table 3.4. A fractional factorial experimental design was selected with five center points (Haaland, 1989) to screen for the effects of the above eight factors. The full factorial was not used as this would have meant doing $2^8 = 256$ separate experiments excluding center points. Instead a resolution IV fractional factorial was chosen with $2^{8-4} = 16$ experiments with five center points that give a total of 21 runs. All chemicals above were obtained from Sigma Scientific.

Table 3.4 Concentrations of variables added per litre of EOE in the first 2^{8-4} screening fractional factorial experiment indicating low, high and center points

Factor	Symbol	Level		
		-1	0	1
Yeast extract	x_1	2.5	3.75	5
Malt extract	x_2	5	7.5	10
Peptone	x_3	0.5	2.75	5
Cornsteep liquor	x_4	30	45	60
K_2HPO_4	x_5	0.2	1.1	2
NaCl	x_6	1	1.5	2
Minerals	x_7	1	1.5	2
Tween 80	x_8	0	0.9	1.8

all chemicals were in $g.l^{-1}$ except minerals and tween 80 solution which were added in ml per l

3.7.1.1.1 Inoculum Preparation

The chosen mutant was grown for four days on O&K agar plates using a three-point stab inoculation technique. A one cm^2 cut out of the leading edge of the growing culture was inoculated into each of two 100 ml O&K liquid media in 500 ml flasks. Flasks were

incubated at 30°C for 27 hours to reach mid-log phase. The inoculum was then centrifuged at 10,000 X *g* in an ALC PK110 centrifuge for 15 minutes and the biomass pellet was washed twice in distilled water before resuspending to the original volume of 100 ml using distilled water. A five ml aliquot was used as inoculum into a final volume of 50 ml.

Experiments were conducted in 300 ml Erlenmeyer flasks with 50 ml working volumes to enhance gas transfer. Media was prepared according to the following experimental design schedule in Table 3.5 and runs were conducted in one block and randomized to prevent experimenter bias. The run order indicates the random order in which each run was carried out. Standard order sorts the experiment into 16 runs and five center points. The random experimental design is presented in Table 3.5.

Table 3.5 Experimental design of an eight-factor 1/16th fractional factorial, FF0816, with five center points, showing coded factor levels and randomized run order to determine effect on riboflavin production of eight medium additives to EOE

Std Order	Run Order	Factor							
		x_1	x_2	x_3	x_4	x_5	x_6	x_7	x_8
11	1	-1	1	-1	1	1	-1	1	-1
10	2	1	-1	-1	1	1	1	-1	-1
1	3	-1	-1	-1	-1	-1	-1	-1	-1
5	4	-1	-1	1	-1	1	1	1	-1
15	5	-1	1	1	1	-1	1	-1	-1
20	6	0	0	0	0	0	0	0	0
18	7	0	0	0	0	0	0	0	0
3	8	-1	1	-1	-1	1	1	-1	1
9	9	-1	-1	-1	1	-1	1	1	1
6	10	1	-1	1	-1	-1	1	-1	1
4	11	1	1	-1	-1	-1	1	1	-1
19	12	0	0	0	0	0	0	0	0
12	13	1	1	-1	1	-1	-1	-1	1
17	14	0	0	0	0	0	0	0	0
14	15	1	-1	1	1	-1	-1	1	-1
7	16	-1	1	1	-1	-1	-1	1	1
21	17	0	0	0	0	0	0	0	0
2	18	1	-1	-1	-1	1	-1	1	1
13	19	-1	-1	1	1	1	-1	-1	1
8	20	1	1	1	-1	1	-1	-1	-1
16	21	1	1	1	1	1	1	1	1

Coded factor levels were analysed using multiple regression and a polynomial relationship for each dependent factor was fitted to a first-order polynomial equation, the general form of which, given in equation 3.1 below:

$$Y = \varepsilon + c_o + \sum a_i x_i + \sum b_{ij} x_{ij} \quad (3.1)$$

where, Y is the predicted riboflavin concentration, a_i and b_{ij} are half the magnitude of effects of single factors x_i and factor interactions x_{ij} , c_o is the intercept term and ε is the random error in the response. The model fit was determined using a probability limit of $p < 0.05$ and all factors that fitted the model were included on this basis as well. A pareto chart with a t-test and Bonferroni post-test were applied to single and two-factor interactions to determine their significance. Four factors were identified as significant and screened further for their effects. This experimental design is shown in Table 3.7.

Also the direction of the experiment towards optimum concentrations of the four factors selected were assessed using response-surface curves.

3.7.1.2 Secondary screening experiment to identify important factors

The four factors identified in the previous experiment as significant, were included in a further experiment to narrow down the choice to two which would be investigated further. Since there were just four factors identified, a full-factorial could be conducted with 16 runs and five center points without compromising resolution in interactions. Inoculum preparation and experimental setup was conducted as described previously in section 3.7.1.1. The four factors and their levels are listed in Table 3.6, and Table 3.7 outlines the randomised experimental design with five center points. All other factors were kept at low concentrations as indicated in Table 3.4.

Table 3.6 Concentrations of variables in the second full factorial experiment indicating low, high and center points

Factor	Symbol	Level		
		-1	0	1
Yeast extract	x_1	5	5.5	6
NaCl	x_2	2	2.25	2.5
K ₂ HPO ₄	x_3	2	2.5	3
Minerals	x_4	2	2.5	3

all chemicals were in g.l⁻¹ except minerals which were added in ml.l⁻¹

Table 3.7 Experimental design of a four-factor full-fractional factorial experiment, FF0416 with five center points, showing coded factor levels and randomized run order to determine effect on riboflavin production of four medium additives to EOE

Std Order	Run Order	Factor			
		x_1	x_2	x_3	x_4
14	1	1	-1	1	1
21	2	0	0	0	0
11	3	-1	1	-1	1
19	4	0	0	0	0
1	5	-1	-1	-1	-1
13	6	-1	-1	1	1
20	7	0	0	0	0
4	8	1	1	-1	-1
15	9	-1	1	1	1
10	10	1	-1	-1	1
2	11	1	-1	-1	-1
9	12	-1	-1	-1	1
16	13	1	1	1	1
3	14	-1	1	-1	-1
6	15	1	-1	1	-1
17	16	0	0	0	0
7	17	-1	1	1	-1
5	18	-1	-1	1	-1
18	19	0	0	0	0
8	20	1	1	1	-1
12	21	1	1	-1	1

A mathematical model describing data was fitted using multiple regression as stated previously and data was used to reduce the number of significant factors to two, which were further investigated in a central-composite design as described below. All analytical steps on assessing the model above were as described in section 3.7.1.1.

3.7.1.3 Response surface experiment to optimize important factors

The two important factors identified in the previous experiment were yeast extract and NaCl. These showed an interaction and a central-composite design with six face-centered points was designed. In addition to the low and center and high values, two additional points at $\alpha = \pm 1.41421$ were also included. A graphical representation of the

design space is shown in Figure 3.1. All levels of the experimental design and factors used are indicated in Table 3.8.

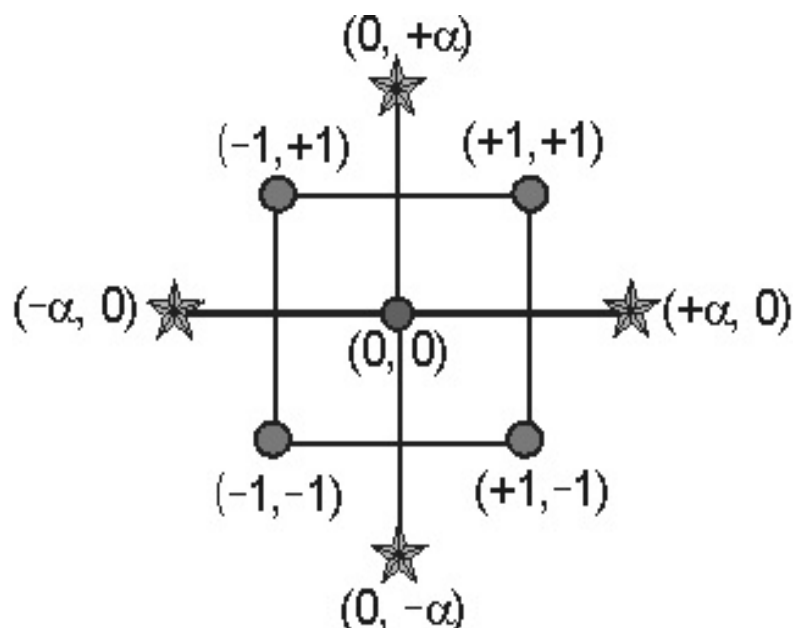


Figure 3.1 Representation of a central composite design for two factors showing six face-centered points around a replicated center point. The four corners of the square represent the factorial (+/- 1) design points and the four star points represent the axial (+/- α) design points (Statease, 2007).

Table 3.8 Concentrations of variables in the central composite experiment indicating low, high and center points along with alpha values ($\alpha = \pm 1.41421$)

Factor	Symbol	Level				
		$-\alpha$	-1	0	1	$+\alpha$
Yeast extract	x_1	6.98	7.5	8.75	10	10.52
NaCl	x_2	2.4	2.5	2.75	3	3.1

Inoculum preparation was conducted as described above and flasks were inoculated and incubated as described in 3.7.1.1. The coded and randomized experiment is presented in Table 3.9.

Table 3.9 Experimental design of a two-factor central-composite experiment showing coded factor levels with randomized run order to determine effect on riboflavin production of two medium additives to EOE

Std Order	Run Order	Factor	
		x_1	x_2
11	1	0	0
4	2	1	1
5	3	-1.41421	0
12	4	0	0
3	5	-1	1
6	6	1.41421	0
8	7	0	1.41421
9	8	0	0
7	9	0	-1.41421
10	10	0	0
2	11	1	-1
13	12	0	0
1	13	-1	-1

The model fitted to the data above was a second-order polynomial function in the general form given below:

$$Y = c_0 + \sum_{i=1}^n a_i x_i + \sum_{j \leq i}^n b_{ij} x_i x_j$$

where Y is the predicted riboflavin response, subscripts i and j take the number 1 to the number of variables ($n=2$) and c_0 is the intercept value, a_i and b_{ij} are the linear and quadratic coefficients, and x_i and x_j are the levels of the independent variables. All designs were constructed and analysed on the platform Design Expert 7.1.6. (Statease, 2007).

An ANOVA was used to determine the goodness-of-fit of experimental data to the model. A quadratic polynomial equation was generated to describe the data based on the model. Three-dimensional and contour graphs were used to visualise the interactions between the two factors used. A point-prediction was made to maximize the amount of riboflavin production while optimizing the two factors tested. The result of the point-prediction was run as a confirmatory experiment.

3.7.1.4 Confirmatory experiment to determine validity of prediction

After conducting the two fractional-factorial and central composite designs, the media components and levels outlined in Table 3.10 were determined as optimal for the maximum production of riboflavin. These were run in triplicate in 50 ml volumes in 500 ml Erlenmeyer flasks. A 2% inoculum of a mid-log phase growth of *A. gossypii* EMS 30/1 mutant was used to inoculate flasks, the preparation of which was described previously. The media components and their concentrations are shown in Table 3.10 below:

Table 3.10 Media components optimized using DOE and RSM and used to confirm predicted results.

Factor	Quantity in EOE (g.l ⁻¹)
Yeast Extract (Biolab)	8.43
NaCl	2.5
K ₂ HPO ₄	2
Peptone (Oxoid)	0.5
Malt extract	5
Minerals	3
Corn steep liquor	30
Edible oil effluent	50 ml

Flasks were incubated at 30°C for 120 h at 130 rpm in a shaking incubator before the entire sample was harvested and biomass was determined gravimetrically using Whatman no.1 filter paper on a five-digit analytical balance after drying at 105°C overnight. Riboflavin was measured spectrophotometrically at 445 nm using a Spectroquant Pharo 3000 spectrophotometer and was converted to mg.l⁻¹ concentrations using a standard curve. The start and end pH values were also recorded using a Beckman PHI 500 benchtop pH meter.

A 2 l batch fermenter (OMNI-CULTURE, VirTis Co. Inc.), was also set up with the factors listed in Table 3.10 with EOE as the diluent. This was prepared in the fermenter and autoclaved at 121°C for 20 minutes and cooled. A 2% inoculum of a mid-log growth phase of *A. gossypii* EMS 30/1 mutant was used to inoculate the fermenter, the preparation of which was described previously. The fermenter was run at 30°C and 130 rpm impeller speed and the starting pH was adjusted to 6.5. At 24-hour intervals, starting at 0 h for 10 successive days, 5 ml aliquots were aseptically drawn and biomass was measured gravimetrically after filtering through a pre-weighed Whatman no. 1 filter paper on a five-digit analytical balance after drying at 105°C overnight. Riboflavin was measured spectrophotometrically at 445 nm using a Spectroquant Pharo 3000 spectrophotometer and was converted to mg.l⁻¹ concentrations using a standard curve. The pH of the fermenter was measured at each sampling using a Beckman pHI 500 benchtop pH meter.

CHAPTER 4 : RESULTS

4.1 RIBOFLAVIN PRODUCTION UNDER DEFINED CONDITIONS

4.1.1 Wild type and Mutant Fungal Growth

The cultures below show varying yellow discolouration of the media on which they grow. This is characteristic of riboflavin production by the organisms which is secreted into the medium. The distribution of the yellow colour is noticed particularly around colonies. Also, at the center of mycelial growth, the yellow colour is strongly evident in Figure 4.1.1 a and b. This is indicative of the late logarithmic to stationary phases in which riboflavin is produced (Schlosser *et al.*, 2007).

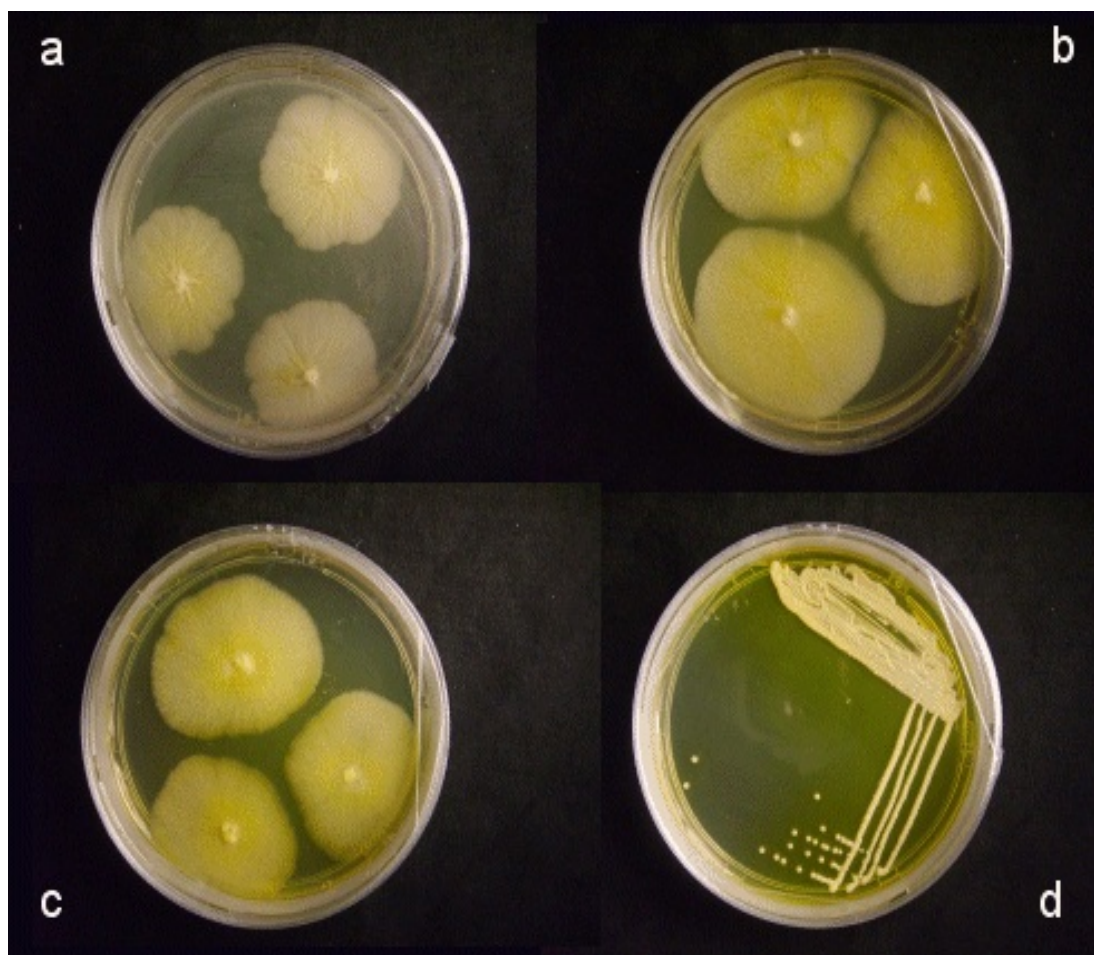


Figure 4.1.1 Seven-day growth of four fungi on Ozbas and Kutsal agar plates (a) *E. gossypii* wild type (ATCC 10895), (b) *E. gossypii* (CBS 109.51), (c) *E. ashbyi* (CBS 206.58), (d) *C. famata* (ATCC 20850).

A colony and microscopic investigation of the four cultures, was conducted in order to establish their growth characteristics. Colonies of the *E. gossypii* wild-type (ATCC 10895) showed an irregular margin and a beige colour, whilst colonies of *E. gossypii* (CBS 109.51) were more filamentous and yellow in colour, indicating more riboflavin production (Figure 4.1.1 a/b). Mycelia of both the *Eremothecium* species showed dichotomous branching and sparing septation when viewed under dark-field microscopy (Figures 4.1.2 a/b). Colonies of *E. ashbyii* (CBS 206.58) also showed filamentous margins similar to the *E. gossypii* (CBS 109.51) strain and dichotomous branching was observed as well (Figure 4.1.2 b). Spore formation in both *E. gossypii* strains were of clavate shape with no asci being observed (Figure 4.1.3 a) and multiple budding was observed in the *C. famata* (ATCC 20850) strain forming short pseudomycelia (Figure 4.1.3 b). A complete description of the colonial morphology and microbial features are presented in Table 4.1.

Table 4.1 Colony and cellular morphologies of four fungi grown on standard Ozbas and Kutsal agar plates after seven days of incubation at 30°C.

	<i>E.gossypii</i> (ATCC 10895)	<i>E.gossypii</i> (CBS 109.51)	<i>E. ashbyii</i> (CBS 206.58)	<i>C.famata</i> (ATCC 20850)
Morphology				
Colony				
Form	irregular	filamentous	filamentous	circular
Margin	undulate	filamentous	filamentous	entire
Surface	wrinkled with radiating furrows	rugrose and undulating	rugrose	smooth, glistening
Elevation	Umbonate	umbonate	umbonate	convex
Colour	white	dark yellow	yellow	light yellow
Cellular				
Mycelia	dichotomous branching	dichotomous branching	sparingly septate	short chains
Spores	clavate	clavate	sickle-shaped with round tips	budding

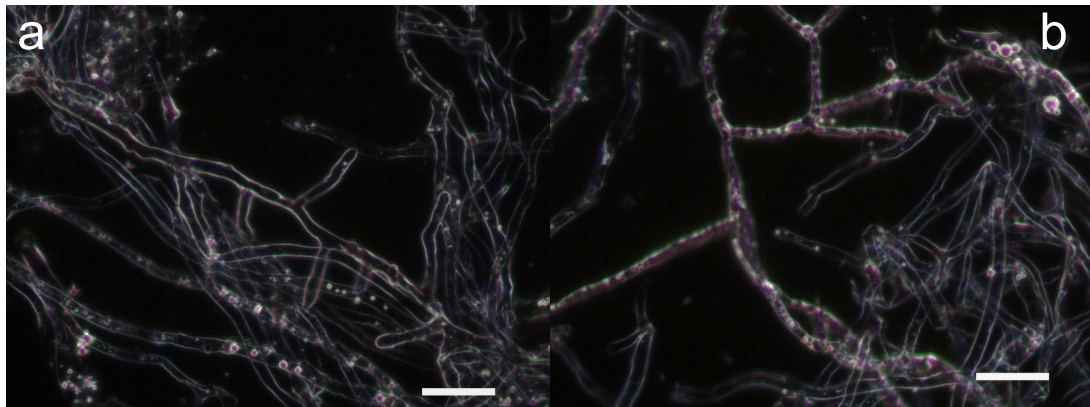


Figure 4.1.2 Sparingly septate mycelia showing dichotomous branching for (a) *E. gossypii* and (b) *E. ashbyi*. Darkfield images at 400 x (bar =25 μ m).

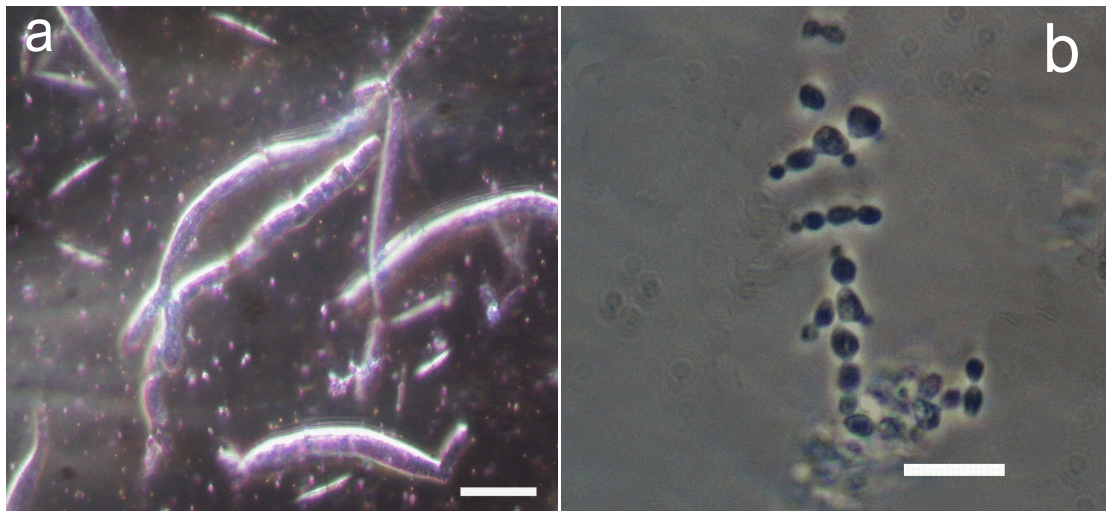


Figure 4.1.3 Spore formation showing (a) needle-like clavate spores in *E. gossypii* Phase contrast image at 400 x (bar=25 μ m) and (b) budding and short chain formation in *C. famata* Phase contrast image at 1000 x (bar=10 μ m).

4.1.2 Localisation of Riboflavin Production

The micrographs in Figure 4.2 indicate the position of riboflavin in the respective cell types. *E. gossypii* has riboflavin produced in vesicles within cells. *Candida famata* has riboflavin produced by a proportion of the entire biomass. This proportion is assumed to be producing riboflavin in the stationary phase as reported by Karos *et al.*, (2004), whereas the remainder of the cells are most likely to be in the lag or logarithmic phases of growth.

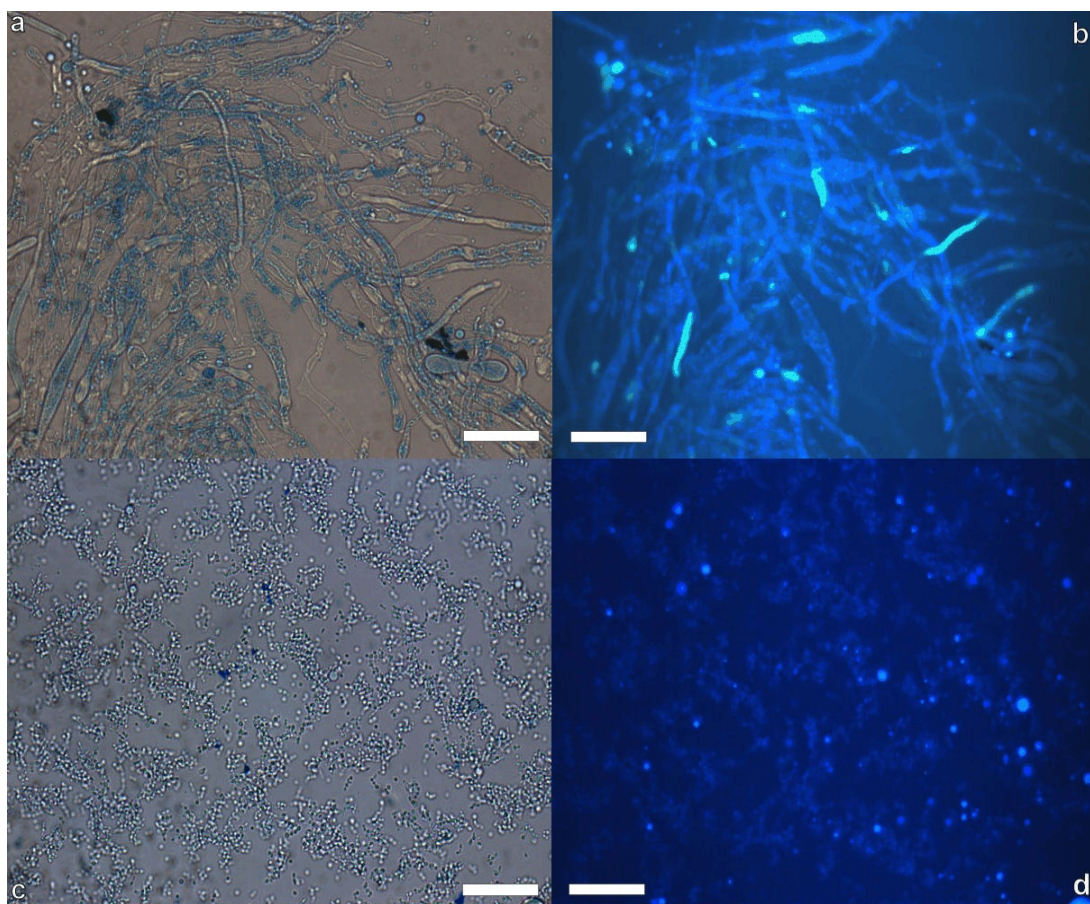


Figure 4.2 Light and UV micrographs at 400x of two fungi showing intracellular localisation of riboflavin. (a) and (b) *E. gossypii* (CBS 109.51) and (c) and (d) *C. famata* (ATCC 20850) light and UV illuminated micrographs respectively. Bar = 25 μm.

4.2 EVALUATION OF FUNGAL GROWTH ON CONVENTIONAL MEDIA

4.2.1 Growth Curve

Four fungi were assessed for their abilities to grow on Ozbas and Kutsal medium using glucose as a carbohydrate source and the resulting growth curves were fitted to the Gompertz growth model in order to determine specific growth rates, doubling times and the times of inoculation (Figure 4.3). Of the four, *E. gossypii* (CBS109.51) and *C. famata*

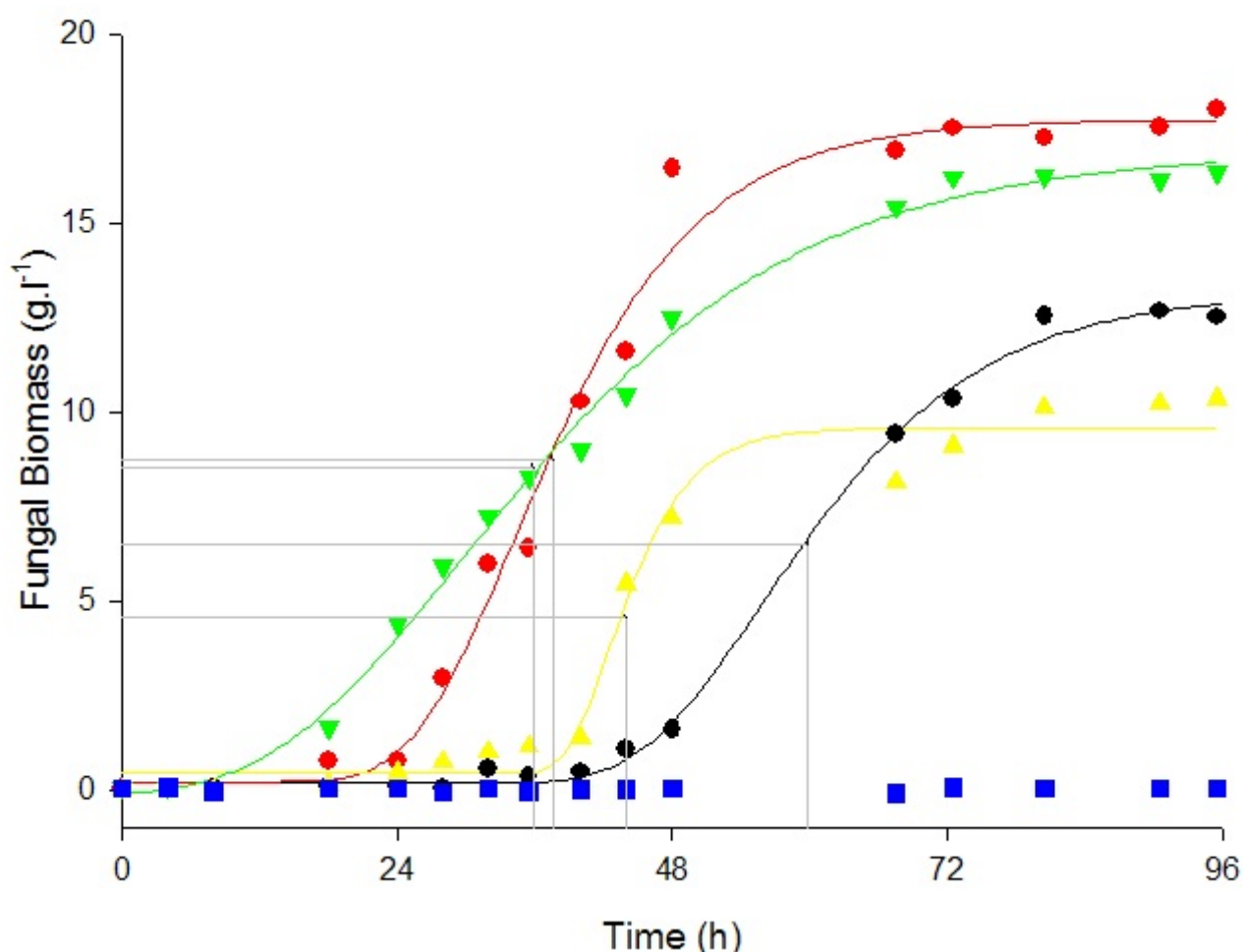


Figure 4.3 Growth curves of four fungi grown on Ozbas and Kutsal liquid medium and fitted to the Gompertz growth model to determine growth parameters. Grey droplines indicate mid-log phases and times of inoculation for each fungus. *E. gossypii* wild type (ATCC 10895) (yellow triangle), *E. gossypii* (CBS 109.51) (red circle), *E. ashbyii* (CBS 206.58), (black circle) and *C. famata* (ATCC 20850) (green inverted triangle).

(ATCC 20850) showed the highest biomass production on glucose indicating an ability to grow on it as a carbohydrate substrate.

4.2.2 Specific Growth Rates and Doubling Times

The growth kinetics of four fungi grown on O&K medium using glucose as a carbon source are shown in Table 4.2. Maximum specific growth rates were calculated using slopes of the fitted Gompertz curves (Figure 4.3). The steeper the curve, the higher the maximum specific growth rates. This showed *E. gossypii* (WT) to have the fastest growth and *C. famata* the slowest (Table 4.2). Doubling times mirrored this trend as they are derived from the specific growth rate calculation. However, mid-log phase times for inoculation purposes indicated otherwise and followed the maximum biomass produced trend, showing both *E. gossypii* and *C. famata* to reach their mid-log phases faster (37.6 and 35.9 h, respectively) whilst *A. gossypii* (WT) reached mid-log phase at 44 h and *E. ashbyi* took 59.8 h to reach mid-log phase (Table 4.2). This was due to the long lag phases observed in both these organisms before growth commenced (Figure 4.3).

Table 4.2 Gompertz parameters and resultant calculations of specific growth rates, doubling times and times of inoculation as well as fit to the curve (R^2).

Organism	Gompertz Parameters	Gompertz Values	Maximum Specific Growth Rates (μ_{max})	Doubling Times (T_d)	Mid-log inoculation times	Curve Fit R^2
<i>E. ashbyi</i>	a	12.9969	0.222	3.1	59.8	0.9977
	b	10.7408				
	x^0	55.9346				
	y^0	0.171				
<i>E. gossypii</i>	a	17.5223	0.357	1.9	37.6	0.9894
	b	9.0168				
	x^0	34.2718				
	y^0	0.2135				
<i>C. famata</i>	a	17.0848	0.188	3.8	35.9	0.9959
	b	16.7542				
	x^0	29.7318				
	y^0	-0.1576				
<i>E. gossypii</i> (WT)	a	9.1518	0.433	1.6	44	0.9803
	b	3.8863				
	x^0	42.5985				
	y^0	0.4228				

4.3 COMPOSITION OF EDIBLE OIL EFFLUENT

Gas Chromatography-Mass Spectroscopy Analysis was carried out on the EOE used and the results are listed below. No significant peaks are noted between 17 and 20 minutes which is the time interval for C10-C20 oils in Figure 4.4 in the Total Ion Chromatograms (TIC) of the sample shown below:

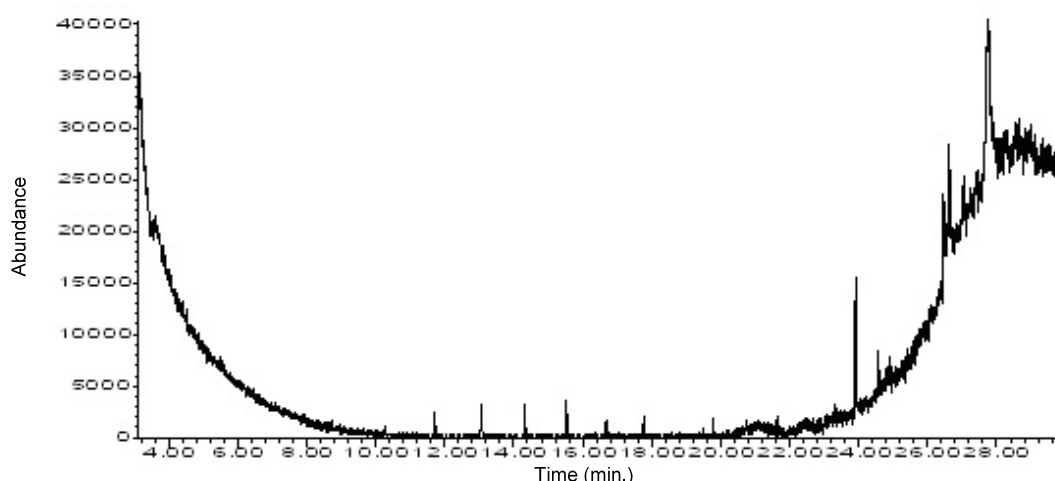


Figure 4.4 Total ion chromatogram of edible oil effluent.

In the Base Peak Chromatogram, two major peaks are observed in Figure 4.5 between 17 and 20 minutes of retention time. These peaks observed in the chromatogram are identified here to be tetradecanoic acid and hexadecanoic acid, with a 98 and 99 percent library match quality, and retention times of 17.44 and 19.53 minutes respectively. Further research into these compounds, confirms the nature of these molecules to be saturated fatty acids, more frequently known as myristic (tetradecanoic acid - C14) and palmitic acid (hexadecanoic acid C-16).

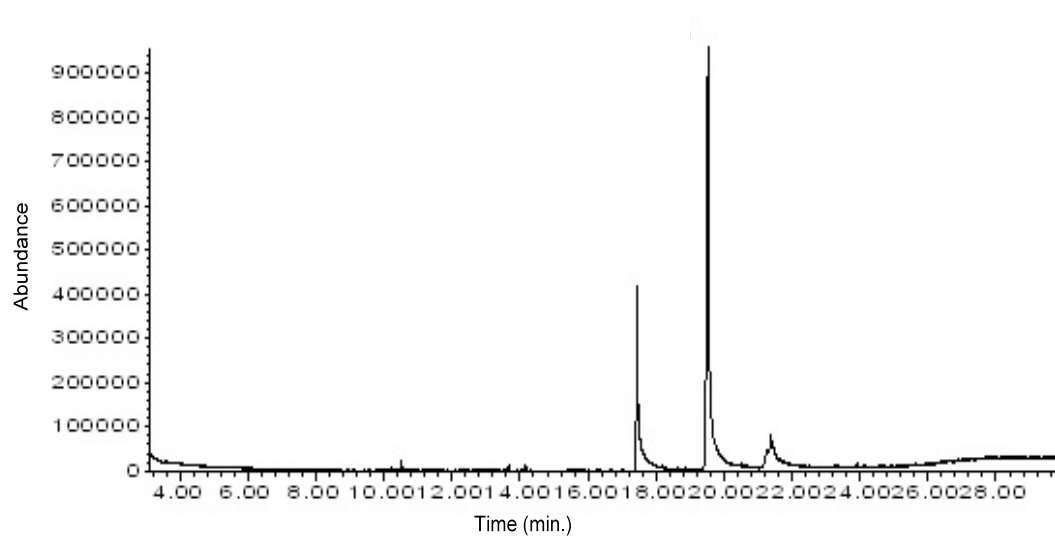


Figure 4.5 Base Peak Chromatogram of edible oil effluent sample showing two peaks that were later identified using mass spectrometry.

Table 4.3 Compounds found in edible oil effluent sample

Compound	Library Match Quality (%)	Retention time (min.)
Tetradecanoic acid	98	17.44
Hexadecanoic acid	99	19.53

4.4 RIBOFLAVIN DETECTION METHOD

A scan of 26 riboflavin concentrations was done over 625 wavelength increments and the results are shown below in a comprehensive three-dimensional scan to show peaks of detection at various wavelengths.

Riboflavin peaks were detected at 265, 347 and 444 nm (Figure 4.6) and these were correlated against concentrations of riboflavin using the square of the Pearson product moment least square correlation coefficient (R^2) for each line.

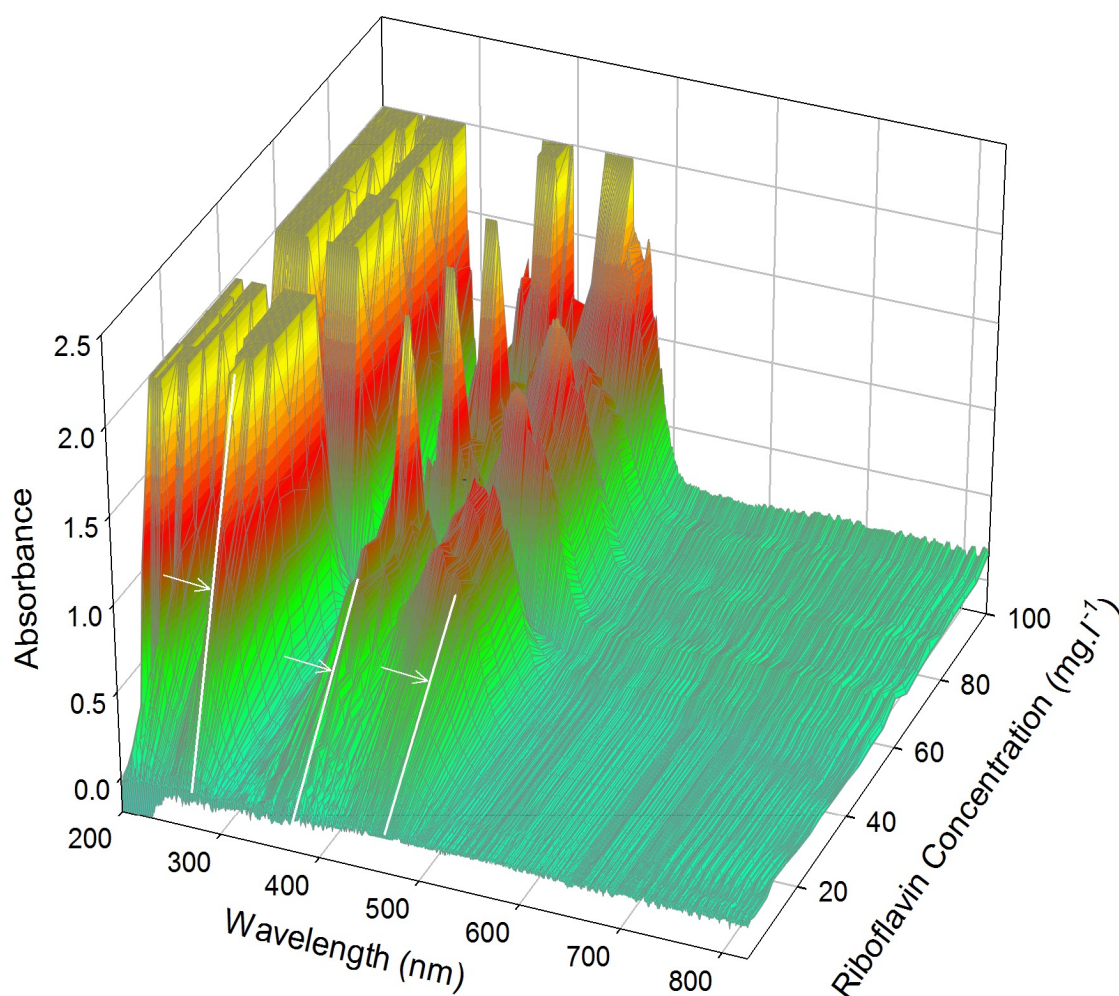


Figure 4.6 Scan of 26 riboflavin concentrations from 200 to 820 nm showing three linear areas (indicated by white arrows) that were further investigated for standard curve preparation.

The three wavelengths were investigated for their sensitivity and range of measurement and results are presented in Figure 4.7 and Table 4.4 below. The wavelength with the widest range was selected to measure riboflavin. This was found to be 444 nm and it also had a very high linear model fit of $R^2 = 0.995$. The wavelength used, concurred with previous researchers who used a similar visible wavelength to measure riboflavin production (Lim *et al.*, 2003; Park and Ming 2004).

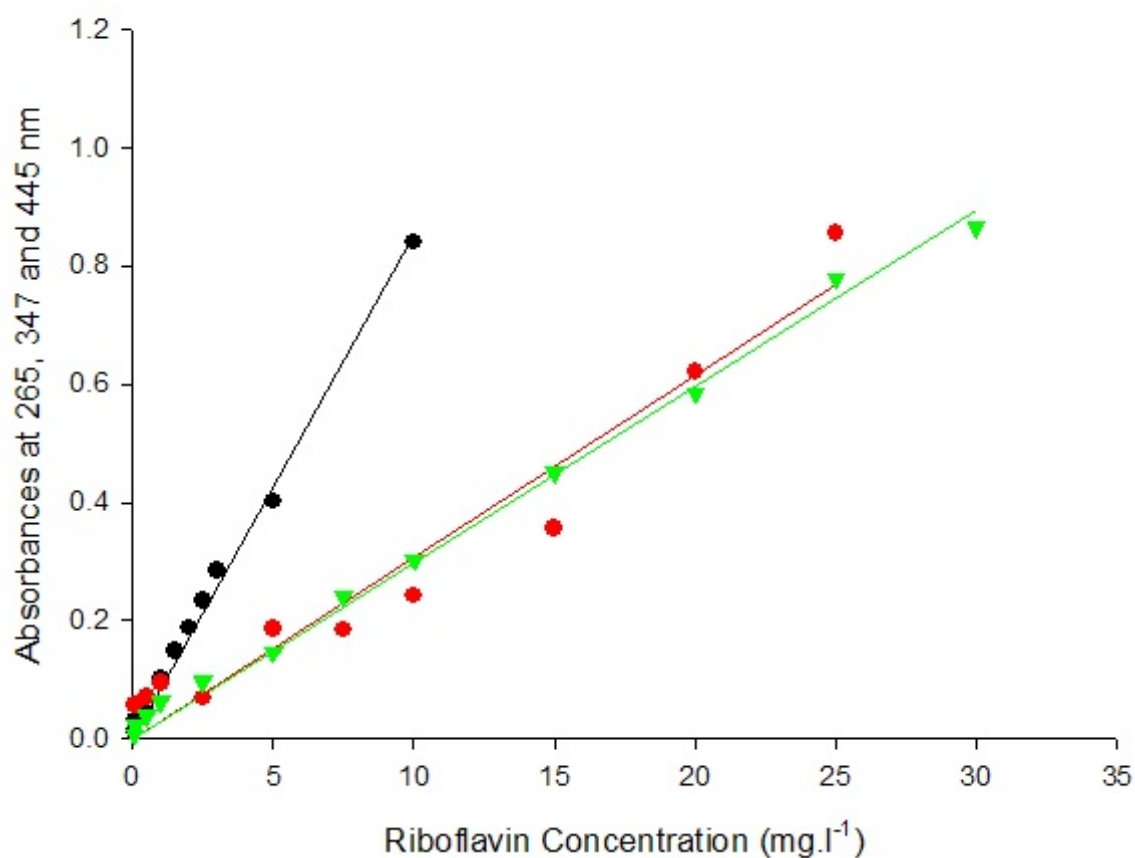


Figure 4.7 Standard curves for three wavelengths, 265 nm (black circle), 347 nm (red circle) and 444 nm (green inverted triangle) investigated for riboflavin measurement.

Table 4.4 Range and sensitivity of riboflavin detection and linear curve fitting values (R^2) calculated by Corel Quattro Pro version 13 spreadsheet for each of the standard curves.

Wavelength (nm)	Range mg/L	Sensitivity (slope)	Linear Fit (R^2)
265	0.05 - 10	0.08506	0.9968
347	0.05 - 25	0.030698	0.9431
444	0.05 - 30	0.029835	0.995

4.5 FUNGAL GROWTH ON EDIBLE OIL EFFLUENT

Figure 4.8 shows four growth curves of *E. gossypii* (wild-type), *E. gossypii* (CBS109.51), *E. ashbyii* (CBS206.58) and *C. famata* (ATCC 208.50) on EOE as carbon source. The graph shows that the model fits all four curves at between 97.9 and 99.7% precision (Table 4.5), hence inferences drawn from the fitted models can be considered precise to those degrees. Both *E. gossypii* CBS (green line) and *C. famata* ATCC (blue line) strains grew better in the effluent over an extended period of time than *E. gossypii* wild-type and *E. ashbyii*. The CBS109.51 mutant form of *E. gossypii* grew five times better on EOE than the wild-type counterpart (green vs red lines). The yeast, *C. famata* grew three times better than the wild-type *E. gossypii* (blue vs red lines).

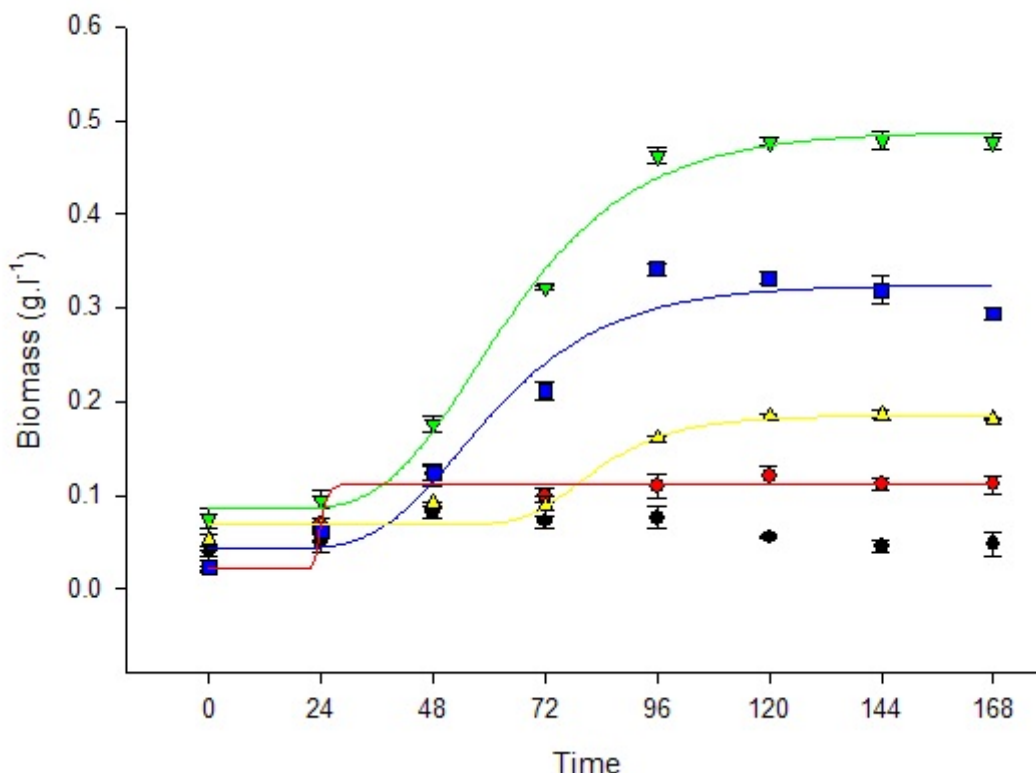


Figure 4.8 Growth curves of four fungi on EOE, fitted to the Gompertz model. *E. gossypii* wild-type (ATCC10895) (red circle) *E. gossypii* (CBS109.51) (green inverted triangle) *E. ashbyii* (CBS206.58) (yellow triangle), and *C. famata* (ATCC 20850) (blue square) and negative control (black circle). Error bars are standard deviations of triplicates.

When examining the model data in Table 4.5, and considering specific growth rates, a slightly different picture emerges. The maximum specific growth rate is calculated on the maximum gradient of each curve and from Figure 4.8, the line with the steepest gradient was found to be *E. gossypii* wild-type which also showed the lowest maximum growth of the four fungi. Hence the largest u_{\max} value of 0.015 h^{-1} although greater than the other three fungi, has to be considered in the context of maximum biomass production as well. Although *E. gossypii* wild-type showed a higher specific growth rate than the other three fungi, the maximum growth of the *E. gossypii* CBS culture and the *C. famata* ATCC culture were far higher. Thus, these latter two cultures were tentatively chosen as candidates for further experiments on EOE.

Table 4.5 Gompertz parameters and resultant calculations of specific growth rates, doubling times and times of inoculation as well as fit to the model (R^2)

Organism	Gompertz Parameters	Gompertz Values	Maximum Specific Growth Rates (μ_{max}) (h^{-1})	Doubling Times (T_d) (h)	Curve Fit (R^2)
<i>E. gossypii</i> (WT)	a	0.091	0.015	45.405	0.979
	b	1.105			
	x^0	23.498			
	y^0	0.021			
<i>E. gossypii</i> CBS	a	0.403	0.004	180.378	0.997
	b	19.388			
	x^0	56.745			
	y^0	0.085			
<i>E. ashbyii</i> CBS	a	0.116	0.002	371.063	0.983
	b	11.435			
	x^0	78.865			
	y^0	0.069			
<i>C. famata</i> ATCC	a	0.281	0.003	237.031	0.981
	b	17.775			
	x^0	53.509			
	y^0	0.043			

4.6 RIBOFLAVIN PRODUCTION ON EDIBLE OIL EFFLUENT

All four fungal types grown on EOE were able to produce riboflavin to varying degrees and production generally increased after 72 hours of incubation (Figure 4.9). Also, shown in the figure are the two highest producers of riboflavin viz., *E. gossypii* CBS culture (green line) and the *C. famata* ATCC culture (blue line). Both these organisms produced significantly more riboflavin than the *E. gossypii* wild-type and *E. ashbyii* CBS culture ($p < 0.05$) on a one-way ANOVA comparison with Tukeys' post-test to compare means. The statistical differences were calculated at the 144-168 h time interval as this is when the riboflavin production levelled off.

The results above were confirmed when examining Table 4.6 which showed that *E. gossypii* CBS culture and the *C. famata* ATCC culture produced riboflavin faster than the other two fungi when grown on EOE. Their production rates were between two and three-times higher than *E. ashbyii* CBS culture and *E. gossypii* wild-type culture, thus

reinforcing the selection of *E. gossypii* CBS culture and the *C. famata* ATCC culture for further mutational studies to improve riboflavin production.

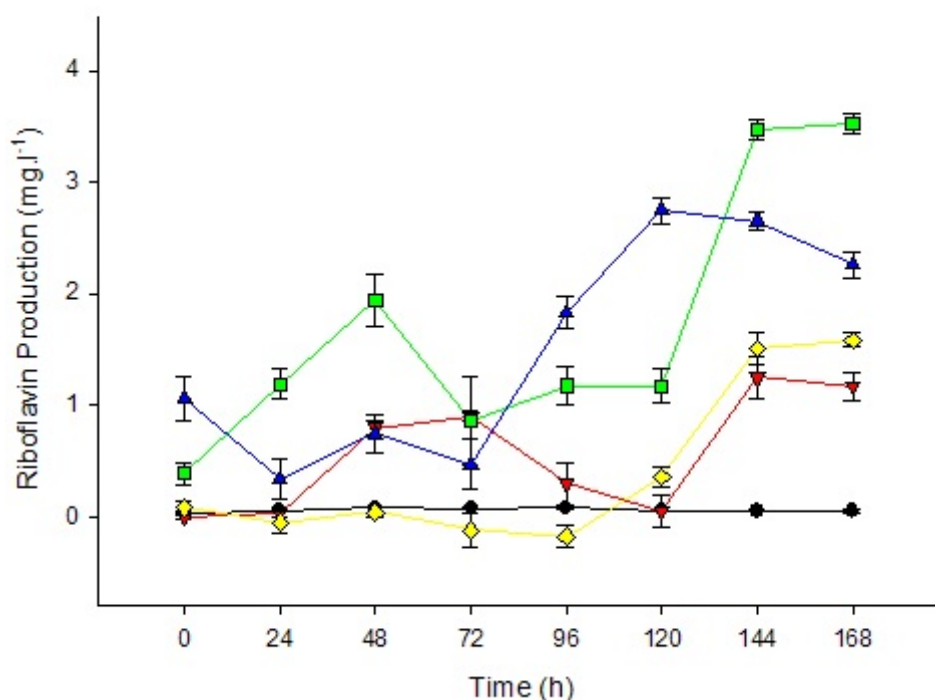


Figure 4.9 Riboflavin production by four fungi grown on EOE after 168 hours. *E. gossypii* wild-type (ATCC 10895) (inverted red triangle), *E. gossypii* CBS 109.51 (green square), *E. ashbyii* (CBS 206.58) (yellow diamond), *C. famata* (ATCC 20850) (blue triangle) and control (black circle). Error bars are standard deviations of triplicates.

Table 4.6 Maximum rate of riboflavin production and the time interval at which they are produced in four fungi grown on EOE.

	Maximum Riboflavin Production Rate (mg.h ⁻¹)	Time Interval of Production (h)
<i>E.gossypii</i> WT	0.052	120-144
<i>E.gossypii</i> CBS	0.147	144-168
<i>E.ashbyii</i> CBS	0.066	144-168
<i>C.famata</i> ATCC	0.114	96-120

4.7 MUTATIONAL STUDIES TO ADAPT MICROORGANISMS FOR GROWTH ON EDIBLE OIL EFFLUENT

The two organisms selected, *E. gossypii* (CBS109.51) and *C. famata* (ATCC 208.50) were subjected to four mutagens at three time intervals and screened on itaconate-containing agar plates to select for riboflavin overproducers. The isolated overproducing colonies were grown on EOE containing liquid media to determine their maximum riboflavin producing potentials.

Of the cultures obtained in mutational studies (Figures 4.10 a-d and 4.11 a-d), those that produced 42 mg/l⁻¹ or more (Table 4.7) were considered as possible candidates for further investigation. These were a sodium azide mutant of *E. gossypii* (43.27 mg.l⁻¹ of riboflavin) and an EMS30 mutant (42.83 mg.l⁻¹ of riboflavin). The mutant derived from sodium azide mutation did not continue to grow after subculture and the EMS 30 mutant produced previously and incorporated into this experiment, was selected and used for further optimization studies. *Candida famata* strains producing riboflavin were not selected because none of the strains produced more than 39 mg.l⁻¹ of riboflavin. Also *C. famata* riboflavin production is known to be inhibited by iron, and scale-up using iron or steel fermenters would then pose an additional problem with this organism.

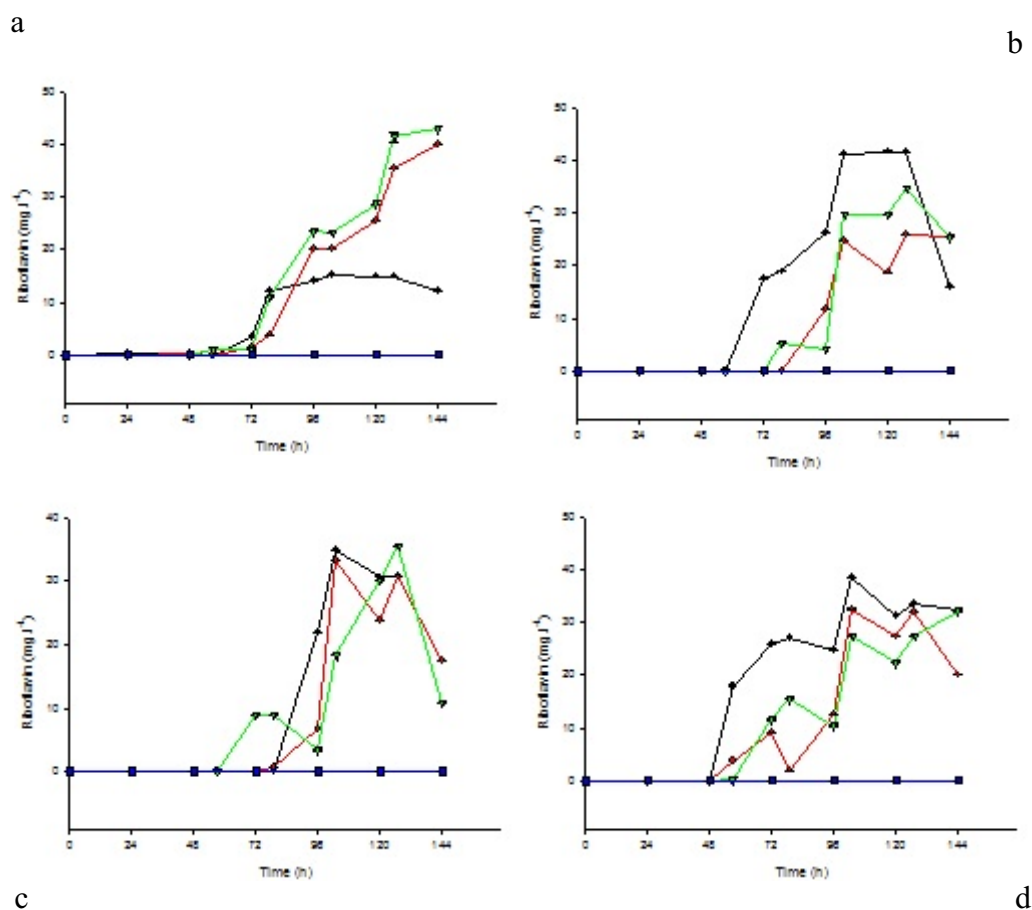
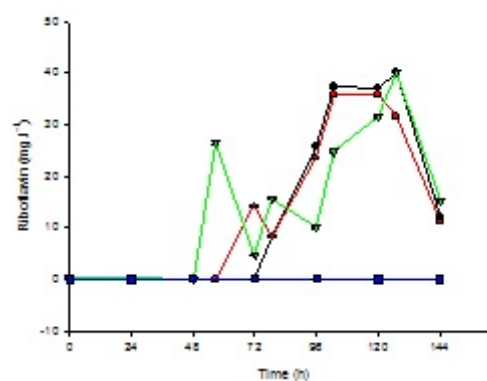
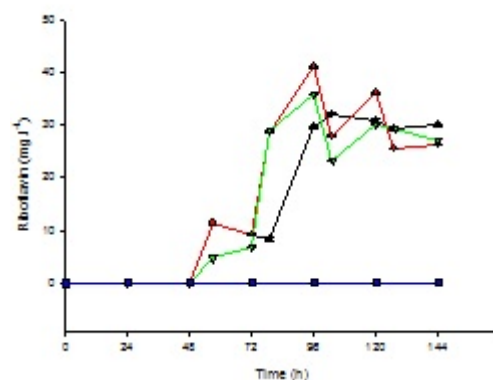
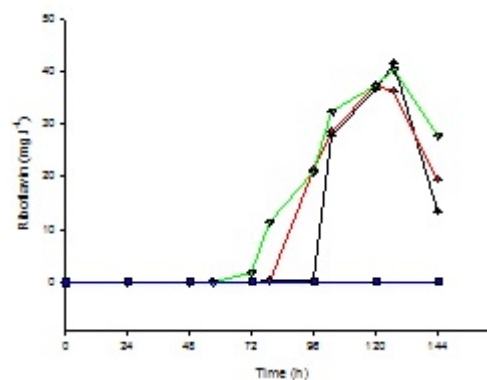
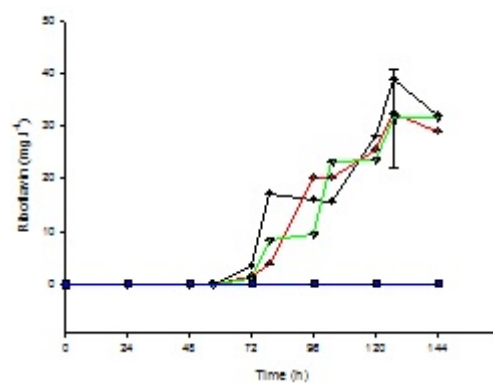


Figure 4.10

Riboflavin production by mutants of *E. gossypii* subjected to mutagens a) EMS, b) U.V. irradiation, c) MNNG and d) sodium azide. Black circle is 10 mins of exposure, red circle is 20 mins of exposure and green inverted triangles are 30 mins of exposure. Control lines are indicated by blue squares.

A summary of the mutant riboflavin production levels is given in Table 4.7.

a



c

d

Figure 4.11

Riboflavin production by mutants of *C. famata* subjected to mutagens a) EMS, b) U.V. irradiation, c) MNNG and d) sodium azide. Black circle is 10 mins of exposure, red circle is 20 mins of exposure and green inverted triangles are 30 mins of exposure. Control lines are indicated by blue squares.

A summary of the mutant riboflavin production levels is given in Table 4.7.

Table 4.7 Composite table showing best mutants of *E. gossypii* and *C. famata* after exposure to each of four mutagenic agents for three time intervals each. Characteristics are ranked within each organism grouping to find the best mutant producer

<i>E. gossypii</i>	Exposure (min)	μ_{\max} (h ⁻¹)	Rank	T _d (h)	Rank	Max Rib (mg.l ⁻¹)	Rank	Prod. Rate (mg.h ⁻¹)	Rank	*Yield (mg.g ⁻¹)	Rank
EMS	10	0.0838	6	8.28	6	15.15	12	0.63	9	4.23	1
	20	0.0731	9	9.48	9	39.94	7	0.89	2	2.59	7
	30	0.0668	12	10.38	12	42.83	2	0.83	6	3.79	2
UV	10	0.0801	7	8.66	7	36.65	9	0.76	7	3.31	3
	20	0.1067	4	6.49	4	37.32	8	0.65	8	2.29	9
	30	0.0724	10	9.57	10	40.2	4	0.84	3	3.04	4
MNNG	10	0.0677	11	10.24	11	32.1	11	0.56	12	2.79	6
	20	0.0734	8	9.4	8	41.01	3	0.57	11	2.09	11
	30	0.0974	5	7.12	5	40.19	6	0.84	3	2.85	5
NaN ₃	10	0.1167	2	5.94	2	43.27	1	0.9	1	2.54	8
	20	0.1079	3	6.43	3	35.77	10	0.63	9	2.21	10
	30	0.4621	1	1.49	1	40.2	4	0.84	3	1.78	12

<i>C. famata</i>	Exposure (min)	μ_{\max} (h ⁻¹)	Rank	T _d (h)	Rank	Max Rib (mg.l ⁻¹)	Rank	Prod. Rate (mg.h ⁻¹)	Rank	*Yield (mg.g ⁻¹)	Rank
EMS	10	0.073	10	9.46	10	38.98	2	0.81	2	3.64	7
	20	0.136	4	5.09	4	32.32	9	0.67	5	3.89	6
	30	0.139	3	5	3	31.74	10	1.32	1	3.36	9
UV	10	0.081	9	8.57	9	41.68	1	0.73	4	3.57	8
	20	0.09	8	7.71	8	25.96	12	0.54	6	8.97	1
	30	0.093	7	7.47	7	34.71	6	0.18	12	6.84	2
MNNG	10	0.071	11	9.77	11	34.79	5	0.48	8	4.43	3
	20	0.15	2	4.63	2	33.19	7	0.46	9	3.9	5
	30	0.163	1	4.25	1	36.61	4	0.76	3	3.3	10
NaN ₃	10	0.106	5	6.49	5	38.5	3	0.53	7	2.29	12
	20	0.093	6	7.43	6	32.55	8	0.45	10	2.6	11
	30	0.055	12	12.52	12	27.48	11	0.38	11	4.12	4

*Yield = yield of riboflavin per unit biomass

4.8 ENZYME ACTIVITY OF SELECTED MUTANT

Since the screening medium contained itaconate which isolates mutants that have an isocitrate lyase enzyme insensitive to feedback by riboflavin production, the isocitrate lyase activities of the pre-and post-mutated *E. gossypii* EMS 30 strain were compared using a Michaelis-Menten plot of the enzyme activity of the two strains.

The mutant showed a higher maximum velocity of enzyme activity ($V_{\max}=0.01328 \text{ U.s}^{-1}$) whereas the wild-type showed a slightly higher substrate affinity ($K_m=46.23 \text{ mM}$) (Figure 4.12 summarised in Table 4.8). This indicated that the speed of the enzyme activity was improved and correlates well with the lower affinity results obtained, since a fast-acting enzyme needs to associate and dissociate with its substrate quicker and would consequently have a lower substrate affinity.

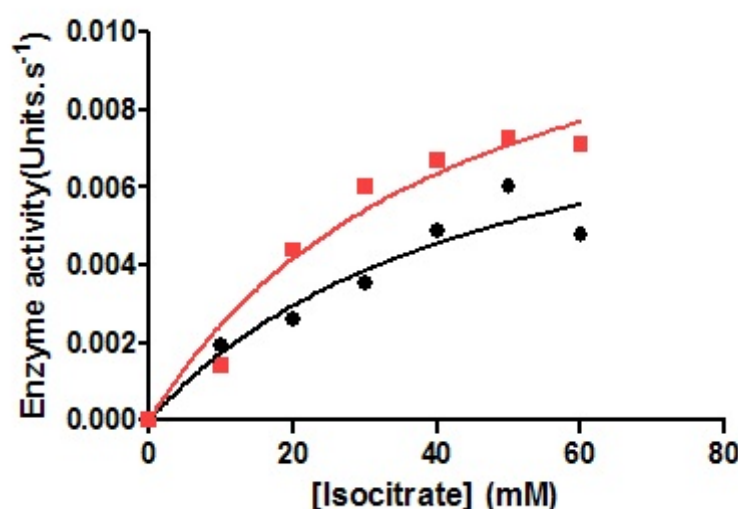


Figure 4.12 Michaelis-Menten plots of enzyme activity of a wild-type *E. gossypii* (black circle) and an EMS 30/1 *E. gossypii* mutant (red square).

Table 4.8 Determination of maximum enzyme velocity (V_{\max}) and Michaelis-Menten constant (K_m) of a wild-type *E. gossypii* and mutant EMS30/1 strain after non-linear curve-fitting. Also included is the goodness-of-fit (R^2)

	V_{\max} (Units.s ⁻¹)	K_m (mM)	R^2
Wild-type <i>E. gossypii</i>	0.009845	46.23	0.9288
Mutant EMS 30/1	0.01328	43.44	0.96

4.9 NUTRIENT SUPPLEMENT SCREENING

4.9.1 Primary Screen

After selecting the mutant, the eight nutrients listed in Table 3.4 were selected from literature to optimize riboflavin production on the EOE-based substrate. Eight supplements (Factors) were initially screened using a fractional-factorial experimental design (Table 4.9) in order to obtain an indication as to which individual and combinations of factors were responsible for both improving, retarding or having no effect on riboflavin production.

Table 4.9 Eight-factor, two-level, half-fraction, resolution IV, fractional factorial design for screening of nutrients to support riboflavin production using EOE as a carbon substrate showing actual/predicted riboflavin production and residuals.

Standard Order	Run Order	Factor levels								Actual	Predicted	Residual
		X_1	X_2	X_3	X_4	X_5	X_6	X_7	X_8	Riboflavin mg.l ⁻¹	Riboflavin mg.l ⁻¹	
1	3	-1	-1	-1	-1	-1	-1	-1	-1	59.26	56.92	2.34
2	18	1	-1	-1	-1	1	-1	1	1	42.50	42.60	-0.10
3	8	-1	1	-1	-1	1	1	-1	1	39.79	36.04	3.75
4	11	1	1	-1	-1	-1	1	1	-1	84.87	90.85	-5.99
5	4	-1	-1	1	-1	1	1	1	-1	11.50	14.83	-3.33
6	10	1	-1	1	-1	-1	1	-1	1	72.83	78.61	-5.78
7	16	-1	1	1	-1	-1	-1	1	1	73.20	63.78	9.42
8	20	1	1	1	-1	1	-1	-1	-1	10.79	11.11	-0.31
9	9	-1	-1	-1	1	-1	1	1	1	59.29	55.96	3.33
10	2	1	-1	-1	1	1	1	-1	-1	70.42	64.64	5.78
11	1	-1	1	-1	1	1	-1	1	-1	22.93	32.35	-9.42
12	13	1	1	-1	1	-1	-1	-1	1	70.02	69.70	0.31
13	19	-1	-1	1	1	1	-1	-1	1	34.86	37.20	-2.34
14	15	1	-1	1	1	-1	-1	1	-1	78.10	77.99	0.10
15	5	-1	1	1	1	-1	1	-1	-1	85.13	88.88	-3.75
16	21	1	1	1	1	1	1	1	1	59.66	53.67	5.99
17	14	0	0	0	0	0	0	0	0	73.40	76.66	-3.26
18	7	0	0	0	0	0	0	0	0	76.79	76.66	0.13
19	12	0	0	0	0	0	0	0	0	76.69	76.66	0.03
20	6	0	0	0	0	0	0	0	0	71.43	76.66	-5.24
21	17	0	0	0	0	0	0	0	0	85.00	76.66	8.34

A half-normal probability plot was used to select factors and the remaining unselected factors were subjected to a Shapiro-Wilk test to determine that they are normally distributed. The probability value of the Shapiro-Wilk test for normalcy was $p > 0.1$.

Individual factors yeast extract (X_1), KH_2PO_4 (X_4) and NaCl (X_6) showed both large (Figure 4.13) and positive effects (Figure 4.14) on the production of riboflavin. In addition, two-factor interactions that were deemed important to investigate since they positively affected riboflavin production were, X_1X_6 and X_1X_7 , with X_7 being a minerals solution (Figure 4.14). Considering the above, factors X_1 , X_4 , X_6 and X_7 were then identified for further screening in a second experiment.

The largest negative factor seems to have been X_5 , corn-steep liquor and this was unusual, considering that literature indicated that this supplement had a positive effect on riboflavin production (Figure 4.14). This factor was then set at low in further experiments because it was found to be involved in one other two-factor positive interactions viz., X_1X_5 although this interaction was below the t -value line. Also, CSL was reduced in previous experiments to below 30 g.l^{-1} and this gave a negative effect for the reduced values, hence the level was kept at 30 g.l^{-1} for the remaining optimization experiments. Other significant negative interactions of note were X_1X_2 (combined yeast and malt extract) and X_1X_3 (combined yeast extract and peptone). All of these except yeast extract were also set at low concentrations for further experiments.

An unusual result to consider was the non-performance of an emulsifier Tween-80 (X_8). It was thought that this factor may enhance solubility of the oil-based effluent and this was not the case. This factor was left out of future experiments.

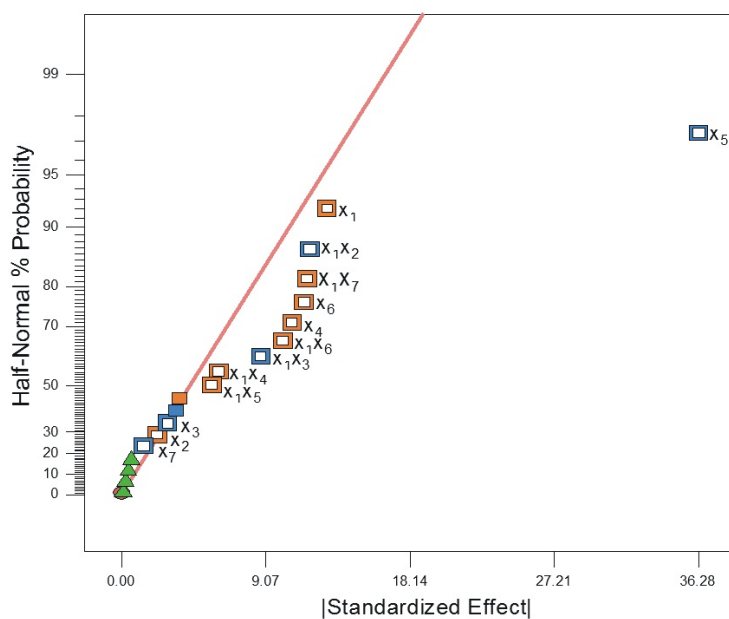


Figure 4.13 Half-normal probability plot to indicate which of the factors were selected to be included in the model. Shapiro-Wilk p -value=0.121.

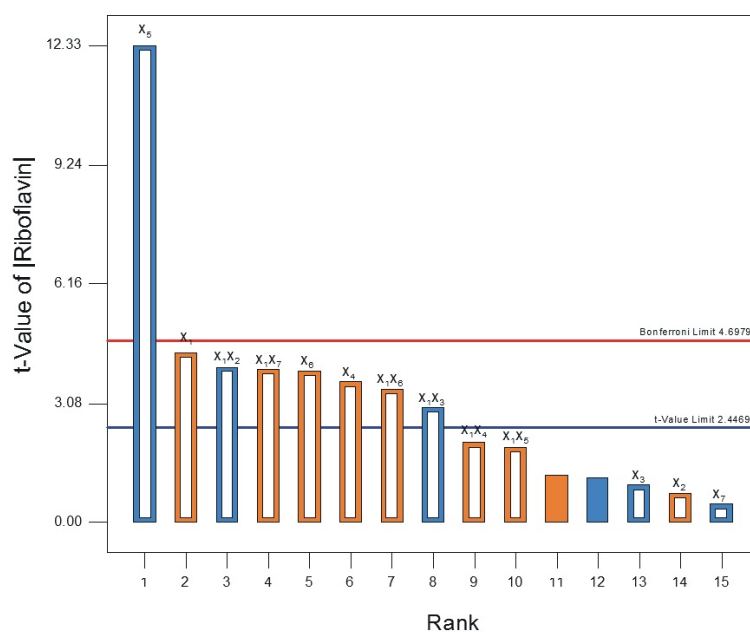


Figure 4.14 Pareto chart to indicate the magnitudes of positive (orange) and negative (blue) effects on riboflavin production in the eight-factor design. Bars above the Bonferroni limit are certainly significant while those above the t-value limit are possibly significant and are included in the model.

The plot shown in Figure 4.15, determines if the data in the model requires mathematical transformation to a logarithmic or quadratic form before interpretation. The power function used relates the standard deviation to a function alpha, the minimum of which is plotted (blue line). Also plotted are the 95% confidence intervals of the power function alpha (red lines) and should the minimum alpha value lie between the 95% confidence intervals, then, a linear mathematical model is sufficient to describe data and no transformation is required.

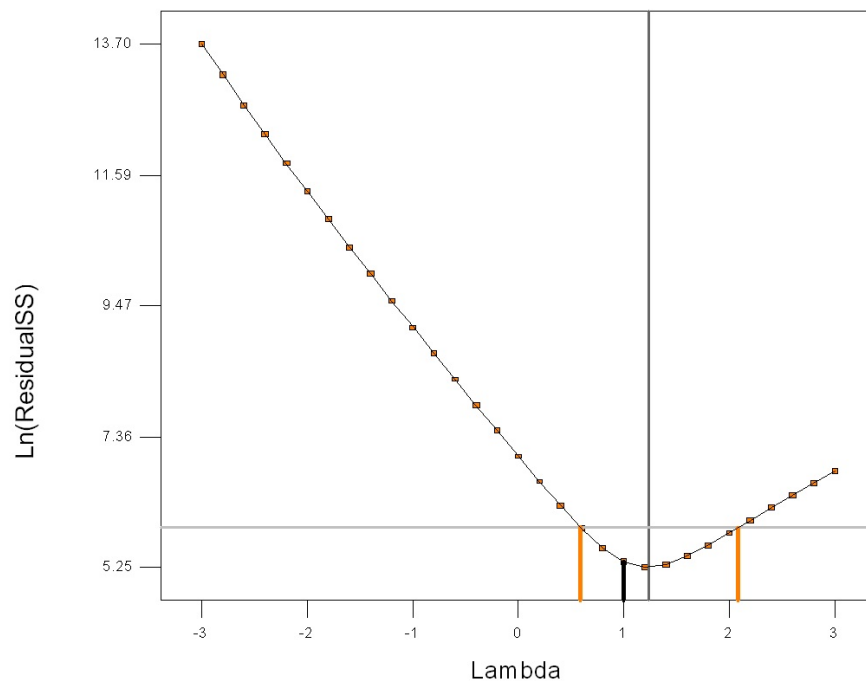


Figure 4.15 Box-Cox plot to determine if a mathematical transformation is required for data to fit a higher-than linear model.

The model generated, given by equation 4.1, was tested using ANOVA and was found to fit selected experimental data significantly ($p=0.0007$) (Table 4.10). Of the eight single factors and five two-factor interactions included in the model, two single-factors malt extract (X_2) and peptone (X_3) did not fit the model significantly. Interactions X_1X_4 and X_1X_5 also were not significant contributors to the effect in the model. Also determined in the fitting of the mathematical model to the data was whether there was curvature in the fit of the data to the model. Since this was a linear model, no curvature was expected, although the curvature value is significant. This is because the center points are clustered higher than the response surface artificially creating a curvature. The lack-of-fit value should not be significant indicating that the model fits the data and this was found to be so (Table 4.10).

Table 4.10 Analysis of variance of the linear model applied to the eight-factor screening experiment, indicating also, significance of one- and two-factor interactions applied to the model. Also shown, are curvature and lack-of-fit results for the applied model

Source	Sum of Squares	df	Mean Square	F Value	p-value Prob > F	
Model	9071.64	13	697.82	20.14	0.0007	significant
X_1 -Yeast Extract	666.08	1	666.08	19.22	0.0046	significant
X_2 -Malt Extract	19.43	1	19.43	0.56	0.4823	
X_3 -Peptone	33.04	1	33.04	0.95	0.3666	
X_4 - K_2HPO_4	458.72	1	458.72	13.24	0.0109	significant
X_5 -Corn Steep Liquor	5265.73	1	5265.73	151.94	< 0.0001	significant
X_6 -NaCl	527.14	1	527.14	15.21	0.008	significant
X_7 -Minerals	7.65	1	7.65	0.22	0.6551	
X_1X_2	559.95	1	559.95	16.16	0.007	significant
X_1X_3	304.94	1	304.94	8.8	0.0251	significant
X_1X_4	148.44	1	148.44	4.28	0.0839	
X_1X_5	128.72	1	128.72	3.71	0.1022	
X_1X_6	409.16	1	409.16	11.81	0.0139	significant
X_1X_7	542.64	1	542.64	15.66	0.0075	significant
Curvature	1837.92	1	1837.92	53.03	0.0003	significant
Residual	207.94	6	34.66			
Lack of Fit	100.36	2	50.18	1.87	0.2677	not significant
Pure Error	107.58	4	26.9			
Cor Total	11117.5	20				

The final equation describing the primary screening experiment incorporating all selected factors is given in equation 4.1. It shows large positive interactions in X_1 alone, X_4 alone,

X_6 alone and the combinations of factors $X_1 X_6$ and $X_1 X_7$ as evidenced by the greater coefficient greater than 5 for each of these single and combination factors in equation 4.1.

$$\text{Riboflavin} = +54.70 + 6.45*X_1 + 1.10*X_2 - 1.44*X_3 + 5.35*X_4 - 18.14*X_5 + 5.74*X_6 - 0.69*X_7 - 5.92*X_1 X_2 - 4.37*X_1 X_3 + 3.05*X_1 X_4 + 2.84*X_1 X_5 + 5.06*X_1 X_6 + 5.82*X_1 X_7 \quad (4.1)$$

Of the five positive significant factors found (X_1, X_4, X_5, X_6 and X_7), there were two sets of large positive interactions also found, $X_1 X_6$ and $X_1 X_7$ (Figure 4.14 and Equation 4.1). It was interesting to observe these three interactions together ($X_1 X_6 X_7$) in a cube plot (Figure 4.16). When all three factors were at their highest, the maximum riboflavin production predicted by the model was 111 mg.l⁻¹. Various other combinations of these factors are shown in the plot and the lowest riboflavin production was predicted when both X_1 and X_6 were low while X_7 was high. Interestingly, this indicated a possible negative interaction of X_7 with the low values of the other two factors and caution with this factor level would have to be exercised in future experiments.

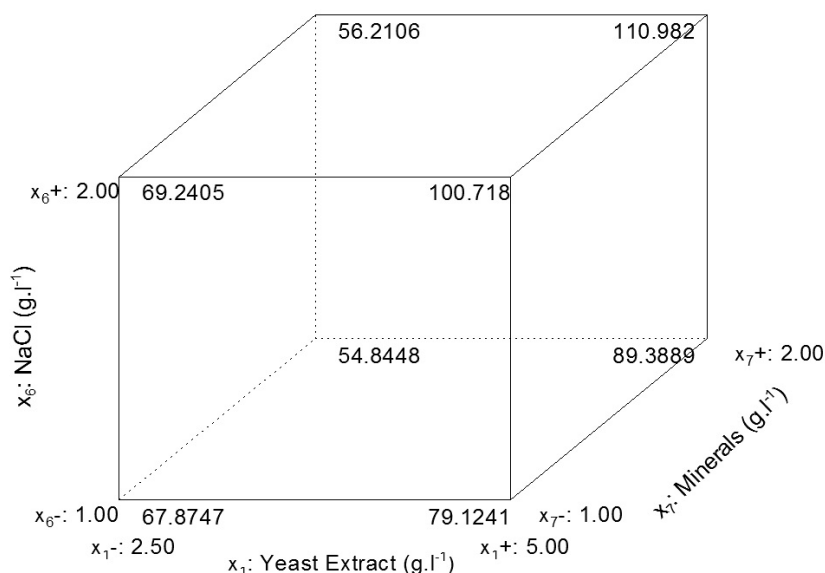


Figure 4.16 Interactions among three factors, yeast-extract, NaCl and minerals to show increased riboflavin production.

The highest two-factor interaction in the pareto chart (Figure 4.14) was found to be the interaction between yeast extract and minerals (X_1X_7). Three-dimensional surface plots (Figures 4.17 and 4.18) were drawn to elucidate the direction that the next experiment should take with regard to these two factors. Both X_1 and X_7 were predicted to increase riboflavin production. Also investigated was the effect of NaCl (X_6) on the shape of the three-dimensional plots Figs 4.17 and 4.18 showing the low and high values of NaCl, a minimum and maximum of 82 and 112 mg.l⁻¹ of riboflavin were predicted. This predicted value was higher than the actual value of 85 mg.l⁻¹ obtained in standard order run 4 of this experiment. The predicted value indicated an increase in NaCl was required as well. The other individual factor to be increased since it was a positive factor was K₂HPO₄ (Figure 4.14). It also interacts with X_1 to have a positive two-factor interaction although, this was not significant.

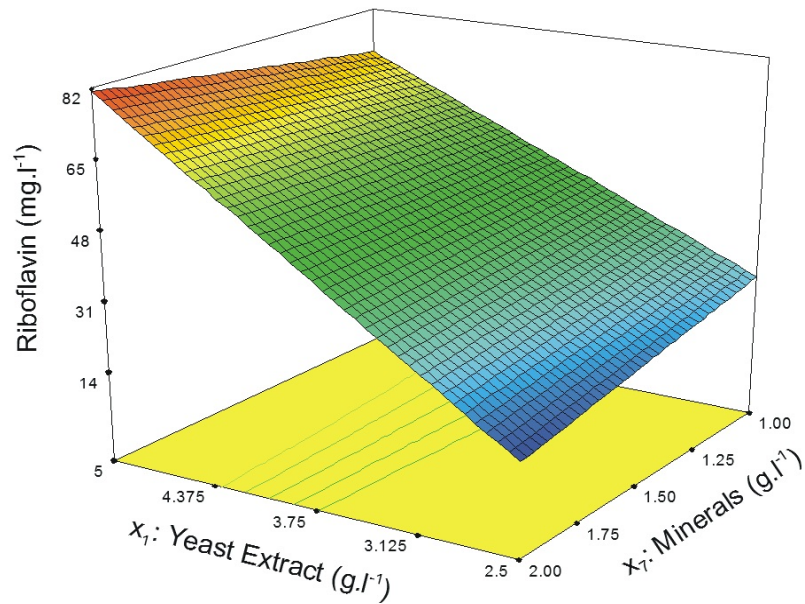


Figure 4.17 Three-dimensional plot to show effect of low NaCl concentration on riboflavin production and the interaction of yeast-extract and minerals.

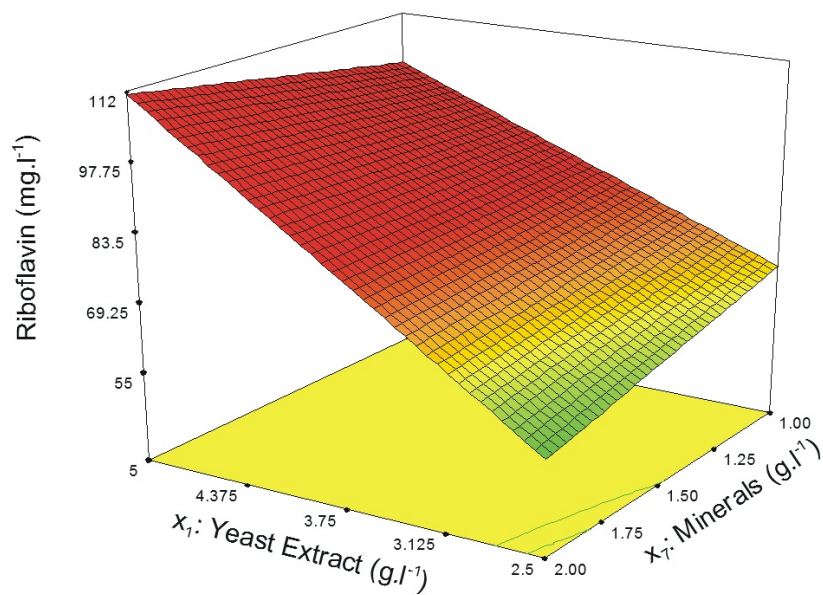


Figure 4.18 Three-dimensional plot to show effect of high NaCl concentration on riboflavin production and the interaction of yeast-extract and minerals.

4.9.2 Secondary Screen

The second screening experiment increased yeast extract, NaCl, K₂HPO₄ and minerals concentrations to determine their effect on riboflavin production by the mutant. The factor levels are detailed in Table 3.6 of the previous chapter. Table 4.11 is a summary of the design of the four-factor full-factorial design. Since this was a full-factorial design, all factors were included in the analysis to follow.

Table 4.11 Four-factor, two-level, full factorial design for screening of nutrients to support riboflavin production using EOE as a carbon substrate

Std Order	Run Order	Factor				Actual	Predicted	Residual
		X_1	X_2	X_3	X_4	Riboflavin mg.l ⁻¹	Riboflavin mg.l ⁻¹	
1	7	-1	-1	-1	-1	39.66	39.66	0
2	1	1	-1	-1	-1	72.78	72.78	0
3	16	-1	1	-1	-1	57.96	57.96	0
4	18	1	1	-1	-1	54.21	54.21	0
5	9	-1	-1	1	-1	71.7	71.7	0
6	17	1	-1	1	-1	59.03	59.03	0
7	10	-1	1	1	-1	40.73	40.73	0
8	5	1	1	1	-1	75.73	75.73	0
9	21	-1	-1	-1	1	90.14	90.14	0
10	4	1	-1	-1	1	87.72	87.73	0
11	14	-1	1	-1	1	40.53	40.53	0
12	19	1	1	-1	1	122.58	122.58	0
13	6	-1	-1	1	1	59.03	59.03	0
14	12	1	-1	1	1	76.06	76.06	0
15	13	-1	1	1	1	28.6	28.6	0
16	8	1	1	1	1	67.82	67.82	0
17	2	0	0	0	0	48.53	47.69	0.84
18	3	0	0	0	0	45.42	47.69	-2.27
19	20	0	0	0	0	47.65	47.69	-0.045
20	11	0	0	0	0	48	47.69	0.31
21	15	0	0	0	0	48.86	47.69	1.17

The half-normal plot (Figure 4.19) shows the selection of all factors to be included in a mathematical model to describe riboflavin production under the influences of these factors. Of note is the highest positive effect of yeast extract (X_1) that is followed by positive interactions for yeast extract and NaCl (X_1X_2) and minerals (X_4). The three-factor interaction predicted to be positive in the previous experiment ($X_1X_2X_4$), showed up as positive in this experiment as well, validating the choice of these three factors. Also shown as a positive interaction were yeast extract and minerals (X_1X_4) which again validated the previous experiment (Figure 4.18).

Of the negative interactions, the four factors together showed the strongest negative interaction with K_2HPO_4 and minerals (X_3X_4) contributing to this negative effect. K_2HPO_4 as a single factor also showed a negative effect on riboflavin production (Figure 4.20).

All factors included in the model were significant ($p < 0.05$) and the model itself was found to significantly fit the data ($p < 0.0001$). Several two- and three-factor interactions were also found to be significant except for $X_2X_3X_4$ which was not significant (Table 4.12). Since $X_2X_3X_4$ contributed a very small effect to overall riboflavin production as inferred by its cofactor below (Eq 4.2), it was ignored as an interaction in further decisions. There was also significant curvature in this model which was investigated in the three-dimensional plots below.

Table 4.12 Analysis of variance of the linear model applied to the four-factor screening experiment, indicating also, significance of one- and two-factor interactions applied to the model. Also shown, are curvature and lack-of-fit results for the applied model

Source	Sum of Squares	df	Mean Square	F Value	p-value	
					Prob > F	
Model	8205.43	15	547.03	298.31	< 0.0001	significant
X_1 -Yeast Extract	2198.76	1	2198.76	1199.03	< 0.0001	significant
X_2 -NaCl	288.77	1	288.77	157.47	0.0002	significant
X_3 - K_2HPO_4	471.72	1	471.72	257.24	< 0.0001	significant
X_4 -Minerals	633.6	1	633.6	345.52	< 0.0001	significant
X_1X_2	862.08	1	862.08	470.11	< 0.0001	significant
X_1X_3	57.89	1	57.89	31.57	0.0049	significant
X_1X_4	443.06	1	443.06	241.61	0.0001	significant
X_2X_3	89.98	1	89.98	49.07	0.0022	significant
X_2X_4	94.48	1	94.48	51.52	0.002	significant
X_3X_4	1089.96	1	1089.96	594.38	< 0.0001	significant
$X_1X_2X_3$	30.96	1	30.96	16.88	0.0147	significant
$X_1X_2X_4$	574.32	1	574.32	313.19	< 0.0001	significant
$X_1X_3X_4$	16.72	1	16.72	9.12	0.0392	significant
$X_2X_3X_4$	6.15	1	6.15	3.35	0.141	
$X_1X_2X_3X_4$	1347	1	1347	734.55	< 0.0001	significant
Curvature	1177.09	1	1177.09	641.89	< 0.0001	significant
Pure Error	7.34	4	1.83			
Cor Total	9389.85	20				

The final equation describing the four-factor screening experiment is given in equation 4.2. Large positive effects are seen for X_1 and X_4 and with interactions of X_1X_2 , X_1X_4 and the three-factor interaction of $X_1X_2X_4$.

$$\begin{aligned}
 \text{Riboflavin} = & +65.27 + 11.72X_1 - 4.25X_2 - 5.43X_3 + 6.29X_4 + 7.34X_1X_2 - 1.90X_1X_3 \\
 & + 5.26X_1X_4 - 2.37X_2X_3 - 2.43X_2X_4 - 8.25X_3X_4 + 1.39X_1X_2X_3 + 5.99X_1X_2X_4 - 1.02X_1X_3X_4 - 0.62X_2X_3X_4 \\
 & - 9.18X_1X_2X_3X_4
 \end{aligned} \quad (4.2)$$

Since $X_1X_2X_4$ was found to be a positive effect, the three factors were plotted on a cube plot to determine the various interaction effects on riboflavin production (Figure 4.21). In this plot a high of 95 mg.l⁻¹ was less than that of the experimental values obtained. Two-factor interactions were then investigated in the following two three-dimensional plots to separate the three factor interactions and determine if a clearer conclusion could be obtained.

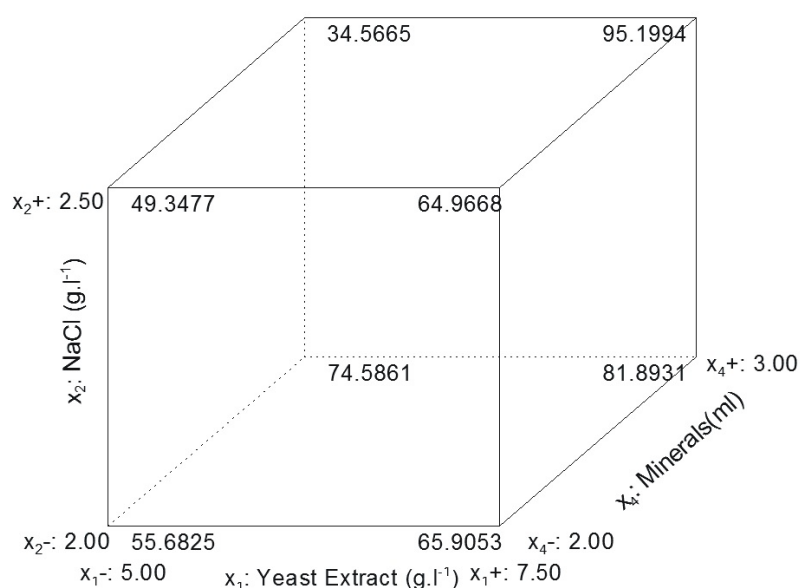


Figure 4.21 Interactions among yeast-extract, NaCl and minerals to show increased production of riboflavin.

Since yeast extract and NaCl (X_1X_2) were the first positive combination effect these were chosen as the axes for the three-dimensional plots while varying minerals concentration (X_4). A decrease in minerals concentration showed a marked effect on predicted riboflavin production reducing it to 73 mg.l⁻¹ (Figure 4.22), while increasing minerals concentrations to their maximum increased riboflavin concentration to 123 mg.l⁻¹ (Figure 4.23). This showed a 9.8% increase in riboflavin production from the previous experiment. The value agreed well with the actual value of 123 mg.l⁻¹ obtained in standard order run 12 of this experiment (Table 4.11) Also of note in Table 4.12 is the curvature value coupled with the shapes of the graph in Figure 4.23 to indicate that the maxima are being reached for these factors (red zone). The following optimization experiment was then designed with an increased mineral concentration, a lowered

K_2HPO_4 concentration and varying yeast extract and NaCl concentrations over a range as shown in Table 3.8.

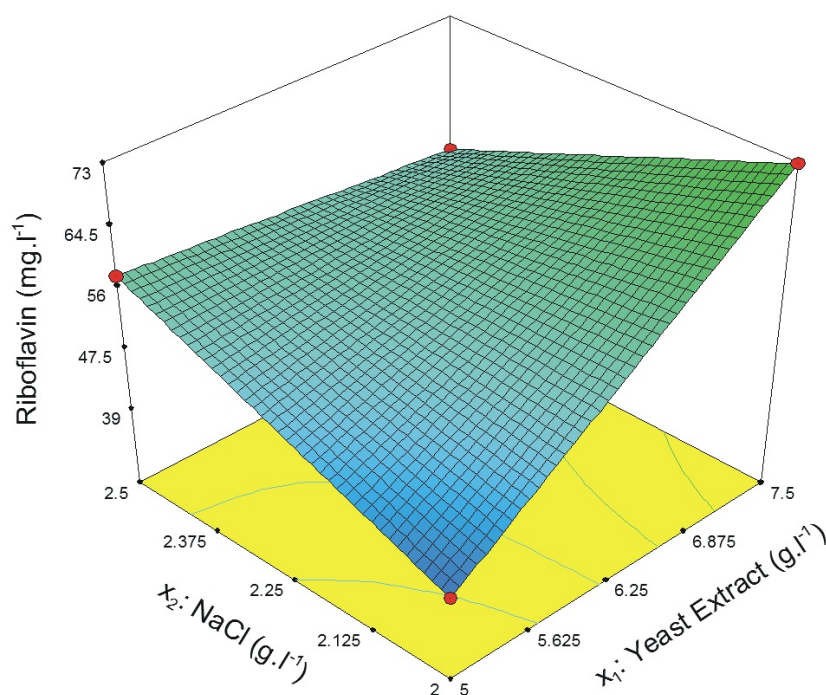


Figure 4.22 Three-dimensional plot to show the effect of low minerals concentration on riboflavin production.

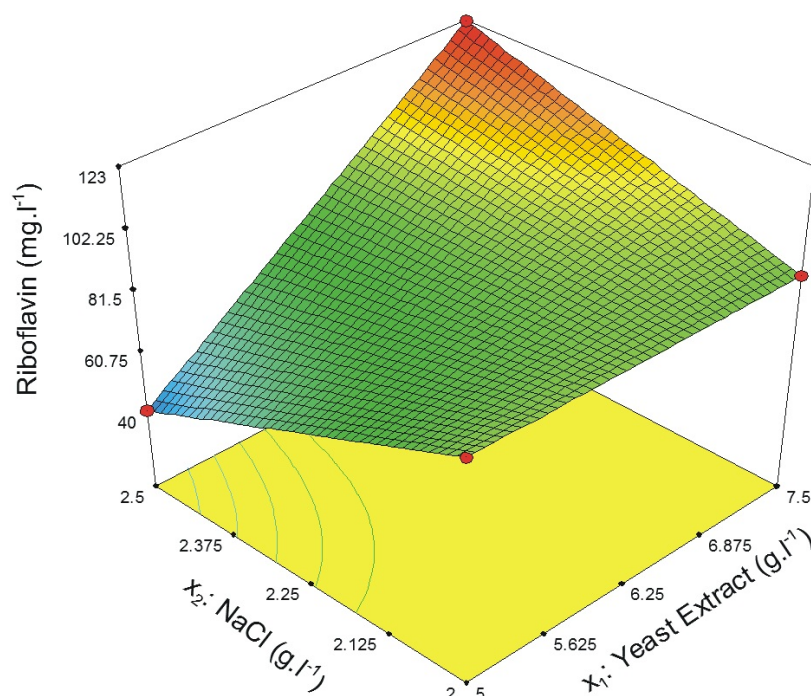


Figure 4.23 Three-dimensional plot to show the effect of high minerals concentration on riboflavin production.

4.9.3 Optimization Experiment

This optimization experiment investigated the effects of yeast extract and NaCl on the production of riboflavin with a two-factor face-centered orthogonal design (Table 4.13). Alpha values are the increased and decreased values above and below the maxima and minima for the experiment. The amounts of increase and decrease were detailed in Table 3.9 of methods.

As seen in Table 4.14, the model was a quadratic transformation of data including squared factors of both X_1 and X_2 . The model was found to significantly fit the data ($p < 0.0001$) with all other factors significantly affecting riboflavin production as well at $p < 0.05$. Also, not shown are the fits of the model to the data using R^2 with both the R^2 and adjusted R^2 giving values of 0.97 and 0.96 respectively, indicating a very good fit to the model of the data points.

Table 4.13 Two-factor, face-centered, central composite design for optimization of nutrients to support riboflavin production using EOE as a carbon substrate showing actual/predicted riboflavin values as well as residuals. Alpha is set at 1.414

Standard Order	Run Order	Factors		Actual Value	Predicted Value	Residual
		X_1	X_2	mg.l ⁻¹	mg.l ⁻¹	
1	3	7.5	2.5	131.559	128.28	3.28
2	1	10	2.5	116.104	114.19	1.92
3	7	7.5	3	101.938	99.11	2.83
4	13	10	3	124.792	123.33	1.47
5	12	6.98	2.75	91.4982	94.84	-3.34
6	10	10.52	2.75	100.594	102	-1.41
7	5	8.75	2.4	138.416	141.11	-2.69
8	4	8.75	3.1	124.888	126.94	-2.06
9	11	8.75	2.75	125.905	125.66	0.25
10	8	8.75	2.75	125.529	125.66	-0.13
11	9	8.75	2.75	125.569	125.66	-0.089
12	2	8.75	2.75	126.453	125.66	0.8
13	6	8.75	2.75	124.832	125.66	-0.83

Table 4.14 Analysis of variance of the quadratic model applied to the two-factor optimizing experiment, indicating also, significance of one- two- and squared-factor interactions applied to the model. Also shown, are curvature and lack-of-fit results for the applied model

Source	Sum of Squares	df	Mean Square	F Value	p-value Prob > F	
Model	2160.47	5	432.09	59.72	< 0.0001	significant
X_1 -Yeast Extract	51.32	1	51.32	7.09	0.0323	significant
X_2 -NaCl	200.64	1	200.64	27.73	0.0012	significant
X_1X_2	366.9	1	366.9	50.71	0.0002	significant
X_1^2	1290.15	1	1290.15	178.31	< 0.0001	significant
X_2^2	121.82	1	121.82	16.84	0.0046	significant
Residual	50.65	7	7.24			
Lack of Fit	49.25	3	16.42	46.92	0.0014	significant
Pure Error	1.4	4	0.35			
Cor Total	2211.12	12				

The final quadratic equation describing the interaction between yeast extract and NaCl is shown in equation 4.3. There is a strongly positive interaction between the two factors as shown by the coefficient of X_1X_2 .

$$\text{Riboflavin} = +125.66 + 2.53*X_1 - 5.01*X_2 + 9.58*X_1*X_2 - 13.62*X_1^2 + 4.18*X_2^2 \quad (4.3)$$

Figures 4.24 and 4.25 indicated a three- and two-dimensional contour plot respectively of the interaction between yeast extract and NaCl. Figure 4.24 shows a typical rising ridge to indicate that the factors can be optimized numerically. Also of note in figure 4.24 is that the ridge does not fall away sharply, indicating that the experiment is robust around the optimum point and riboflavin values would not decrease dramatically were the parameters to vary slightly. Figure 4.25 shows the contours to be converging on a point (red region) which could be predicted using equation 4.3. The point prediction was done using Design Expert 7.1.6 and the resultant five possible solutions were presented in Table 4.15. Of the solutions, the most viable choice was one with a yeast extract concentration of 8.43 g.l⁻¹ and NaCl concentration of 2.5 g.l⁻¹ producing a possible maximum of 135.76 mg.l⁻¹ riboflavin as it had the lowest standard error of mean of the five solutions. This represented an increase of 11% over the previous experiment and an overall increase from the start of experimentation from 3.52 mg.l⁻¹ to the current

predicted maximum of 135.71 mg.l^{-1} . This represents an overall increase of 3757% from the unmutated unoptimized culture.

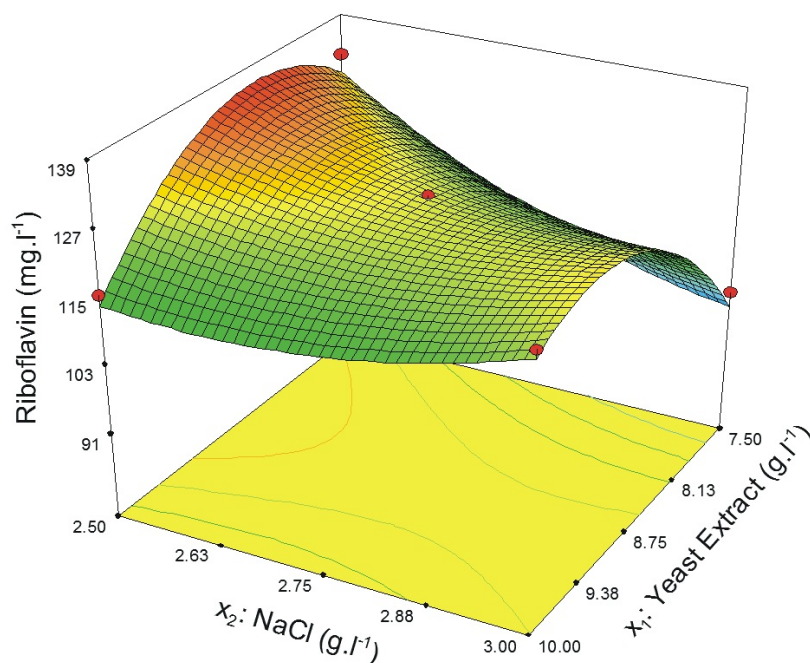


Figure 4.24 Interaction between yeast extract and NaCl to show a peak riboflavin production.

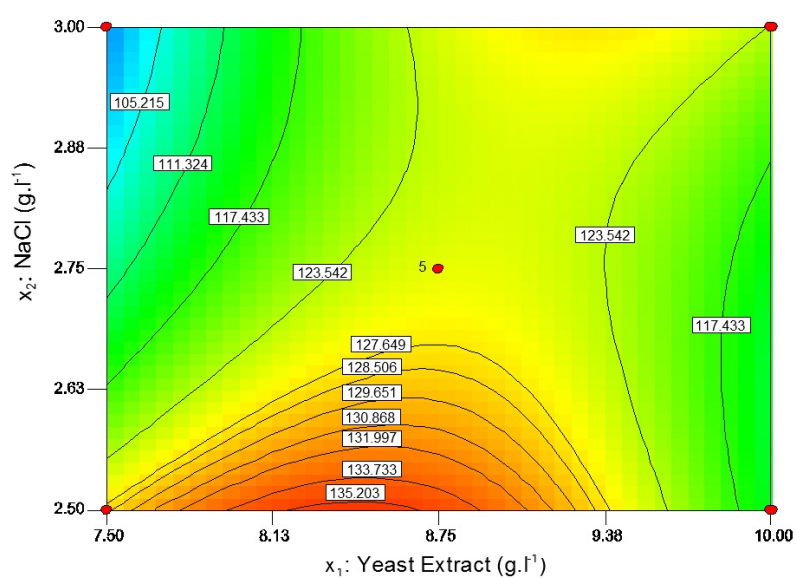


Figure 4.25 Contour plot to show location of peak riboflavin production with varying yeast extract and NaCl concentrations.

Table 4.15 Optimized solutions from the model generated for the two remaining factors, yeast extract and NaCl to maximize riboflavin production

Solution	Yeast Extract	NaCl	Riboflavin	Std Error of Mean	Desirability	
Number	g.l ⁻¹	g.l ⁻¹	g.l ⁻¹			
1	8.43	2.5	135.761	±1.43	0.943	Selected
2	8.39	2.5	135.748	±1.44	0.943	
3	9.3	3	127.526	±1.51	0.768	
4	9.34	3	127.517	±1.52	0.768	
5	9.36	3	127.501	±1.53	0.767	

4.9.4 Confirmatory Experiment

A confirmatory experiment was done to determine whether the optimized parameters above would produce predicted riboflavin values under the conditions stated in Table 4.15. The graph (Figure 4.26) indicated that riboflavin production increased to 132.28 mg.l⁻¹ which was close to the absolute predicted value of 135.76 mg.l⁻¹ after 144 hours and that the production was delayed to after the biomass optimum (Figure 4.27). Also shown is the overall increase in riboflavin production and the sharp increase after 48 h compared to the unoptimized mutant and the unmutated wild-type. Biomass increases are faster than riboflavin production, tapering off at between 48 and 72 h. The quantities are significantly different though and riboflavin production after optimization is definitely more ($p < 0.01$) than both the unoptimized mutant and the wild-type. This successfully demonstrated the progressive strategy of mutation and statistical optimization for increasing riboflavin production on EOE.

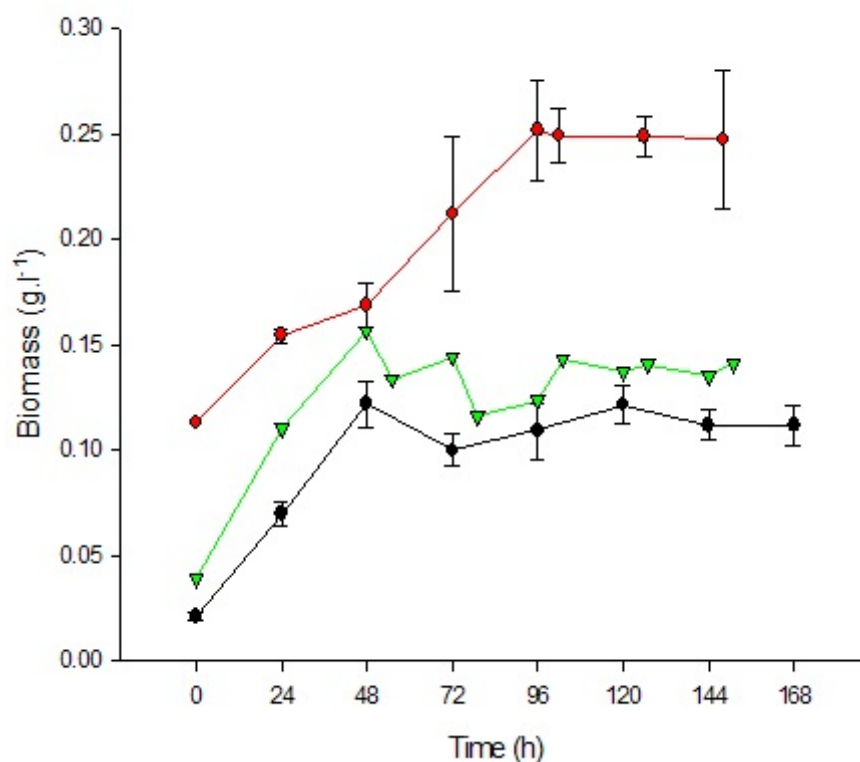


Figure 4.26 A comparison of biomass production by *E. gossypii* prior to mutation (black circle), after mutation (green inverted triangle) and after statistical media optimization (red circle).

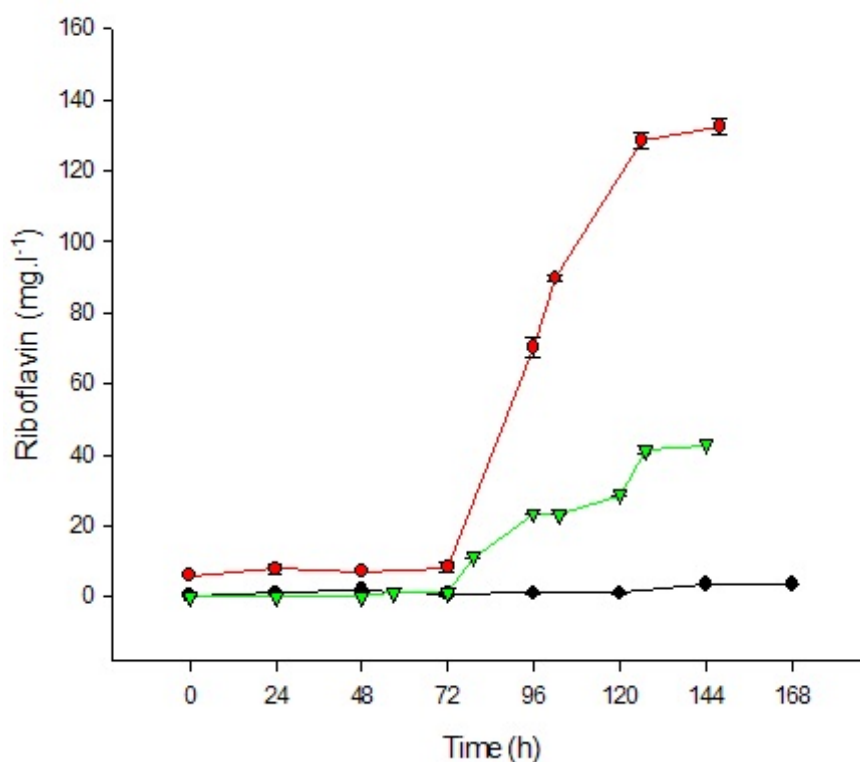


Figure 4.27 A comparison of riboflavin production by *E. gossypii* prior to mutation (black circle), after mutation (green inverted triangle) and after statistical media optimization (red circle).

A 2-litre fermenter was also run to determine if the flask experiments were repeatable in a laboratory fermentation. The maximum riboflavin produced was 130 mg.l^{-1} which was slightly less than flask experiments (Figure 4.28 vs Figure 4.27). The biomass production increased slightly compared to flask experiments (Figure 4.26). Also shown is the decrease in oil concentration over the incubation period to show that oil was used as a substrate for riboflavin production with a reduction in oil content from 5309 to 2519 mg.l^{-1} . This indicated that the yield for riboflavin was 46.59 mg.g^{-1} oil. The pH increased over incubation to approximately pH 8. Riboflavin production was thus shown to be upscalable with little loss in yield.

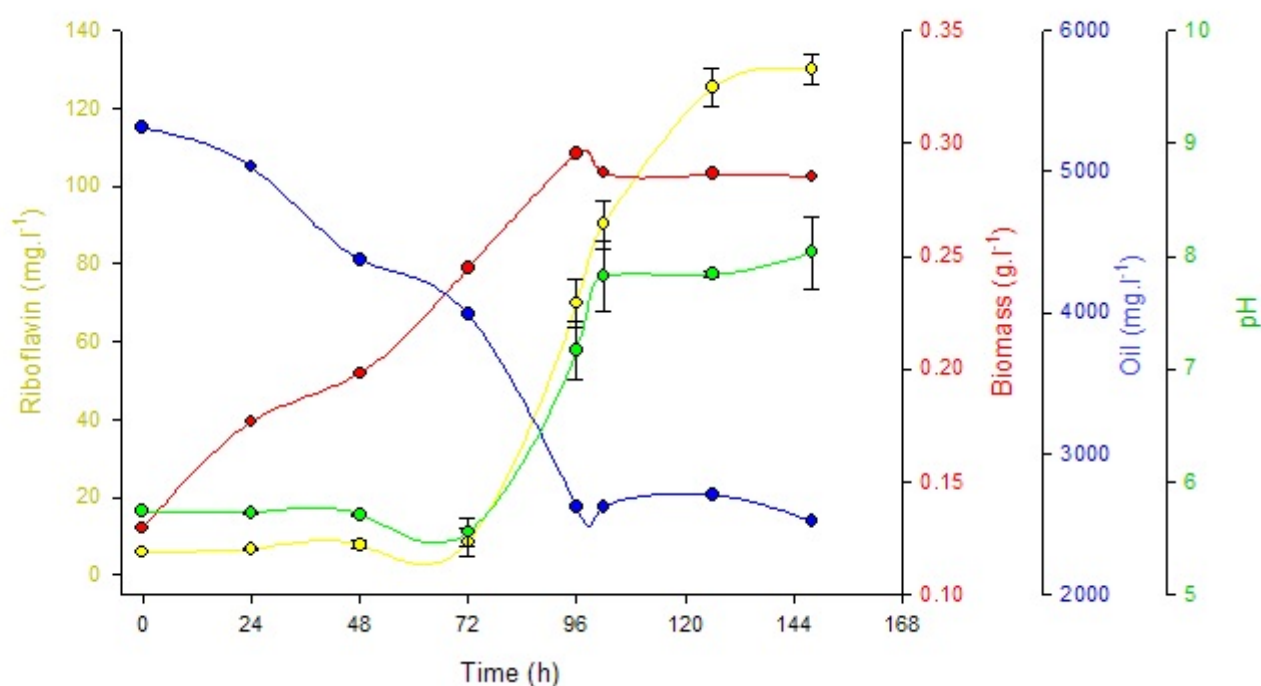


Figure 4.28 Riboflavin production in a 2-litre fermenter confirmatory test using a mutated strain of *E. gossypii* and optimized growth conditions. Show are riboflavin production (yellow), biomass (red), residual oil in medium (blue) and pH (green).

CHAPTER 5 : DISCUSSION

INTRODUCTION

Edible oil effluents have been poorly characterized in the literature and have previously not been reported as a substrate for any form of biological product. The only previous fate of these effluents reported is one of treatment by various means before disposal (Matsumiya, *et al.*, 2007; Sugimori, 2009). Since this effluent is produced in quantities up to 90 megalitres per day in just one industrial plant, and there are two refining factories in kwa-Zulu Natal, the effluent was considered as a possible substrate for fermentative development.

The aim was to find an organism that would utilize the effluent and produce a useful product in order to offer an alternative to the treat-and-dispose method used so that the effluent could be considered a valued product. Fungal species, *E. gossypii* (Lim, *et al.*, 2003; Sugimoto *et al.*, 2010), *E. ashbyii* (Kalingan and Krishnan, 1997, Kalingan and Liao, 2002) and *C. famata* (Heefner *et al.*, 1992; Yatsyshyn, *et al.*, 2009) have previously been reported in the literature to grow on edible oils and produce riboflavin. The most obvious solution was then to attempt to adapt one of these fungi to grow on the EOE and produce riboflavin as a valuable by-product.

FUNGAL STRAINS CHOSEN

Four fungi were obtained from various sources. The wild-type *E. gossypii* was kindly provided by Dr K.P. Stahmann of the Institut für Biotechnologie, Jülich, Germany, whilst two strains, *E. gossypii* and *E. ashbyii* were obtained from the Centraalbureau voor Schimmelcultures and a *C. famata* strain was obtained from the American Type Culture collection. The latter three were selected from the respective culture-collection websites specifically for their high riboflavin production yields on conventional media.

All four strains were grown on solid and liquid media according to a recipe by Ozbas and Kutsal (1986). The colony morphologies conformed to their descriptions from the respective culture banks and riboflavin production was evident from yellow

discolouration on solid media plates as shown in Figure 4.1.1. The filamentous fungi, particularly the two mutants (Figures 4.1.1 b and c), showed production towards the center of the mycelial mass, indicating that media depletion and possible growth stress were contributors to riboflavin production. This is in keeping with conclusions of Schlosser *et al.*, (2007), who concluded similarly, after observing growth of these organisms in relation to media depletion. The yeast culture (Figure 4.1.1 d) showed secretion of riboflavin into the medium around colonies indicating overproduction of riboflavin in excess of its requirements. This extracellular secretion was also found in a patented strain of *C. famata* produced by Heefner *et al.*, (1992). A bacterial strain *B. subtilis* used by Bretzel *et al.*, (1999) also demonstrated high concentrations in solution and even produced crystals of riboflavin in the medium.

INTRACELLULAR RIBOFLAVIN LOCALIZATION

An attempt to locate the production within biomass microscopically, was conducted by comparing distribution of riboflavin under UV fluorescence with the corresponding light micrograph of the same field of view (Figure 4.2). Two fungi, *E. gossypii* (CBS 109.51) and *C. famata* (ATCC 20850) are shown. Riboflavin in the filamentous fungus was shown to be produced strongly within the biomass and localized within vacuoles. This corresponded to some results presented by Lim *et al.*, (2003) who showed the localization of riboflavin in the filamentous fungus *E. gossypii* over a time period of 108 hours microscopically and whose micrographs show sparse distribution of riboflavin across mycelia. Riboflavin production by the yeast was shown to be more distributed within the field of view, with some cells producing riboflavin while others were not. This again was possibly indicative of the age of cells having an influence on riboflavin production.

GROWTH CURVE MODEL-FITTING

In order to differentiate among the four fungi with respect to their growth profiles, a growth modeling method needed to be chosen from literature. There are several types: logistic, Gompertz, Richards, Schnute, Stannard and Weibull (Zweitering *et al.*, 1990). Of the four-parameter sigmoid functions that fit growth curves, two that were most utilized in literature were the sigmoid and the Gompertz model. The latter was proposed by Benjamin Gompertz in 1825 and has found favour in some analyses of growth data (Windsor, 1932). The arguments for this growth model against the logistical model center around the inflection point. The inflection of the logistical model is exactly at 50%

between the asymptotes, whereas the Gompertz curve has a point of inflection when approximately 37% of growth is completed (Windsor, 1932). In selecting a model, the profile least likely to deviate from sample data should be selected. The arguments for the Gompertz model are that microorganisms have various responses to environmental stress such as mutation, adaptation to produce different enzyme sets, antibiotic production and adaptation to pollutants (Vanderpitte *et al.*, 1995). These would drive the inflection point to the left changing the growth profile of the microorganism to one resembling the Gompertz more than the logistic model.

The four fungi all demonstrated the ability to grow on Ozbas and Kutsal liquid medium with glucose as a carbohydrate source to varying degrees of growth saturation (Figure 4.3). All four growth curves were fitted to the Gompertz model with R^2 for fitting of curves in the range of 0.98 to 0.99 showing very good agreement with the Gompertz model (Table 4.2). Two of the four fungi showed short lag times of less-than 24 hours and maximum biomass production in the region of 17 mg.l⁻¹ (Figure 4.3 and parameter a of Table 4.2). These were *E. gossypii* (CBS109.51) and *C. famata* (ATCC 208.50) while *E. ashbyii* (CBS206.58) and *E. gossypii* wild-type (ATCC 10895) produced approximately 13 and 9 mg.l⁻¹ respectively. This showed that the two former organisms demonstrated the ability to adapt faster to the medium and produce biomass faster and to a higher concentration.

An examination of the maximum specific growth rates of the four fungi produces a slightly different picture though, with the *E. gossypii* wild-type (ATCC 10895) having the largest U_{\max} of 0.433 h⁻¹ followed by *E. gossypii* (CBS109.51) with 0.357 h⁻¹, *E. ashbyii* (CBS206.58) with 0.222 h⁻¹ and *C. famata* (ATCC 208.50) with 0.188. This may imply that *E. gossypii* wild-type (ATCC 10895) is the fastest growing organism on glucose but examining Figure 4.3, it can be seen that U_{\max} is closely related to the slopes of the curves and the *E. gossypii* wild-type (ATCC 10895) strain has indeed got the sharpest incline in curve, although its lag phase is the slowest and its maximum production is the least, as discussed in the previous paragraph.

A more meaningful understanding of the growth on glucose by these four organisms can be related to the mid-log growth times that were calculated using the Gompertz parameters as outlined in Eq. 3.4 of methods (Table 4.2). These values then show both

E. gossypii (CBS109.51) and *C. famata* (ATCC 208.50) reach mid-log at 38 and 36 hours respectively and that *E. gossypii* wild-type (ATCC 10895) takes 44 hours to reach mid-log while *E. ashbyii* (CBS206.58) takes approximately 60 h to reach mid-log phase. These four mid-log times were then taken as the times to bulk up inocula for all four fungi in order to inoculate further experiments. These mid-log time parameters also agree with the maximum biomass production data and the two factors were used in further Gompertz growth-curve transformations as primary parameters for ranking of data.

ANALYSIS OF EDIBLE OIL EFFLUENT

In order to determine if EOE was capable of supporting growth of fungi, its components were analyzed using GC-MS. The ion-spectra of EOE (Figure 4.4) showed no significant peaks in the expected range of 17 to 20 minutes where the components were likely to elute. A further chromatogram scanning for carbon chains showed two peaks (Figure 4.5) that were identified as tetradecanoic and hexadecanoic acids respectively with library matches of between 98 and 99% (Table 4.3). Tetradecanoic acid is also known as myristic acid and is a common component of palm and coconut oils and butter fat. This oil has a C14 chain that can possibly serve as a substrate for riboflavin production. Hexadecanoic acid is also known as palmitic acid and is one of the most common saturated fatty acids in plants, being derived from palm oil. It is a C16 fatty acid that can also be used as a possible substrate to synthesise riboflavin. The presence of these fatty acids was indicative that this effluent could serve as a complex carbon substrate for fungal growth and possible riboflavin production.

VALIDATION OF RIBOFLAVIN MEASUREMENT METHOD

Of the three methods encountered during literature searches for riboflavin detection, both UV and light spectrophotometry showed promise as fast, accurate methods for riboflavin detection (Ozbas and Kutsal, 1986; El-Refai *et al.*, 2009), with authors showing preferences for slightly different wavelengths for detection. The only drawback was the light-degradation of sample after measurement (Ahmad *et al.*, 2004). This method was thus investigated for its suitability for riboflavin measurement. The full-spectrum scan of riboflavin conducted is shown in Figure 4.5 with 26 riboflavin concentrations being scanned over a wavelength range of 200 to 820 nm at one nanometer scan intervals. Three linear regions were identified, two in the UV range 265 nm and 347 nm and one in the visible range at 444 nm (Figure 4.6). These three linear

ranges were further investigated for sensitivity and range of measurement. These results are shown in Figure 4.7 and summarized in Table 4.4. Although the lowest wavelength showed the highest sensitivity it also showed a very narrow range of linearity with increasing riboflavin concentration. The intermediate wavelength of 347 nm showed less linearity than the other two with an R^2 of 0.94. The wavelength chosen to measure riboflavin spectrophotometrically was 444 nm because it had a wider linear range of up to 30 mg.l⁻¹ riboflavin and was also linear up to this range with an R^2 of 0.995. A similar wavelength was also chosen by both Ozbas and Kutsal, (1986) and El-Refai, (2009) to measure riboflavin.

SCREENING FOR GROWTH ON EDIBLE OIL EFFLUENT

All four fungi were investigated for their growth potential on EOE. The medium comprised EOE as the sole carbon source with added nitrogen, phosphate and minerals. This was done in order to determine which of the four were capable of utilizing the carbon components detected earlier in EOE. The Gompertz model was employed to fit growth data and the model had a high goodness-of-fit to all data sets with high R^2 values. Vanderpitte *et al.*, (1995) essentially used the same fit characteristics to determine goodness-of-fit and found it acceptable. The two fungi that showed the highest growth on EOE in Figure 4.8 were *E. gossypii* (CBS109.51) and *C. famata* (ATCC 208.50) with maximum predicted biomass values of 0.401 mg.l⁻¹ and 0.281 mg.l⁻¹ growth respectively. This is far lower than the maximum predicted on glucose media in Table 4.2 with 17.522 and 17.085 mg.l⁻¹ produced using glucose as a carbon source. However, these two fungi did demonstrate the ability to grow on EOE better than *E. ashbyii* (CBS206.58) and *E. gossypii* (CBS109.51).

The maximum specific growth rates again show that *E. gossypii* (CBS109.51) had the highest U_{max} of 0.015 h⁻¹ (Table 4.5) and upon examination of the graph in Figure 4.8 it is again seen that the transition between low and high values is quite sharp for this organism, hence the steep slope of the graph and the high U_{max} value compared to other values. *E. gossypii* (CBS109.51) and *C. famata* (ATCC 208.50) are ranked second and third in growth rates with U_{max} of 0.004 and 0.003 h⁻¹ respectively (Table 4.5). These U_{max} values are again far below those obtained in Table 4.1 with glucose as a carbon substrate indicating a lower affinity for the more complex C 14 to C 16 carbon sources present in EOE. Nevertheless, all four organisms did demonstrate the ability to grow on this effluent

source and of the four, *E. gossypii* (CBS109.51) and *C. famata* (ATCC 208.50) produced the highest biomass concentrations and this assisted in their choice for further study on EOE.

RIBOFLAVIN PRODUCTION ON EDIBLE OIL EFFLUENT

In addition to growth, all four fungi were assessed for riboflavin production on EOE and showed the ability to produce nominal amounts without adaptation to the medium (Figure 4.9). The maximum amount of riboflavin produced was 3.52 mg.l⁻¹ riboflavin by *E. gossypii* (CBS109.51) followed by 2.74 mg.l⁻¹ produced by *C. famata* (ATCC 208.50). These maximum production values were significantly larger than the *E. ashbyii* (CBS206.58) and *E. gossypii* wild-type (ATCC 10895). In addition, the maximum riboflavin production rate was also calculated and both *E. gossypii* (CBS109.51) and *C. famata* (ATCC 208.50) demonstrated the fastest and second-fastest rates of production on EOE with 0.147 and 0.114 mg.h⁻¹ when calculating over measured time intervals (Table 4.6). In their seminal article, Tanner *et al.*, (1949), showed that *E. gossypii* showed an affinity for glucose over other more complex carbohydrates having a poor set of enzymes for break-down of the more complex sources. Their strain was a *E. gossypii* wild-type and the ones used here have since been mutated several times and would most likely have acquired some complex carbon catabolysing capabilities. The above results, however, show that the organisms used still prefer simple carbohydrates to more complex ones for growth.

Considering the fact that *E. gossypii* (CBS109.51) and *C. famata* (ATCC 208.50) both produced higher biomass values than their counterparts and that they produced more riboflavin at a higher rate on EOE, these two fungi were chosen to determine if either could be mutated to produce more riboflavin on EOE.

MUTATION AND STRAIN SELECTION

Both fungal cultures selected were exposed to four mutagens at three time intervals. The selection medium contained itaconate which is a known inhibitor of isocitrate lyase (Stahmann *et al*, 2000). This allowed selection of mutants whose isocitrate lyase was insensitive to inhibition. Colonies producing riboflavin were then picked off each medium and the resulting 24 organisms were screened for their riboflavin production. Figure 4.8 shows riboflavin production results for the mutants of *E. gossypii*

(CBS109.51) and the sodium azide mutagen at 10 minutes exposure produced the highest riboflavin levels (Figure 4.10d) followed by the EMS mutagen at 30 minutes exposure (Figure 4.10a). The particular EMS culture was from a previous round of mutations conducted by a researcher S. Govender (unpublished). These two organisms produced 43.27 and 42.83 mg.l⁻¹ respectively (Table 4.7). This was an approximately 12-fold increase in production over the unmutated strains (Figure 4.9) of this organism.

Isocitrate lyase (ICL) has been the target enzyme for several authors using strains of *E. gossypii* (Schmidt *et al*, 1996; Park *et al*, 2007). Schmidt *et al*, (1996) used soybean oil and glucose as substrates and found a correlation between ICL activity and riboflavin production particularly with soybean oil. They found a 25-fold increase in riboflavin yield by the mutant strain compared to its wild-type with a corresponding 15% increase in ICL activity using soybean oil. They also found that even though riboflavin production by the mutant increased 8-fold using glucose, the ICL activity decreased by 33%. This implied that ICL is a bottle-neck enzyme in organisms producing riboflavin with oil as a substrate as opposed to glucose. Park *et al*, (2007) used a UV mutant of *E. gossypii* and grew it on activated bleaching earth which contained vegetable oil. They found that itaconate selected mutants were able to increase riboflavin production nine-fold from the wild-type.

Figure 4.11 shows the respective mutants of *C. famata* (ATCC 208.50) and their riboflavin production after exposure to mutagens. A UV mutant exposed for 10 minutes (Figure 4.11b) produced the highest riboflavin concentration of 41.68 mg.l⁻¹ while an EMS exposure of 10 minutes (Figure 4.11a) produced the second-highest riboflavin concentration of 38.98 mg.l⁻¹ (Table 4.6). These were not as high as the amounts produced by mutants of *E. gossypii* (CBS109.51). A *C. famata* strain isolated using tubercidin as a riboflavin analogue, was patented by Heefner *et al.*, (1992) although they failed to mention in their patent application the method they used to create the mutant.

A composite table of growth and riboflavin production of all mutants (Table 4.7) showed that the *E. gossypii* (CBS109.51) mutants produced higher riboflavin concentrations, and higher specific growth rates. However, the *C. famata* (ATCC 208.50) mutants produced higher rates of riboflavin production and more riboflavin per unit biomass. The deciding factor in choosing a mutant to continue optimization was maximum riboflavin production

and in this instance *E. gossypii* (CBS109.51) mutants produced more riboflavin. The two mutants of *E. gossypii* (CBS109.51) chosen also had high rankings in most other categories of measurement. Literature has also indicated that *E. gossypii* is more suited to complex oil media and this also assisted in the choice of the filamentous fungus for further optimization studies.

ISOCITRATE LYASE ACTIVITY

The two mutants chosen for further investigation were the NaAz 10/1 mutant and the EMS 30/1 mutant. Since these were selected on the basis of resistance to inhibition of isocitrate lyase, the activity of isocitrate lyase was determined. The sodium azide mutant was not subculturable so the EMS 30/1 strain was used for further experiments. The mutant's enzyme activity was compared to the original *E. gossypii* (CBS109.51) culture and Figure 4.12 showed that it had a higher activity than the original culture. A non-linear curve-fitting in the form of Michaelis-Menten type plots was also used to determine the maximum enzyme reaction velocity (V_{\max}) and the substrate affinity of the enzyme (K_m). The results showed that the mutant had a faster reaction velocity but the original culture had a slightly higher affinity for the substrate (Table 4.8). These results agreed with those of Park *et al.*, (2007) who also examined ICL activity by a mutated *E. gossypii* strain and found that activity was increased by 50% in the mutant after two days of incubation. Both curves in the current study fitted the model to precision of between 0.93 and 0.96 when R^2 was used as a goodness-of-fit criterion. This indicates that the conclusions were reliable and that the mutant did indeed produce a faster-acting enzyme. The substrate affinity of faster acting enzymes needs to be lower in order to associate and dissociate faster to catalyze reactions. Hence, the lower substrate affinity is in keeping with the faster reaction rate of the enzyme.

SUBSTRATE OPTIMIZATION

Design of experiments was chosen as a method to optimize nutrient supplements required to produce riboflavin because it is a comprehensive and advanced set of analyses to analyze both single and multi-factor interactions using a single set of experiments (Haaland, 1989). The design also allows for many factors to be assessed at the same time making screening less expensive and less time consuming. Keeping this in mind, eight factors were selected from literature that would most likely improve riboflavin production using EOE as a carbon source. Ordinarily, running eight factors at two levels

with five center points would require a total of 261 experimental runs to complete, however, using DOE, the experiment could be completed in just 21 runs (Table 4.9). This obviously allows for a reduction in resources, time and effort to obtain results. There is a trade-off in this exercise in that some two and three-factor interactions may not be resolved, being aliased with each other. Being a Resolution IV design, (Table 4.8) no four-factor interactions could be resolved and a full list of aliased factors can be found in both the design software and literature (Haaland, 1989, Statease, 2007). This was not necessarily a problem as only one and two-factor interactions needed to be investigated and resolved at this stage.

Actual and predicted values shown in Table 4.9 did not vary greatly from each other, as evidenced by the residual column. The ratio of data (not shown) from minimum to maximum was 7.88 so no transformation of data was required and a linear model was used to analyse this data set. Figure 4.13, a half-normal plot, showed the selected factors after completing the experiment and both single and two-factor interactions were selected. The half-normal plot was used in preference to the full-normal plot because the sign of the effect is ignored and large effects are all grouped to the right of the graph giving a good pictorial idea of large effects. The smaller effects, those indistinguishable from noise that are unselected normally follow the line drawn and are subjected to a Shapiro-Wilk test and the probability of them being normally distributed is calculated. In this instance, a probability of $p > 0.3$ (value should be $p > 0.1$) was found for the unselected data points implying that they were normally distributed.

The largest effect was found to be corn-steep liquor which also was found to be a strong negative effect (Figure 4.14). This could be for one of two reasons. The concentration of CSL was high, at 60g.l^{-1} and this could have influenced it to be a negative effect. Alternatively, the presence of yeast extract in the medium, a direct substitute of CSL, could have meant that it was used preferentially to CSL which is the more likely scenario. This is borne out by the fact that the largest positive effect was yeast extract (Figure 4.14). Another possible explanation is that the CSL might have contained inhibiting chemical compounds, being a complex nutrient source, and increasing its concentration would have increased the inhibitors as well.

Pujari and Chandra, (2000) used CSL between 20 and 60 g.l⁻¹ for production of riboflavin by a UV mutant *E. ashbyii* strain and found an optimum of 29-32 g.l⁻¹ CSL. Sugimoto *et al.*, (2010) also used CSL in their optimization process using an oxalate resistant strain of *E. gossypii* and found that their maximum riboflavin production was at approximately 60 g.l⁻¹ CSL using a Box-Behnken experimental design. They also included glycine in their experiments and this is a direct precursor to riboflavin production so the contribution of CSL can be brought into question.

Competing substrates could also have provided the negative interaction between yeast extract and malt extract, both being nitrogen sources for the medium. The two positive interactions were between yeast extract/minerals and yeast extract/sodium chloride. Also of interest were positive interactions for NaCl by itself as a single factor and K₂HPO₄ as a single factor. The supplement NaCl can be tolerated by *E. gossypii* up to a concentration of 0.2 M (Forster, *et al.*, 1998). This is 11.688 g.l⁻¹ and the concentrations used here are well within that range.

Yeast extract and KH₂PO₄ were among five factors used in a full-factorial design to assess growth on flax-seed oil by *C. famata* strains by Suzuki *et al.*, (2009). They used a large concentration range of 30-60 g.l⁻¹ and found yeast extract to have a negative effect on riboflavin production. A possible explanation for this is that the high value of this nutrient was too high for the organism to tolerate. Their finding with the phosphate source was that a maximum of 105.7 mg.l⁻¹ riboflavin was produced with an optimum of 40 g.l⁻¹ KH₂PO₄. This is a lower amount of riboflavin than the current study with 20 times more phosphate.

The function of the Box-Cox plot was explained previously and the value obtained for lambda, a transformational indicator was 1. This fell within the 95% confidence interval of 0.59 and 2.08 shown in the graph (Figure 4.15). This tool showed that there was no transformation required for data to be further analyzed as it could fit a linear model.

Data was fitted to a mathematical model, and the probability of each single and dual-factor interaction as well as the overall model fit were calculated using ANOVA to compare the fit of each to the predicted model. In Table 4.10, the model probability was $p < 0.0007$ which indicates a very good fit of data to the predicted model. Of all factors

chosen in the pareto chart (Figure 4.14), the only insignificant one was minerals as an individual factor. All the other single and dual-factor interactions chosen were significant at the $p < 0.05$ threshold. This implies that further assessment with significant factors can be determined with reasonable certainty. Also of interest were the curvature which was significant implying that there was curvature in the response surfaces and the lack-of-fit value which was not significant implying that the values fitted the model. Lack-of-fit measured the variation around the actual and fitted model.

Since two two-factor interactions were found to be significant earlier in Figure 4.14, a cube plot was drawn to include the three factors involved viz., yeast extract, NaCl and minerals (Figure 4.16). This would possibly show whether a three-factor interaction occurred among the three, as was indeed the case. The high values of all three factors combined to give a predicted maximum of 111 mg.l⁻¹ of riboflavin whereas, by contrast, a combination of the lows of each of these factors would produce a predicted 68 mg.l⁻¹ (Figure 4.16). This showed that all three of these factors would have to be increased in further experiments.

A combination of yeast extract and minerals in three-dimensional plots (Figures 4.17 and 4.18) show the effect of NaCl as it had been reduced in Figure 4.17 and increased in Figure 4.18. The maximum predicted values for each were shown to be 82 and 112 mg.l⁻¹ respectively clearly showing the need to increase yeast extract, minerals and NaCl concentrations in the following experiment. Also of interest in Figure 4.17 is the slight curvature implied in the ANOVA table (Table 4.10). This shows a curvature around the yeast extract/minerals axis particularly at low yeast extract concentrations, whereas there was more linearity at the upper end of yeast extract concentration implying that there was further scope for optimizing yeast extract supplementation levels.

The four factors chosen to increase were yeast extract, NaCl, minerals and K₂HPO₄. The other factors were kept to a minimum except Tween 80 which had no effect on experiments and was removed from solution with little effect on subsequent experiments. Tween 80 was used as a 1.8% supplement by Pujari and Chandra (2000) in the production of riboflavin by *E. gossypii* as mentioned previously, and after their screening experiments, no mention was made of it in their optimization experiments. It is presumed they left it out of succeeding experiments as well.

Because there were just four factors to test, a full-factorial design ($n=2^4$) was chosen with five center points making a total of 21 (n) runs in total, the same number of runs as the previous experiment, but with a complete resolution of all factors and all interactions. This is the most powerful experimental design level with all interactions being resolved from each other. The design and actual and predicted results showed in Table 4.11 gave an extremely good fit between the values with small variations in the center points only. This would then give a very significant mathematical model with which to investigate the design space.

The half-normal probability plot (Figure 4.19) had yeast extract as the most significant positive effect with the first positive double-interaction being a combination of yeast extract/NaCl. Also showing positive effects were a triplicate combination of yeast extract/NaCl/minerals and a double combination of yeast extract/minerals.

The pareto chart (Figure 4.20) elucidated some of the negative interactions. One of the largest was a combination of all four factors which indicates that there was some overshoot in the experimental design particularly when all four factors were set at their high values. The individual factor that might have been increased too far was K_2HPO_4 as it showed a negative individual effect and was involved in several other negative effects, implying that it might have been a contributor to those combinations. This factor was then set at its low value of 2 g.l⁻¹ for further experiments. Pujari and Chandra (2000) used KH_2PO_4 in optimization experiments and found a range of 1.2 - 1.5 g.l⁻¹ allowed production of maximal riboflavin using an *E. ashbyii* UV mutant.

The ANOVA table for the model showed that the model fit the data with high precision ($p < 0.0001$) as the predicted values were similar to experimental ones. All other factors significantly fit the mathematical model as well ($p < 0.05$) (Table 4.12). Curvature was also shown to be significant with some curvature in the model being indicated.

Having seen the positive effects of the yeast extract/NaCl combination, the individual mineral factor and the three-factor combination of yeast extract/NaCl/minerals (Figure 4.18), the combination of these three factors was plotted in a cube plot to investigate their effects at each combination (Figure 4.21). This plot showed that in combination at their

low values, the maximum predicted riboflavin was 56 mg.l⁻¹ whereas increasing all three to their maximum values increased riboflavin to 95 mg.l⁻¹.

An investigation of the two-factor interaction between yeast extract/NaCl, while varying the concentration of minerals, provided a more complete picture. Figure 4.22 shows the two-factor combination with minerals at its low value producing a maximum of 73 mg.l⁻¹ riboflavin while increasing the minerals concentration in Figure 4.23 changed the shape of the graph to show a maximum prediction of 123 mg.l⁻¹. This was then used as an indicator as to the direction the response-surface method would take in the following experiment. Minerals concentration was set at its high value, the K₂HPO₄ was set at its low value and both yeast extract and NaCl were investigated as varying factors in the optimization experiment.

The experiment was run as a central composite, face-centered design. Two factor variation allowed for the design to be completed in eight runs with five center points for a total of 13 runs. The variation around the peripheral points was set at 1.414 times the low and high values. This design type thus produces five points across the face of the design crossing over at the center point and is a very efficient method to investigate factor effects. For clarification, a graphical schematic of the design is shown in Figure 3.1.

The variation in runs is shown in Table 4.13, with predicted and actual values being close to each other as evidenced by small residual values. Table 4.14 shows the ANOVA for the model and the predicted p value is $p < 0.0001$ which is an excellent fit for the model. The mathematical model for all central composite designs is a quadratic one, thus including the squares of the individual factors. All other factors were found to be significant at a threshold of $p < 0.05$. Worryingly, the lack of fit value was also significant, but an investigation of R² and adjusted R² values gave 0.97 and 0.96 respectively. These two values along with the strong p-value for the model and individual factors allowed the model to be analyzed further with some assurance.

The interaction graph between yeast-extract and NaCl showed a typical rising ridge (Figure 4.24). This is a common feature in optimization experiments. Yeast extract shows an obvious maximum value on this graph while the NaCl value required some further

investigation. A contour plot showed the optimization point slightly outside the design space for NaCl (Figure 4.25). This was then calculated using an optimization algorithm to yield five solutions shown in Table 4.15. Of the five, the most desirable was one predicting production of 135.761 mg.l⁻¹ riboflavin with yeast extract set at 8.43 g.l⁻¹ and NaCl set at 2.5 g.l⁻¹. The maximum predicted value was some 38.5-fold higher than the riboflavin produced by this strain on EOE without mutation and media optimization.

CONFIRMATION EXPERIMENT

Having established the nutrient requirements for the optimum production of riboflavin, the solution with the highest desirability and lowest standard error of mean was chosen from Table 4.15 to confirm if results were reproducible in triplicate shake-flask experiments. Figure 4.26 showed the progressive improvement in biomass yield for *E.gossypii* EMS30/1 and showed an increase in biomass from 0.11 mg.l⁻¹ to 0.25 mg.l⁻¹ which is a 2.2 fold increase in biomass production. Also shown in Figure 4.27 is the steep increase in riboflavin production after statistical optimization of media components with a maximum of 132.28 mg.l⁻¹ of riboflavin being produced compared to the mutated strain (42.83 mg.l⁻¹) and the unmutated strain (3.52 mg.l⁻¹) of *E. gossypii*. This is a 3-fold increase over the mutated strain and a 37.6 fold increase over the wild-type indicating that the strategy was successful at improving riboflavin production.

The laboratory scale fermentatation in a 2-litre bioreactor showed an average of 130 mg.l⁻¹ of riboflavin produced which was within the 95% confidence interval for the prediction of maximum riboflavin production (Figure 4.28). Also of note is the phase in which riboflavin was produced, and this was shown to be after the biomass peaked at 96 h. This is in agreement with the typical production curve seen earlier in Figure 2.3 and in general agreement with the trends shown by Karos *et al.*, (2004). Also, pH, oil depletion and biomass were monitored and results are shown in Figure 4.26.

The depletion of the oil fraction was shown and this indicated a decrease from 5,309 mg.l⁻¹ to 2,519mg.l⁻¹. This occurred over the duration of growth showing that the organism was using oil to produce biomass, and more sharply when riboflavin production began during the time interval 72 to 96 h (Figure 4.28) indicating that this was the carbon source used for riboflavin production. The efficiency of riboflavin production on the carbon source was 46.59 mg.g⁻¹. This were lower than the yield amount of riboflavin

produced by Lim *et al.*, (2003) who produced 320 mg.g⁻¹ riboflavin on soybean oil substrate. The production in this process was on an oil effluent and could not be directly compared to a pure oil additive. This process has thus been shown to produce riboflavin using the oil effluent carbon, along with supplements.

A progressive increase in riboflavin production has been achieved over the duration of this study. This involved a strategy of mutation and selection to increase yield from 3.52 mg.l⁻¹ for the unmutated culture to 42.83 mg.l⁻¹ for the mutated culture. This was a 12.2 fold or 1117% increase in production. Over the two screening and one optimization experiment using DOE and predictive modelling, a 38.6-fold increase was predicted with an increase of 3757% over the initial producer. The actual production was slightly lower than predicted, but nevertheless just as impressive, and in a 2-litre fermenter culture, 130.15 mg.l⁻¹ was produced, a 37-fold or 3597% increase from the unmutated unoptimized culture. The progression of these increases in riboflavin production is summarised in Table 5.1.

Table 5.1 Progressive increase in riboflavin production over the various steps including mutation, screening, optimization, batch and fermenter production.

Experimental steps	Riboflavin on EOE (mg.l ⁻¹)	Increase (fold)	Increase (%)
<i>E. gossypi</i> without modification	3.52	-	-
<i>E. gossypi</i> mutant EMS 30/1	42.83	12.2	1117%
<i>E. gossypi</i> EMS30/1 after primary screen (predicted)	112	31.8	3082%
<i>E. gossypi</i> EMS30/1 after secondary screen (predicted)	122.58	34.8	3382%
<i>E. gossypi</i> EMS30/1 after optimization (predicted)	135.76	38.6	3757%
<i>E. gossypi</i> EMS30/1 optimized flask (actual)	132.28	37.6	3658%
<i>E. gossypi</i> EMS30/1 optimized 2-litre fermenter (actual)	130.15	37.0	3597%

FEASIBILITY OF PRODUCTION

The South African oil industry produces minimally 6 x 10⁸ litres of wastewater per annum. This wastewater often exceeds 20,000 mg.l⁻¹ COD, far higher than the average level measured effluents in this study. A differentiation must be made between wastewater and effluent, the effluent being treated whereas the wastewater is not. This is most likely the reason for the discrepancy in COD measurements reported and observed. These are the basic assumptions for production of riboflavin used in this

estimation, excluding infrastructure, which will be financed through loans and repaid from operating profits as expenses before taxation. This is the reason why capital repayment is not included in the cost of product calculation in Table 5.2.

The costings of each of the chemicals added are listed per litre in Table 5.2.

Table 5.2 Cost of medium and purification for riboflavin production on edible oil effluent in South African cents.

	Quantity per litre	Cost SA cents/g	Cost per litre SA cents
Yeast Extract	8.43 g	2.51	21.16
NaCl	2.5 g	0.60	1.50
K ₂ HPO ₄	2 g	2.30	4.60
Malt Extract	5 g	1.18	5.90
Peptone	0.5 g	2.86	1.43
CSL	30 ml	0.0375	1.13
Minerals 17 mg.ml ⁻¹	3 ml	3.92	0.20
Effluent	1000 ml		No cost
Base cost			35.92
Labour cost percentage - 50% of base cost			17.96
Purification and packaging cost percentage - 30% of base cost			10.78
Final cost			64.66

The amount of riboflavin produced per litre was approximately 130 mg from an effluent of 5,000 mg.l⁻¹ C₁₄ - C₁₆ oils. Production from an untreated wastewater of 20,000 mg.l⁻¹ COD is estimated to quadruple the yield with 520 mg being produced at the base cost of 35.92 cents. Costs for purification usually are 30% and labour would be 50% of production costs and this would make the total price for production 64.41 cents (Table 5.2). The production cost would thus be :

$$64.66 \text{ cents} \times \frac{1000}{520} \text{ g} = R124 \text{ per gram}$$

The feed grade sale price of riboflavin which is a lower estimate than food grade is approximately R2.04 per gram and will produce a resultant profit margin of R0.80 per gram produced. The major contributors to this cost are yeast and malt extract. The feed market would be more amenable to riboflavin produced from EOE. Previous research has suggested that CSL could replace at least yeast extract as a nitrogen source but this was not found to be the case in this study. If just 10% of the market adopted this production process, the effluent volume directed towards this process would be 6 x 10⁷ litres

providing a volumetric production of riboflavin of approximately 31.2 tonnes per annum with a market value of approximately 63.65 million rands per annum and a profit margin of approximately 24.96 million rands. Clearly this technology is an attractive and marketable solution to use EOE for the production of riboflavin.

CONCLUSIONS

- Four fungi tested in this study were able to grow on edible oil effluent to varying degrees and produce small quantities of riboflavin.
- Two of the four, *E. gossypii* (CBS109.51), and *C. famata* (ATCC 208.50) were able to produce more riboflavin than *E. gossypii* wild-type (ATCC 10895) and *E. ashbyii* (CBS206.58).
- Both were mutated and produced in the range of 40 mg.l⁻¹ riboflavin on EOE. An *E. gossypii* EMS 30/1 mutant was then used to optimize riboflavin production using Design of Experiments and Response Surface Methods.
- Using the above statistical design methods, an iterative increase in riboflavin production was achieved up to a theoretical maximum of 136 mg.l⁻¹, of which a maximum of 130 mg.l⁻¹ was achieved in a laboratory-scale fermentation..
- The cost implications for production of riboflavin on EOE were calculated and with the current market value, a 10% technology uptake by the edible oil industry could yield a riboflavin industry with a 63.65 million rands per annum and 24.96 million rands gross profit margin.
- This technology can be profitably scaled-up to provide a valuable product from what would ordinarily be an effluent stream requiring treatment.

REFERENCES

- Adrio, J.L. and Demain, A.L. 2003. Fungal Biotechnology. *International Microbiology*, **6**: 191-199.
- Ahmad, I., Fasihullah, Q., Noor, A., Ansari, I.A. and Ali, Q.N.M. 2004. Photolysis of riboflavin in aqueous solution: a kinetic study. *International Journal of Pharmaceutics*, **280**: 199-208.
- Anon. 2002. B vitamin requirements and lean growth potential. [online]. Available from: http://www.dsm.com/en_US/html/dnpus/an_art_2_1_b_requirements_swine.htm. [Accessed 19 April 2002].
- Anderson, M.J. and Whitcomb, P.J. 2000. *DOE Simplified. Practical Tools for Effective Experimentation*. Productivity Press, New York, USA. ISBN: 978-1563272257.
- Anderson, M.J. and Whitcomb, P.J. 2005. *RSM Simplified. Optimizing Processes Using Response Surface Methods for Design of Experiments*. Productivity Press, New York, USA ISBN-13: 978-1563272974.
- Bacher, A. and Mailander, B. 1973. Biosynthesis of riboflavin: The structure of the purine precursor. *The Journal of Biological Chemistry*, **248**: 6227-6231.
- Bacher, A., Eberhardt, S., Fischer, M., Kis, K. and Richter, G. 2000. Biosynthesis of vitamin B₂. *Annual Review of Nutrition*, **20**: 153-67.
- Bailey, R.B., Lauderdale, G.W., Heefner, D.L., Weaver, C.A., Yarus, M.J., Burdzinski, L.A. and Boyts, A. 1992. A Fermentation Process for Riboflavin-Producing Organisms, World Intellectual Property Organization Patent Number WO 92/01060, Coors Biotechnology Incorporated, North Pecos, Colorado.

Barichevich, E.M and Calza, R.E.1996.Mutagen killing and photoreactivation in the anaerobic fungus *Neocallimastix frontalis* EB188. *Fungal Genetics*, **43**:17-19.

Begoude, B.A.D., Lahlali, R., Friel, D., Tondje, P.R., and Jijakli, M.H. 2007. Response surface methodology study of the combined effects of temperature, pH, and a_w on the growth rate of *Trichoderma asperellum*. *Journal of Applied Microbiology*, **103**: 845-854.

Bigelis, R. 1989. Industrial products of biotechnology: application of gene technology. In: Rehm, H.J and Reed, G. (ed.) *Biotechnology*, VCH, Weinheim. pp. 243. ISBN-13: 978-3527283101.

Box, G.E.P. 2005. *Statistics for Experimenters - Second Edition*. Hoboken, N.J,Wiley-Interscience. ISBN: 0-471-09315-7.

Breen, C., Crowe, A., Roelfsema, H.J., Saluja, I.J. and Guenter, D. 2003. High-dose riboflavin for prophylaxis of migraine. *Canadian Family Physician*, **49**: 1291-1293.

Bretzel, W., Schurter, W., Ludwig, B., Kupfer, E., Doswald, S., Pfister, M., and van Loon, A.P.G.M. 1999. Commercial riboflavin production by recombinant *Bacillus subtilis*: down-stream processing and comparison of the composition of riboflavin produced by fermentation or chemical synthesis. *Journal of Industrial Microbiology and Biotechnology*, **22**: 19-26.

Burgess, C.M., O'Connell-Motherway, M., Sybesma, W., Hugenholtz, J. and van Sinderen, D. 2004. Riboflavin production in *Lactococcus lactis*: Potential for in-situ production of vitamin-enriched foods. *Applied and Environmental Microbiology*, **70**(10): 5769-5777.

Burgess, C.M., Smid, E.J., Rutten, G. and van Sinderen, D. 2006. A general method for selection of riboflavin-overproducing food-grade microorganisms. *Microbial Cell Factories*, **5**: 24.

- Burgess, C.M., Smid, E.J., and van Sinderen, D. 2009. Bacterial vitamin B2, B11 and B12 overproduction: An overview. *International Journal of Food Microbiology*, **133**: 1-7.
- Chell, R.M., Sundaram, T.K., and Wilkinson, A.E. 1978. Isolation and characterization of isocitrate lyase from a thermophilic *Bacillus* sp. *Biochemistry Journal*, **173**:165-177.
- Choe, E., Huang, R. and Min, D.B. 2005. Chemical Reactions and Stability of Riboflavin in Foods. *Journal of Food Science*, **70**(1): 28-36.
- Cocaign, M., Monnet, C., and Limdley, N.D. 1993. Batch kinetics of *Corynebacterium glutamicum* during growth on various carbon substrate: use of substrate mixtures to localise metabolic bottlenecks. *Applied Microbiology and Biotechnology*, **40**: 526-530.
- Costa, J.A.V., Colla, L.M., Filho, P.D., Kabke, K., and Weber, A. 2002. Modelling of *Spirulina platensis* growth in fresh water using response surface methodology. *World Journal of Microbiology and Biotechnology*, **18**: 603-607.
- Dauner, M., Sonderegger, M., Hochuli, M., Szyperski, T., Wuthrich, K., Hohmann, H., and Sauer, U. 2002. Intracellular carbon fluxes in riboflavin-producing *Bacillus subtilis* during growth on two-carbon substrate mixtures. *Applied and Environmental Microbiology*, **68**: 1760-1771.
- De Baets, S., Vanderdrinck, S., Vandamme, E.J. 2000. Vitamins and Related Biofactors. *Encyclopaedia of Microbiology - 2nd Edition*. Academic Press, USA. ISBN: 0-12226-800-8.
- De Lucas, J.R., Amor, C., Diazl, M., Turner, G., and Laborda, F. 1997. Purification and properties of isocitrate lyase from *Aspergillus nidulans*, a model enzyme to study catabolite inactivation in filamentous fungi. *Mycological Research*, **101**:410-414.

Diogo, H.C., Sarpieri, A., and Pires, M.C. 2005. Fungi preservation in distilled water. *Annals of Brazilian Dermatology*, **80**: 591-594.

Drossler, P., Holzer, W., Penzkofer, A. and Hagamann, P. 2002. pH dependence of the absorption and emission behavior of riboflavin in aqueous solution. *Chemical Physics*, **282**:429–39.

Dunne, L.J. 1990. *Nutrition Almanac - Third Edition*. McGraw-Hill, New York. ISBN:0071389326.

El-Refai, H.A., Allam, R.F., and El-Shafei, M.S. 2009. Fermentative parameters and kinetic studies of riboflavin production by local isolate of *Aspergillus terreus*. *Journal of Applied Sciences Research*, **5**: 601-604.

Ertrk, E., Erkmen, O., and Oner, D. 1998. Effects of various supplements on riboflavin production by *Ashbya gossypii* in whey. *Turkish Journal of Engineering and Environmental Sciences*, **22**:371-376.

Fischer, M., Schott, A., Romisch, W., Ramsperger, A., Augustin, M., Fidler, A., Bacher, A., Richter, G., Huber R., and Eisenreich, W. 2004. Evolution of Vitamin B2 Biosynthesis. A Novel Class of Riboflavin Synthase in Archaea. *Journal of Molecular Biology*, **343**: 267-278.

Food and Nutrition Board, 1998. Riboflavin. *Dietary Reference Intakes: Thiamin, Riboflavin, Niacin, Vitamin B₆, Vitamin B₁₂, Pantothenic Acid, Biotin, Folate and Choline*. National Academies Press, Washington DC, 87–122.

Forster, C., Marienfeld, S., Wendisch, V.F., and Kramer, R. 1998. Adaptation of the filamentous fungus *Ashbya gossypii* to hyperosmotic stress: different osmoreponses to NaCl and mannitol stress. *Applied Microbiology and Biotechnology*, **50**: 219-226.

Fuller, T.E. and Mulks, M. H. 1995. Characterisation of *Acinobacillus pleurpneumoniae* riboflavin biosynthesis genes. *Journal of Bacteriology*, **177**(24): 7265-7270.

- Fung, M., and Triulzi, D.J. 2003. Pathogen inactivation of blood products, *Transfusion Medicine Update* Issue 7 [online]. Available from: <http://www.itxm.org/tmu/tmu2002/issue7.htm> [Accessed 4 March 2003].
- Garrison, R.H. and Somers, E. 1990. *The Nutrition Desk Reference*. Keats Publishing Inc., Connecticut, USA. ISBN-13: 978-0879838263.
- Gyure, D.C. and Lauderdale, G.W. 1992. Method for Recovery of Riboflavin. United States Patent Number 5,103,005. Coors Biotechnology Incorporated, Westminster, Colorado.
- Haaland, P.D. 1989. *Experimental Design in Biotechnology*. Marcel Dekker, Inc, New York, Basel. ISBN-13: 978-0824778811.
- Heefner, D.L., Weaver, A.C., Yarus, M.J., and Burdzinski, L.A. 1992. Methods for producing riboflavin with *Candida famata*. ZeaGen, Inc, **5**: 435-466.
- Heefner, D.L., Weaver, A.C., Yarus, M.J., Burdzinski, L.A., Gyure, D.C. and Foster, E.W. 1994. Riboflavin Producing Strains of Microorganisms, Methods for Selecting and Method for Fermentation. European Patent Number 0 365 560 B1. Archer Daniels Midlands Company, Decatur Illinois.
- Hickey, R.J. 1954. Production of riboflavin by fermentation. In: Underkofler, L.A. and Hickey, R.J (eds) *Industrial Fermentations*, Chemical Publishing Co. Inc. New York, USA.
- Hoffmann, F. 2000. Vitamin B₂. La-Roche LTD. [online]. Available from: www.reche.com/vitamins/what/anh/vits/vitb2.html [Accessed 19 April 2002].
- Howe, C.A. 1957. Process for producing riboflavin. United States Patent Office, Patent Number 2,807,611.

- Hustad, S., Ueland, P.M. and Schneede, J. 1999. Quantification of riboflavin, flavin mononucleotide and flavin adenine dinucleotide in human plasma by capillary electrophoresis and laser-induced fluorescence detection. *Clinical Chemistry*, **45**(6): 862-868.
- Hutchens, S.A., Leon, R.V., O'Neill, H.M., and Evans, B.R. 2007. Statistical analysis of optimal culture conditions for *Gluconacetobacter hansenii* cellulose production. *Letters in Applied Microbiology*, **44**: 175-180.
- Jiminez, A., Santos, M.A., Pompejus, M., and Revuelta, J.L. 2005. Metabolic engineering of the purine pathway for riboflavin production in *Ashbya gossypii*. *Applied and Environmental Microbiology*, **71**:5743-5751.
- Kalingan, A.E. and Krishnan. M.R.V. 1997. Application of agro-industrial by-products for riboflavin production by *Eremothecium ashbyii* NRRL 1363. *Applied Microbiology and Biotechnology*, **47**: 226-230.
- Kalingan, A.E. and Liao, C.-M. 2002. Influence of type and concentration of flavogenic factors on production of riboflavin by *Eremothecium ashbyii* NRRL 1363. *Bioresource Technology*, **82**: 219-224.
- Karos, M., Vilari, C., Bollschweilera, C. and Revuelta, J.L. 2004. A genome-wide transcription analysis of a fungal riboflavin overproducer. *Journal of Biotechnology*, **113**: 69–76.
- Kato, T. and Park, E.Y. 2006. Expression of alanine:glyoxylate aminotransferase gene from *Saccharomyces cerevisiae* in *Ashbya gossypii*. *Applied Microbiology and Biotechnology*, **71**:46-52.
- Khan, M. N. and Akhtar, W. 1998. Wastes from edible oil and fat industry of Karachi. 24th WEDC Conference - Sanitation and Water For All. 144-146. Pakistan.
- Koizumi, S. and Teshiba, S. 1998. Riboflavin biosynthetic genes of *Corynebacterium ammoniagenes*. *Journal of Fermentation and Bioengineering*, **86**: 130-133.

- Koizumi, S., Yonetani, Y., Maruyama, A. And Teshiba, A. 2000. Production of riboflavin by metabolically engineered *Corynebacterium ammoniagenes*. *Applied Microbiology and Biotechnology*, **53**: 674-679.
- Kolonne, S., Seviour, R.J., and McDougall, B.M. 1994. Effect of pH on Exocellular riboflavin production by *Eremothecium ashbyii*. *Biotechnology Letters*, **16**:79-84.
- Kurtzman, C.P. 1995. Relationships among the genera *Ashbya*, *Eremothecium*, *Holleya* and *Nematospora* determined from rDNA sequence divergence. *Journal of Industrial Microbiology*, **14**: 523-530.
- Kurtzman, C.P. and Fell, J.F. 1998. *The Yeasts, A Taxonomic Study - Fourth Edition*. Elsevier, Amsterdam, ISBN: 078174797X.
- Lago, B.D. and Kaplan, L. 1981. Vitamin fermentations: B₂ and B₁₂. *Advances in Biotechnology*, **3**: 241-246.
- Leathers, T.D. and Gupta, S.C. 1997. Xylitol and riboflavin accumulation in xylose-grown cultures of *Pichia guilliermondii*. *Applied Microbiology and Biotechnology*, **47**:58-61.
- Lee, K.H., Park, Y.H., Han, J.H, Lee, K.H. and Choi, H. 2006. Microorganisms for producing riboflavin and method for prducing riboflavin using the same. U.S. Patent 7078222.
- Li, Y., Liu, Z., Cui, F., and Liu, Z. 2007. Application of Plackett-Burman experimental design and Doehlert design to evaluate nutritional requirements for xylanase production by *Alternaria mali* ND-16. *Applied Microbiology and Biotechnology*, **77**: 285-291.
- Lim, S.H., Ming H., Park, E.Y., and Choi, J.S. 2003. Improvement of riboflavin production using mineral support in the culture of *Ashbya gossypii*. *Food Technology and Biotechnology*, **41**: 137-144.

- Liu, B-A. and Tzeng, Y.M. 1998. Optimization of growth medium for the production of spores from *Bacillus thuringiensis* using response surface methodology. *Bioprocess Engineering*, **18**: 435-438.
- Liu, G.Q. and Wang, X.L. 2007. Optimization of critical medium components using response surface methodology for biomass and extracellular polysaccharide production by *Agaricus blazei*. *Applied Microbiology and Biotechnology*, **74**: 78-83.
- Long, A. R. 2000. Vitamins and Other Minerals. In: Horwitz, W. (ed.) *Official Methods of Analysis of AOAC International*, **45**: 9-10. Gaithersburg, USA: AOAC International.
- Maeting, I., Schmidt, G., Sahm, H., Revuelta, J.L., Stierhof, Y.D., and Stahmann, K.P. 1999. Isocitrate lyase of *Ashbya gossypii* - transcriptional regulation and peroxisomal localization. *FEBS Letters*, **444**: 15-21.
- Maisels J.M., and Watchko J.F. 2000. Neonatal Jaundice. USA: Informal Health Care.
- Matsumiya, Y., Wakita, D., Kimura A., Sanpa S and Kubo M. 2007. Isolation and characterization of a lipid-degrading bacterium and its application to lipid-containing wastewater treatment. *Journal of Bioscience and Bioengineering* **103**: 325–330.
- Montgomery, D.C. 2005. *Design and Analysis of Experiments, Sixth Edition*. John Wiley and Sons Inc, USA. ISBN-13: 978-0471316497
- Morehouse, A.L. 1958. Riboflavin Recovery. United States Patent Number 2,822,361. Grain Processing Corporation, Muscaline, Iowa.
- Moses, K. 2009. EMS Mutagenesis [online]. Available at: <http://fruitfly4.aecom.yu.edu/labmanual/16a.html>. [Accessed 20 September 2009].
- Osman, H.G. and Chenouda, M.S. 1965. Biosynthesis of riboflavin by *Eremothecium ashbyii*. *Journal of Microbiology*, **11**:625-628.

Ozbas, T. and Kutsal, T. 1986. Comparative study of riboflavin production by two microorganisms: *Eremothecium ashbyii* and *Ashbya gossypii*. *Enzyme and Microbial Technology*, **8**: 593-596.

Ozbas, T. and Kutsal, T. 1991. Effect of growth factors on riboflavin production by *Ashbya gossypii*. *Enzyme and Microbial Technology*, **13**:594-597.

Park, E.Y. and Ming H. 2004. Oxidation of Rapeseed Oil in Waste Activated Bleaching Earth and Its Effect on Riboflavin Production in Culture of *Ashbya gossypii*. *Journal of Bioscience and Bioengineering*, **97**(1): 59-64.

Park, E.Y., Tajima, Z.S., and Dwiarti, L. 2007. Isolation of *Ashbya gossypii* mutant for an improved riboflavin production targeting for biorefinery technology. *Journal of Applied Microbiology*, **103**: 468-476.

Pasternak, R and Ellis, V. 1943. Purification of Riboflavin, United States Patent Number 2,324,800, Charles Pfizer and Company, Brooklyn, N.Y.

Perkins, J.B., Sloma, A., Hermann, T., Theriault, K., Zachgo, E., Erdenberger, T., Hannet, N., Chatterjee, N.P., Williams, V., Rufo, G.A., Hatch, R. and Pero, J. 1999. Genetic engineering of *Bacillus subtilis* for the commercial production of riboflavin. *Journal of Industrial Microbiology and Biotechnology* **22**: 8-18.

Pujari, V. and Chandra, T.S. 2000. Statistical optimization of medium components for enhanced riboflavin production by a UV-mutant of *Eremothecium ashbyii*. *Process Biochemistry*, **36**: 31-37.

Roux-Van der Merwe, M.P., Badenhorst, J and Britz, T.J. 2005. Fungal treatment of an edible-oil-containing industrial effluent. *World Journal of Microbiology & Biotechnology*, **21**: 947-953.

Sandor, P.S., Afra, J., Ambrosini, A. and Schoenen, J. 2000. Prophylactic treatment of migraine with beta-blockers and riboflavin: differential effects on the intensity dependence of auditory evoked cortical potential. *Headache* **40**: 30-35.

- Sapra, V.T., Hughes, J.L. and Sharma, G.C. 2004. Effect of sodium azide and N-nitroso-N-methylurea on M₁ and M₂ generations of hexaploid *Triticale* (x *Triticosecale*). [online]. Available at: <http://www.grs.nig.ac.jp/wheat/wis/No41-42/p52/1.html>. [Accessed 20 March 2004].
- Satoh, D. 2003. A measure to distinguish between a logistic curve model and a Gompertz curve model. *Fast Abstract ISSRE*, Chillarege Press. [online]. Available at: <http://www.chillarege.com/fastabstracts/issre2003/127-FA-2003.pdf>. [Accessed 20 March 2004].
- Sauer, U. and Bailey, J.E. 1999. Estimation of P-to-O ratio in *Bacillus subtilis* and its influence on maximum riboflavin yield. *Biotechnology and Bioengineering* **64**: 750-754.
- Sauer, U., Cameron, D.C. and Bailey, J.E. 1998. Metabolic capacity of *Bacillus subtilis* for the production of purine nucleosides, riboflavin and folic acid. *Biotechnology and Bioengineering*, **59**: 227-238.
- Sauer, U., Hatzimanikatis, V., Hohmann, H.P., Manneberg, M., van Loon, A.P.G.M. and Bailey, J.E. 1996. Physiology and metabolic fluxes of wild-type riboflavin-producing *Bacillus subtilis*. *Applied and Environmental Microbiology*, **62**: 3687-3696.
- Sayyad, S.A., Panda, B.P., Javed, S., and Ali, M. 2007. Optimization of nutrient parameters for lovastatin production by *Monascus purpureus* MTCC 369 under submerged fermentation using response surface methodology. *Applied Microbiology and Biotechnology*, **73**: 1054-1058.
- Schallmeyer, M. Singh, A. and Ward, P. 2004. Developments in the use of *Bacillus* species for industrial production. *Canadian Journal of Microbiology*, **50**(1): 1-17.
- Schlosser, T., Wiesenberg, C.G., Funke, A., Viets, U., Vijayalakshmi, S., Nieland, S., and Stahmann, K.P. 2007. Growth stress triggers riboflavin overproduction in *Ashbya gossypii*. *Applied Microbiology and Biotechnology*, **10**: 569-578.

Schmidt, G., Stahmann, K.P., Kaesler, B. and Sahm H. 1996. Correlation of isocitrate lyase activity and riboflavin formation in the riboflavin overproducer *Ashbya gossypii*. *Microbiology*, **142**: 419-426.

Sierra, S., Rodelas, B., Martinez-Toledo, M.V., Pozo, C., and Gonzales-Lopez, J. 1999. Production of B-group vitamins by two *Rhizobium* strains in chemically defined media. *Journal of Applied Microbiology*, **86**: 851-858.

Silviera, S.T., Burkett, J.F.M., Costa, J.A.V., and Kalil, S.J. 2007. Optimization of phycocyanin extraction from *Spirulina platensis* using factorial design. *Bioresource Technology*, **98**: 1629-1634.

Stahmann, K.P., Arst Jr, H.N., Althofer, H., Revuelta, J.L., Monschau, N., Shlupen, C., Gatgens, C., Weisenburg, A., and Schlosser, T. 2001. Riboflavin, overproduced during sporulation of *Ashbya gossypii*, protects its hyaline spores against ultraviolet light. *Environmental Microbiology*, **3**: 545-551.

Stahmann, K.P., Böddecker, T. and Sahm, H. 1997. Regulation and properties of a fungal lipase showing interfacial inactivation by gas bubbles, or droplets of lipid or fatty acid. *European Journal of Biochemistry*, **244**: 220-225.

Stahmann, K.P., Revuelta, J.L., and Seulberger, H. 2000. Three biotechnical processes using *Ashbya gossypii*, *Candida famata* or *Bacillus subtilis* compete with chemical riboflavin production. *Applied Microbiology and Biotechnology*, **53**: 509-16.

Statease. 2007. Design Expert 7.1.6 [online] Available at: <http://www.statease.com>. [Accessed 11 September 2007].

Steffen, Roberts and Kirsten [SRK (CE) Inc.] 1989. Water and Wastewater Management in the Edible Oil Industry. WRC Report No. TT 40/89. Water Research Commission, Pretoria.

- Sugimori, D. 2009. Edible oil degradation by using yeast coculture of *Rhodotorula pacifica* ST3411 and *Cryptococcus laurentii* ST3412. *Applied Microbiology and Biotechnology*, **82**: 351-357.
- Sugimoto, T., Morimoto, A., Nariyama, M., Kato, T., and Park, E.Y. 2010. Isolation of an oxalate-resistant *Ashbya gossypii* strain and improved riboflavin production. *Journal of Industrial Microbiology and Biotechnology*, **37**: 57-64.
- Survase, S.A., Bajaj, I.B., and Singhal, R.S. 2006. Biotechnological Production of Vitamins. *Food Technology and Biotechnology*, **44**: 381-396.
- Suryadi, H., Yoshida, N., Yamada-Onodera, K., Katsuragi, T., and Tani, Y. 2000. Characterization of a flavogenic mutant of methanol yeast *Candida bodinii* and its extracellular secretion of riboflavin. *Journal of Bioscience and Bioengineering*, **90**:52-56.
- Suzuki, G.T., Fleuri, L., and Macedo, G.A. 2009. Influence of nitrogen and carbon sources on riboflavin production by wild strains of *Candida* sp. *Food Bioprocess Technology*, [online]. Available at: <http://www.springerlink.com/content/tq17638612826248/fulltext.pdf>. [Accessed 4 June 2009].
- Tanner, F.W., Vojnovich, C., and Van Lanen, J.M. 1949. Factors affecting riboflavin production by *Ashbya gossypii*. *Agricultural and Industrial Chemistry*, **58**:737-745.
- Takeda Vitamin and Food USA, Inc. 2002. Product data - Riboflavin USP/FCC.[online]. Available at <http://www.mrathcliffe.com/tusa/products.html#Bcomplex>, Accessed 19 April 2002.
- Umgeni Water Methods Manual. 2002. Laboratory Services, Method 113 - GC-MS Screening.

Usui, N., Yamamoto, Y. and Nakamatu, T. 1994. Process for Producing Riboflavin by Fermentation. United States Patent Number 5,334,510. Ajinomoto Corporation, Incorporated, Tokyo, Japan.

Vandamme, E.J. 1989. *Biotechnology of Vitamins, Pigments and Growth Factors*. ISBN: 978-1-85166-325-5.

Vanderpitte, V., Quataert, P., De Rore, H. and Verstraete, W. 1995. Evaluation of the Gompertz function to model survival of bacteria introduced into soils. *Soil Biology and Biochemistry*, **27**(3): 365-372.

van Loon, A.P., Hohmann, H.P., Bretzel, W., Humbelin, and M., Pfister, M. 1996. Development of a fermentation process for the manufacture of riboflavin. *Chimia* **50**: 410–412.

Wendland, J. and Walther, A. 2005. *Ashbya gossypii*: A model for fungal developmental biology. *Nature Reviews Microbiology*, **3**:421-429.

Windsor, C.P. 1932. The Gompertz Curve as a Growth Curve. *Proceedings of the National Academy of Sciences*. **18**(1): 1-8.

Wolf, R., Reiff, F., Wittman, R. and Butzke, J. 1982. Process for the preparation of riboflavin. United States Patent Number 4,355,158.

World Bank Group. 2007. Environmental \Health and Safety Guidelines Vegetable Oil Processing. [online] available at: [http://www.ifc.org/ifcext/enviro.nsf/AttachmentsByTitle/gui_EHSGuidelines2007_VegetableOilProc/\\$FILE/Final+-+Vegetable+Oil+Processing.pdf](http://www.ifc.org/ifcext/enviro.nsf/AttachmentsByTitle/gui_EHSGuidelines2007_VegetableOilProc/$FILE/Final+-+Vegetable+Oil+Processing.pdf). Accessed 12 November 2007.

Wu, Q.L., Chen, T., Gan, Y., Chen, X., and Zhao, X.-M. 2007. Optimization of riboflavin production by recombinant *Bacillus subtilis* RH44 using statistical designs. *Applied Microbiology and Biotechnology*, **76**: 783-794.

Xiao, Z.J., Liu , P.H., Qin, J.Y., and Xu, P. 2007. Statistical optimization of medium components for enhanced acetoin production from molasses and soybean meal hydrolysate. *Applied Microbiology and Biotechnology*, **74**: 61-68.

Yatsyshyn , V.Y., Ishchuk, O.P., Voronovsky, A.Y., Fedorovych, D.V., and Sibirny, A.A. 2009. Production of flavin mononucleotide by metabolically engineered yeast *Candida famata*. *Metabolic Engineering*, **11**: 163-167.

Zhi, W., Song, J., Ouyang, F., and Jingxiu, B. 2005. Application of response surface methodology to the modeling of amylase purification by aqueous two-phase systems. *Journal of Biotechnology*, **118**: 157-165.

Zweitering, M.H., Jongenburger, I., Rombouts, F.M. and Van't Riet, K. 1990. Modeling of the bacterial growth curve. *Applied and Environmental Microbiology*, **56**(6): 1875-1881.